



Title	INTRAMOLECULAR OH π HYDROGEN BOND AND SOLVENT EFFECTS
Author(s)	Ueji, Sinichi
Citation	大阪大学, 1978, 博士論文
Version Type	VoR
URL	https://hdl.handle.net/11094/27740
rights	
Note	

The University of Osaka Institutional Knowledge Archive : OUKA

<https://ir.library.osaka-u.ac.jp/>

The University of Osaka

INTRAMOLECULAR OH... π HYDROGEN BOND

AND

SOLVENT EFFECTS

1978

Shinichi Ueji

80SC00375

INTRAMOLECULAR OH... π HYDROGEN BOND

AND

SOLVENT EFFECTS

1978

Shinichi Ueji

General Abstract

It is now well known that the π -electron systems in olefins and aromatics can act as the proton acceptors, as the lone-pair electrons in nitrogen and oxygen atoms do. The phenomenon of π hydrogen bonding, as well as that of the ordinary hydrogen bonding, is of fundamental importance in chemistry, physics and biology. For this reason, a number of studies in the field have been reported in the last twenty years.

Hitherto the intramolecular OH... π hydrogen bonding has been discussed on the basis of the relationship between the strength of the interaction and the stereochemistry, while the intermolecular one has been mainly examined in relation to the hydrogen bond strength (or energy) and/or the structure and the strength of π base. However, definite information as to the following points is still lacking, in spite of its great importance. i) Although all studies so far have been carried out in the so-called "inert" solvents, the effects of solvents on the OH... π hydrogen bonding have been generally neglected, because of the complexity of the problem. ii) The nature of the two hydroxyl IR stretching bands (*cis* and *trans* isomers) observed for biphenyl-2-ol has been studied by many workers, but unfortunately no one has reported any reliable ratio of the two isomers. iii) Little is known about the stereochemistry of the OH... π hydrogen bonding in crystalline state.

In order to contribute to the elucidation of the above mentioned problems, present author's study has been conducted on the intramolecular OH... π hydrogen bonded systems. For

this purpose, 2-arylphenols and 2,6-diarylphenols have been selected as a suitable model system. In the inert solvents such as CCl_4 , the former phenol shows the $\text{OH}\dots\pi$ bonded hydroxyl group and the free hydroxyl group; while the latter possesses only the $\text{OH}\dots\pi$ bonded one, because of the presence of aryl groups at the 2,6-positions of phenol. The present thesis is divided into six chapters.

In Chapter I, the IR spectra of the intramolecular $\text{OH}\dots\pi$ hydrogen bonding are investigated in a range of nonpolar solvents which can not act as proton acceptors. The geometry for the solvent-solute association model can be shown on the basis of the relationship between the solvent-induced IR shifts and the stereochemical environment around the $\text{OH}\dots\pi$ bonded systems. This geometry is also verified by the Proton NMR results.

In basic solvents acting as proton acceptors, there is a competition between the intramolecular $\text{OH}\dots\pi$ and intermolecular $\text{OH}\dots(\text{base})$ hydrogen bonds in 2,6-diarylphenols, which are regarded as the sterically hindered phenol. The thermodynamics of the competitive hydrogen bonded system is studied by means of IR spectroscopy. The steric effects on the intermolecular hydrogen bond formation are discussed on the basis of the variation of the thermodynamic parameters caused by the structural factors. These results are given in Chapter II.

Chapter III presents a study of the equilibrium of biphenyl-2-ol by IR spectroscopy. The proportion of the *cis* ($\text{OH}\dots\pi$) and *trans* (free OH) isomers is estimated by applications of Hammett treatment and solvent effects. The two

different methods lead to the concordant results.

In Chapters IV and V, studies of the solvent effects are extended to those of systems other than the OH... π bonding. Chapter IV discusses the effects of solvents on the carbon-13 NMR spectra of the carbonyl carbon systems. The dipolar association between a carbonyl-containing solute and acetonitrile solvent is deduced from the correlation between the ^{13}C chemical shifts and the G values (solvent polarity parameter). Chapter V describes the effects of solvents on the UV-VIS spectra of sodium 4-nitrophenoxide in the presence of 15-crown-5 ether. A marked difference in the solvent shifts between hydroxylic and nonhydroxylic solvents is discussed.

In the final chapter, three-dimensional X-ray analysis reveals the stereochemistry of the intramolecular OH... π hydrogen bonding in 4-substituted (NO_2 , H and OC_2H_5) 2,6-diphenylphenols. The IR spectra in the solid state can be explained on the basis of the crystal and molecular structures.

Most of these studies have already been reported in the following journals.

- 1) The Effects of Solvents on the Intramolecular OH... π Bonded System
S. Ueji and T. Kinugasa, *Tetrahedron Letters*, 2037 (1976).
- 2) The Effects of Solvents on the IR and PMR Spectra of Intramolecular OH... π and OH...O Hydrogen Bonded Systems
S. Ueji, *Bull. Chem. Soc. Jpn.*, 51, 1799 (1978).
- 3) Infrared Spectroscopic Study of the Interaction between 2,6-Diarylphenols and Alkyl Cyanides

- S. Ueji, T. Kinugasa, and N. Ueda, *J. Chem. Soc., Perkin Transaction 2*, 178 (1976).
- 4) Equilibrium Study of Biphenyl-2-ol by Infrared Spectroscopy
T. Kinugasa, M. Nakamura, and S. Ueji, *J. Chem. Soc., Perkin Transaction 2*, 1663 (1976).
- 5) The Effects of Solvents on Carbon-13 Chemical Shifts of the Carbonyl Carbon System
S. Ueji and M. Nakamura, *Tetrahedron Letters*, 2549 (1976).
- 6) The Effects of Solvents on the Electronic Absorption Spectra of Sodium 4-Nitrophenoxide in the Presence of 15-Crown-5 Ether
S. Ueji and M. Kitadani, *Bull. Chem. Soc. Jpn.*, 50, 2819 (1977).
- 7) 2,6-Diphenylphenol: The structure Containing an Intramolecular OH... π Hydrogen Bond
K. Nakatsu, H. Yoshioka, K. Kunimoto, T. Kinugasa, and S. Ueji, *Acta Crystallogr., Sect. B*, in press.

Acknowledgements

The author is greatly indebted to Professor Emeritus Toshio Kinugasa for his invaluable guidance and constant encouragement throughout the course of this study.

The author is also deeply grateful to Professor Ichiro Murata, Osaka University, for his stimulating discussions and invaluable advice on the preparation of this thesis.

Greatful thanks are also made to Dr. Masayuki Kitadani for his helpful suggestions and active collaborations.

Finally the author's grateful acknowledgement is also due to all the members of Kinugasa laboratory and to all fellow researchers of chemical laboratory of college of general education.

Shinichi Ueji

Department of Chemistry
College of General Education
Kobe University

May, 1978.

C O N T E N T S

CHAPTER I	Effects of Nonpolar Solvents on the IR and PMR Spectra of Intramolecular OH... π and OH...O Hydrogen Bonded Systems	
		page
	Abstract.....	1
	Introduction.....	2
	Results and Discussion.....	4
	Experimental.....	23
	References.....	26
CHAPTER II	Effects of Basic Solvents on Intramolecular OH... π Hydrogen Bonded System. Steric Effects on Intermolecular Hydrogen Bond Formation of 2,6-Diarylphenols with Base	
	Abstract.....	31
	Introduction.....	31
	Experimental.....	33
	Results and Discussion.....	37
	References.....	56
CHAPTER III	Equilibrium Study of Biphenyl-2-ol by IR Spectroscopy	
	Abstract.....	58
	Introduction.....	58
	Results and Discussion.....	60
	Experimental.....	65
	References.....	66

CHAPTER I. Effects of Nonpolar Solvents on the IR
 and PMR Spectra of Intramolecular OH... π
 and OH...O Hydrogen Bonded Systems

Abstract. The effects of solvents on the intramolecular OH... π and OH...O hydrogen bonding in 2-arylphenols and 2,6-diarylphenols have been studied by examining the OH stretching IR absorption spectra in a range of solvents. The solvent shifts of the hydrogen bonded bands, $\nu_{\text{OH...}\pi}$ and $\nu_{\text{OH...O}}$, followed the G correlation and the BHW plot. The success of both correlations suggests that the solvent shifts are primarily due to a specific solvent-solute association, even in relatively non-polar solvents. The temperature effects on the frequencies of $\nu_{\text{OH...}\pi}$ and $\nu_{\text{OH...O}}$ also furnish some support to a specific solvent-solute association mechanism in solvation of the intramolecular hydrogen bonded systems. The solvent sensitivity of the OH... π and OH...O hydrogen bonded bands depended on the stereo-chemical environment around the hydrogen bonded system rather than on such electronic factors as the strength of the hydrogen bonding. On the basis of the relationship between the solvent sensitivity and the structural changes over a group of phenols, a simplified model for the solvent-solute association is put forward. Furthermore, this simplified model is also discussed in terms of the aromatic solvent-induced shifts in the PMR spectra.

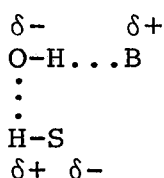
Introduction

Since the first observation of the solvent sensitivity of the hydrogen bonded OH frequency,¹⁾ considerable attention has been focused on the solvent effects on IR frequency shifts.²⁻⁵⁾ However, the problem is not yet completely settled.

In the IR study of the solvent effects on the hydrogen bonded bands, Bellamy, Morgan, and Pace²⁾ attributed the origin of solvent shifts to the specific association of solvents with the hydrogen bonded complex,



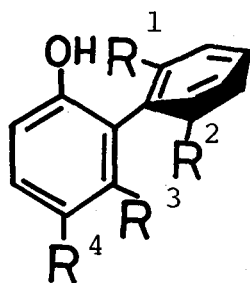
where S-H denotes the solvent molecule. Later, Yoshida and Ōsawa⁴⁾ interpreted the solvent shifts in terms of the dipolar association model, in which the solvent is preferentially oriented with its bond dipole toward the lone pair dipole of the hydroxyl group in the hydrogen bonded system. Furthermore, they assumed that the dipolar association exists as the following geometry.^{3a)}



Most of the studies in this field have been concerned with the intermolecular hydrogen bonding. However, there has been little systematic study of the intramolecular hydrogen bonding, primarily because of the complexity of the factors affecting the solvent sensitivity. In case of the intramolecular hydrogen bonding, the solvent shifts can be expected to be affected by the geometric effects as well as the electronic effects if the specific solvent-solute association is an important factor in determining the solvent shifts.

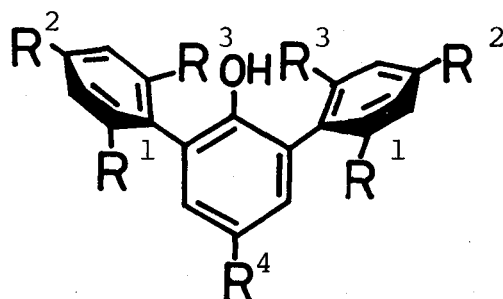
In this chapter, the effects of solvents on the intramolecular OH... π and OH...O hydrogen bonding in 2-arylphenols (I - 7) and 2,6-diarylphenols (8 - 14) are investigated by means of IR spectroscopy, and the solvent-solute association model is discussed through the geometric effects on the solvent sensitivity.

2-arylphenols



- 1 $R^1=R^2=R^3=R^4=H$
 2 $R^1=R^2=R^4=H, R^3=CH_3$
 3 $R^1=R^3=CH_3, R^2=R^4=H$
 4 $R^1=OH, R^2=R^3=R^4=H$
 5 $R^1=OH, R^2=R^3=CH_3, R^4=H$
 6 $R^1=OCH_3, R^2=R^3=R^4=H$
 7 $R^1=R^2=R^3=H, R^4=NO_2$

2,6-diarylphenols



- 8 $R^1=R^2=R^3=R^4=H$
 9 $R^1=CH_3, R^2=R^3=R^4=H$
 10 $R^1=R^2=R^3=H, R^4=NO_2$
 11 $R^1=CH_3, R^2=R^3=H, R^4=NO_2$
 12 $R^1=R^3=CH_3, R^2=H, R^4=NO_2$
 13 $R^1=R^3=H, R^2=CH_3, R^4=NO_2$
 14 $R^1=R^3=H, R^2=C(CH_3)_3, R^4=NO_2$

1H NMR spectroscopy is also a powerful method for the study of the geometry for the solvent-solute association model. The aromatic solvent-induced shifts in the PMR spectra of compound (8) are nicely explained in terms of the model.

derived from the IR study,

Results and Discussion

IR Spectra. In nonpolar solvents such as CCl_4 , 2-arylphenols (1, 2, 3, 5, and 7) show the doublet νOH absorptions, corresponding to the free and the intramolecularly $\text{OH}\dots\pi$ hydrogen bonded hydroxyl groups, while 2,6-diarylphenols (8 - 14) have only a singlet νOH due to the intramolecular $\text{OH}\dots\pi$ hydrogen bonding. In addition to the observed doublet, the other 2-arylphenols (4 and 6) exhibit a broad third band centered at about 3450 cm^{-1} , indicating the presence of intramolecular $\text{OH}\dots\text{O}$ hydrogen bonding. These assignments are based on the reported IR spectra of similar compounds.^{6,7)} Some typical νOH absorption spectra are reproduced in Fig. 1.

Table 1 summarizes the intramolecular $\text{OH}\dots\pi$ and $\text{OH}\dots\text{O}$ hydrogen bonded OH stretching frequencies in the same set of solvents, together with the solvent constants. The $\text{OH}\dots\pi$ and $\text{OH}\dots\text{O}$ frequencies in the vapor phase were estimated by interception at $G=0$ in the G correlations (see Fig. 2), according to the previously reported procedure.^{1,3)} The G value is the solvent constant empirically assigned to the solvent by Allerhand and Schleyer in order to explain the solvent sensitive IR bands.¹⁾ The relative solvent shifts, $\Delta\nu/\nu$, of the $\text{C}=\text{O}$ of acetophenone are used as the reference value in the Bellamy-Hallam-Williams (BHW) plot.⁸⁾ The choice of solvents was limited to inert solvent which can not act as proton acceptors, because the proton acceptor

Table 1. Intramolecular OH... π and OH...O hydrogen bonded OH stretching frequencies (cm^{-1}) in the same set of solvents and the solvent constants

Solvents	Solvent constants		1	2	3	4		5
	G	$\Delta\nu/\nu$				OH... π	OH...O	
(Vapor)	0	0	(3587)	(3580)	(3571)	(3569)	(3538)	(3553)
Hexane	44	7.0	3573.0	3566.6	3558.3	3558.4	_____a)	3544.3
Cyclohexane	49	7.6	3570.2	3564.2	3557.5	3556.6	_____a)	3543.9
Decalin	58	8.8	3566.6	3563.0	3555.7	3555.7	3483	3542.0
Tetrachloro- ethylene	64	9.4	3565.7	3560.2	3553.0	3554.8	3478	3541.1
Carbon tetrachloride	69	9.9	3564.8	3561.1	3553.9	3555.7	3474	3542.0
Benzene	80	11.1						
Dichloro- methane	100	14.0	3554.8	3550.5	3542.7	3549.3	3440	3534.8
Bromoform	118	17.0	3547.5	3544.0	3539.4	3540.3	3429	3530.5

a) The apparent intensity was too weak to obtain a reliable value.

Table 1 (Continued).

6		7	8	9	10	11	12	13	14
OH...π	OH...0								
(3579)	(3499)	(3569)	(3573)	(3567)	(3554)	(3545)	(3534)	(3547)	(3546)
3566.6	3460	3551.1	3560.2	3554.8	3539.3	3532.0	3521.0	3533.0	3533.0
3564.4	3456	3548.4	3558.5	3553.8	3536.6	3531.4	3520.8	3531.4	3531.4
3563.9	3450	3543.9	3555.5	3551.0	3533.9	3525.7	3517.0	3527.5	3526.6
3561.4	3442	3542.0	3555.7	3549.4	3531.1	3524.8	3514.1	3525.0	3526.4
3562.0	3441	3543.9	3555.7	3550.0	3532.0	3527.5	3516.6	3527.5	3527.5
			3549.3	3544.1	3524.0	3518.6	3508.1	3518.0	3516.7
3551.7	3409	3527.6	3543.8	3539.0	3519.7	3513.0	3504.3	3512.8	3513.0
3545.5	3397	3520.9	3540.2	3535.7	3514.1	3511.0	3501.4	3510.5	3511.0

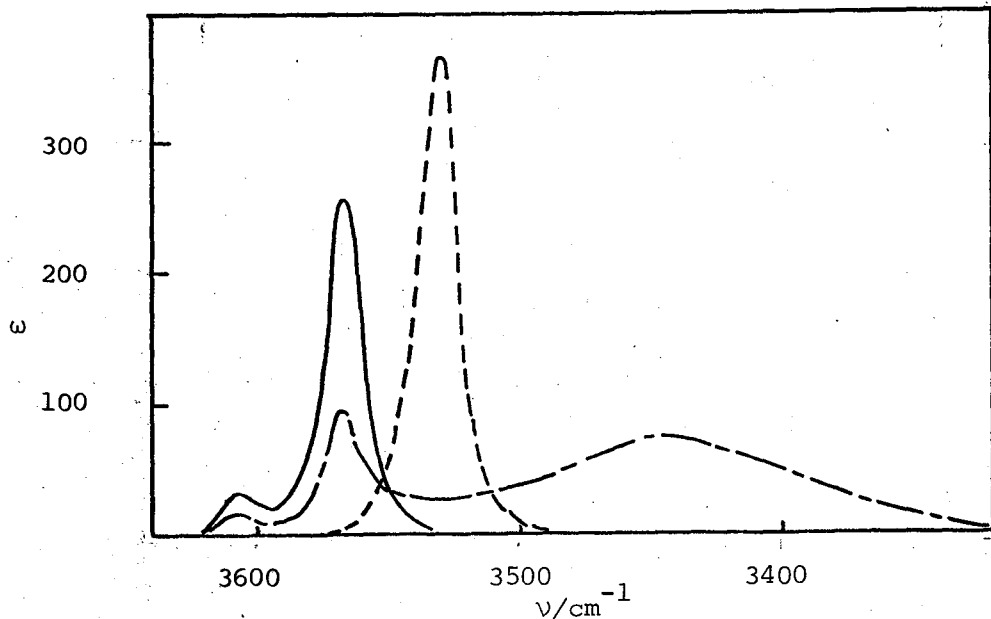


Fig. 1. VOH Absorptions of 1(—), 6(---), and 10(-·-·) in CCl_4 .

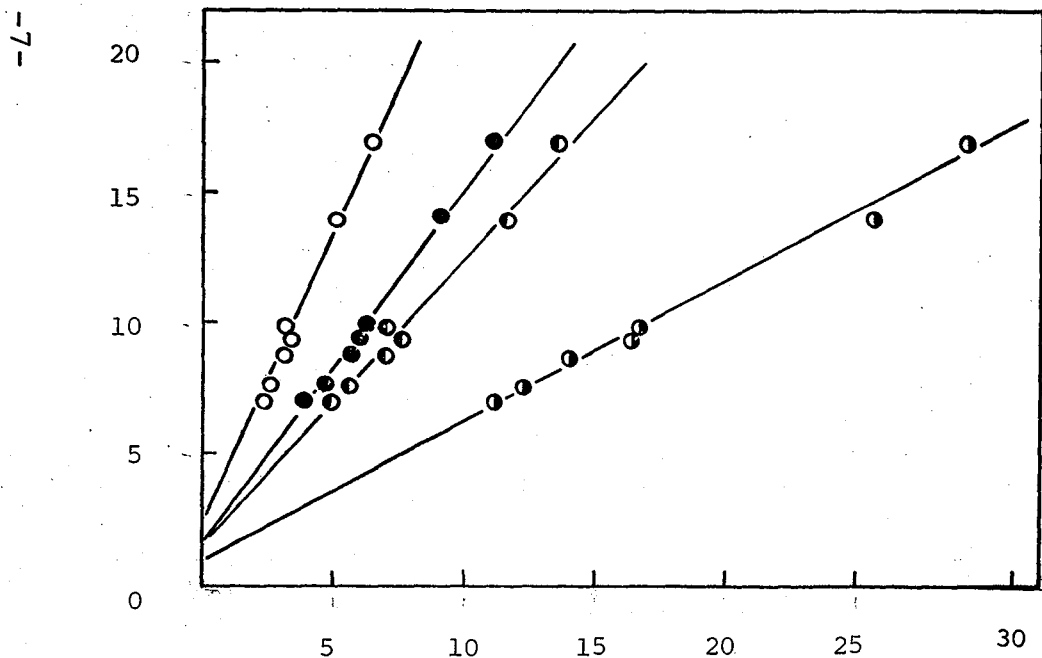


Fig. 3. BHW plots of $\nu\text{OH}\dots\pi$ and $\nu\text{OH}\dots\text{O}$ frequencies against the $\nu\text{C}=\text{O}$ frequencies of acetophenone. 1(●), 5(○), 7(⊙), 6(OH..O;⊙).

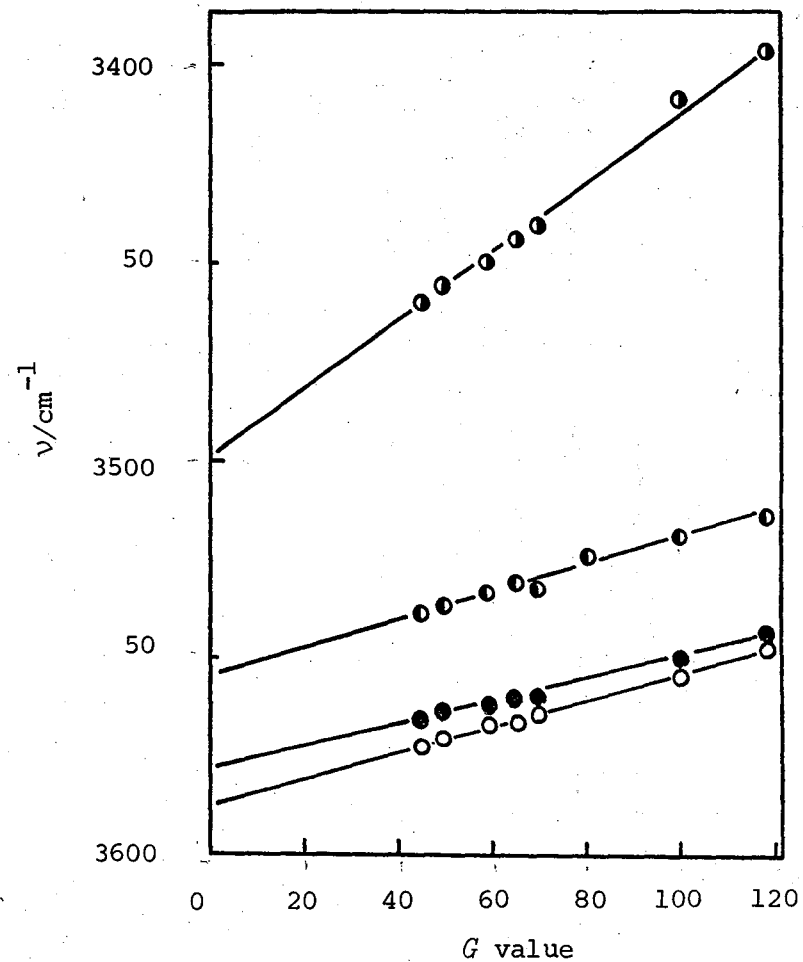


Fig. 2. Correlation of the OH stretching frequencies of $\text{OH}\dots\pi$ and $\text{OH}\dots\text{O}$ hydrogen bonds with the G values of the solvents. 1(○), 6($\text{OH}\dots\pi$, ● ; $\text{OH}\dots\text{O}$, ⊙), 10(⊙).

solvents produce intermolecular hydrogen bonding.⁹⁾

It is found from Table 1 that the frequencies of the hydrogen bonded bands, $\nu_{\text{OH}} \dots \pi$ and $\nu_{\text{OH}} \dots \text{O}$, are fairly sensitive to the change of solvent. These solvent shifts correlate linearly with both the G and $\Delta\nu/\nu$ values. Figures 2 and 3 show the G correlation and the BHW plot respectively. The success of both correlations suggests that the operation of the solvation mechanism in the $\text{OH} \dots \pi$ bonded system is similar to that in the carbonyl group¹⁰⁾ and that the solvent shifts are mainly produced by a specific solvent-solute association rather than by general dielectric effects, because (1) Bellamy *et al.* showed that the solvent dependency of the $\nu_{\text{C=O}}$ frequency is primarily due to a specific solvent-solute association,⁸⁾ and (2) the G value does not fit the KBM, pullin, and Buckingham equations based on the dielectric theory.¹⁾

As can be seen from Figs. 2 and 3, the slopes in both correlations vary widely from compound to compound. It is known that the slope of the G correlation (a)¹⁾ and the reciprocal slope of the BHW plot ($1/S$)¹¹⁾ become direct measures of the solvent sensitivity.

Table 2 lists the a and $1/S$ values, the IR spectral data, and the dihedral angle between the phenol ring and the proton acceptor ring. In the IR data, both A_i/A_f and $\Delta\nu_{\text{max}}$ can indicate the strength of the hydrogen bonding in 2-arylphenols.¹²⁾ With 2,6-diarylphenols without a free hydroxyl group, both A_i and ν_{max} are adopted as a measure of the strength of the $\text{OH} \dots \pi$ bonding.¹³⁾ The dihedral

Table 2. Solvent sensitivity, spectral data, and dihedral angle for the OH... π and OH...O hydrogen bonded systems

	<i>a</i> value	1/ <i>S</i> value	$\Delta\nu_{\max}/\text{cm}^{-1}$ ^{a)}	A_i/A_f ^{b)}	Dihedral angle(θ)/deg	K band λ_{\max}/nm
2-arylphenols						
1	0.33	0.69	42.2	6.7	50° ^{c)}	245.5
2	0.30	0.64	47.5	11.2	60° ^{c)}	245.5
3	0.27	0.56	54.5	16.4	70° ^{c)}	240.0
4	OH... π	0.23	0.50	44.5	9.1	
	OH...O	0.94	2.00	126	— ^{d)}	
5		0.19	0.40	62.7	42.0	70°–90°
	OH... π	0.28	0.60	42.8	7.8	
6	OH...O	0.85	1.90	164	39.7	
7		0.40	0.87	47.3	9.6	

a) $\nu_{\text{OH}}(\text{free}) - \nu_{\text{OH}}(\text{OH}\dots\pi \text{ or } \text{OH}\dots\text{O})$. b) $A_i(\text{OH}\dots\pi \text{ or } \text{OH}\dots\text{O})/A_f(\text{free})$. c) See Ref. 7.

d) The A_i value could not be determined owing to very weak intensity.

Table 2(Continued).

	a value	$1/S$ value	$\nu_{i_{\max}}/\text{cm}^{-1}$	$A_i \times 10^{-4} \text{e}^{\text{e}}$	Dihedral angle(θ)/deg	K band λ_{\max}/nm
2,6-diarylphenols						
8	0.28	0.61	3555.7	1.89	60° (52°) ^{f)}	241.0
9	0.27	0.58	3550.0	2.01	70°	236.0
10	0.34	0.74	3532.0	2.60	g) (58°) ^{f)}	
11	0.30	0.67	3527.5	2.85	g)	
12	0.29	0.65	3516.6	2.85	g)	
13	0.32	0.74	3527.5	2.73		
14	0.32	0.75	3527.5	3.04		

e) $\text{mol}^{-1} \text{l cm}^{-2}$. f) Our X-ray results(see chapter VI). g) The dihedral angle is supposed to increase in the order; $12 > 11 > 10$.¹⁹⁾

angle was roughly estimated from the K-band maxima of these compounds in heptane in the UV spectra, according to the established method.^{7,14)} From the data in Table 2, the strength of the OH... π hydrogen bonding is found to increase with the increase in the dihedral angle. This trend is consistent with those reported by Ōki and Iwamura,⁷⁾ who studied the steric effects on the OH... π hydrogen bonding in 2-arylphenols.

For the intermolecular hydrogen bonding, Yoshida *et al.*³⁾ reported the parallelism between the l/S value and the strength of the hydrogen bonding. This fact is consistent with the dipolar association theory, in which the bond dipole of the solvent associates with the lone pair dipole of the hydrogen bonded system, because the lone pair dipole increases with the strength of the hydrogen bonding.

In case of the OH... π hydrogen bonding, the component of the dipole electric field is in the $\overset{\delta-}{\text{O}} \leftarrow \overset{\delta+}{\text{H}}$ direction, because the charge-transfer plays an important role in this hydrogen bonded system.¹⁵⁾ Furthermore, the oxygen lone pair dipole on the OH group reinforces the component of the dipole due to the charge-transfer. Therefore, the dipolar association theory can also be applied to the intramolecular OH... π hydrogen bonded systems now being studied, as with the ordinary hydrogen bonding.

In contrast to Yoshida's result, it is clear from Table 2 that the proportional correlation between the solvent sensitivity and the strength of the OH... π bonding does not hold in this case; rather, both the α and l/S values seem to be inversely proportional to the A_i , A_i/A_f , v_i , and Δv values.

This result suggests that the solvent sensitivity is not due to the electronic effect. However, it seems that our observation can be reconciled with Yoshida's dipolar association theory by considering the difference between inter- and intramolecular hydrogen bonded system.

For the intermolecular hydrogen bonding, such electronic effects as the strength of the hydrogen bonding are important factors in the dipolar association. On the other hand, for the intramolecular hydrogen bonding, the steric effects on the dipolar association seem to play a larger part than the electronic effects, since the OH... π bonded system is fixed in the same molecule by the molecular geometry. This consideration may be justified, because the interdipolar distance greatly affects the dipolar association energy, according to the Keesom equation.¹⁶⁾ Therefore, the lack of the correlation proposed by Yoshida *et al.* can be interpreted by assuming that the steric effects are so great that the electronic effects are masked.

By comparing the solvent sensitivity for the compound pairs of 1 and 7, 8 and 10, 9 and 11, it is noted that the nitrophenols (7, 10, and 11) show α and $1/S$ values larger than those for the corresponding phenols without the nitro group (1, 8, and 9) (see Table 2). The electron withdrawing nitro substituent produces a stronger OH... π hydrogen bonding, but does not greatly alter the stereo-chemical environment around the dipole of the OH... π bonded system. For these pairs of compounds, therefore, only the electronic effects can be operative in determining the solvent sensitivity.

This result supports the dipolar association theory.

In order to investigate the steric effects on the dipolar association, both α and $1/S$ values are compared with the structural changes over a group of phenols. As can be seen from Table 2, both α and $1/S$ values appear to decrease with an increase in the dihedral angle; the observed order in the solvent sensitivity for the similar structural class is as follows; $7 > 1 > 2 > 3$, $4 > 5$, $8 > 9$, $10 > 11 \approx 12$, $10 \approx 13 \approx 14$. This suggests that the solvent sensitivity is greatly affected by the steric factors.

From the dihedral angular dependence of the solvent sensitivity, we propose a simplified model with the geometry (I) for the dipolar association between the dipole of the OH... π bonded system (involving the lone pair dipole) and the bond dipole of the solvent molecule, as is shown in Fig. 4.

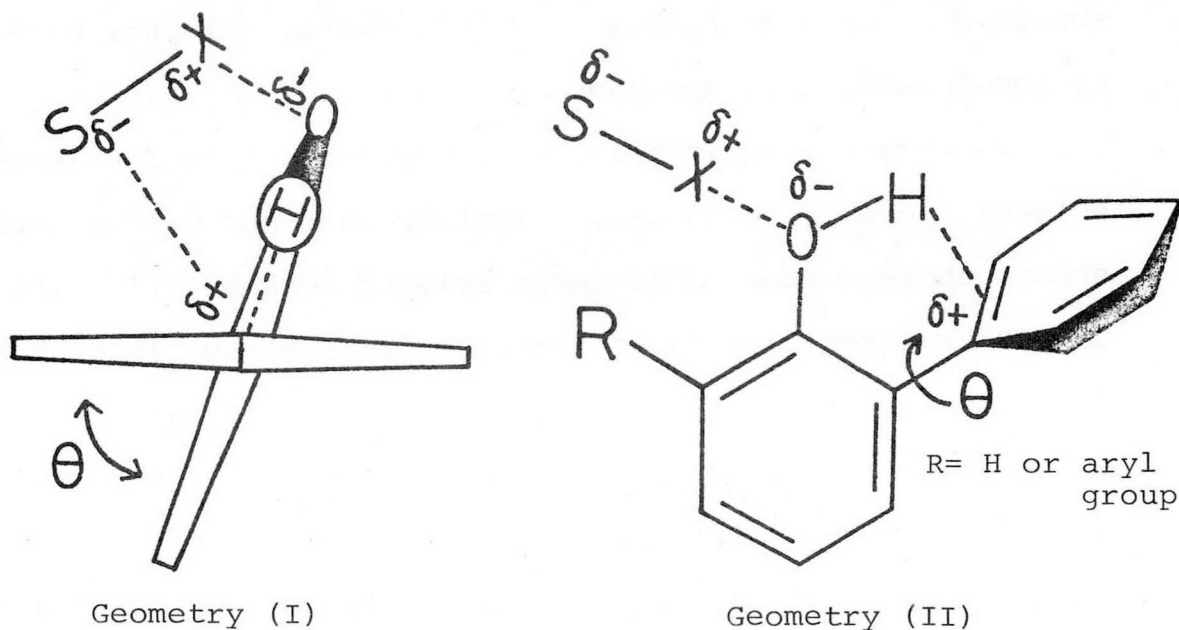


Fig. 4. Schematic representation of the dipolar association between the bond dipole of the solvent and the dipole of the OH... π bonded system. S-X; solvent, θ ; dihedral angle.

This model is based on a specific 1:1 solvent-solute interaction. The geometry (I) indicates that the approach of the bond dipole of the solvent to the dipole of the OH... π bonded system is made difficult by the larger dihedral angle, since the steric repulsion between the solvent molecule and the proton acceptor ring becomes more severe with an increase in the dihedral angle.

As another model, the geometry (II), in which the positive end of the dipole of the solvent associates with the negative end of the dipole (the lone pair electrons) of the OH... π bonded system, is also shown in Fig. 4. This model seems to be consistent with the Bellamy's theory. In this geometry, however, there are no steric effects on the solvent-solute association, and so Yoshida's correlation should be held throughout all the phenols studied here. This model is supposed to be significant only in a protic solvent, because of the formation of hydrogen bonding.

In competitive intramolecular hydrogen bond formation between the OH... π and OH...O systems in 4 and 6, the latter system shows a remarkably large solvent sensitivity. The OH...O hydrogen bonding in the biphenyl skeleton is possible only in either a planar or nearly planar conformation,^{6b)} while the OH... π hydrogen bonding is favored for the conformation in which the dihedral angle becomes larger.⁷⁾ For example, 2-arylphenol (5), with a nearly perpendicular conformation, shows no OH...O bonding, but a strong OH... π interaction (see Table 2). Furthermore, in general, the strength of the OH...O bonding is greater than that of the OH... π bonding

(see Table 2). Therefore, the trend in the observed solvent sensitivity can be interpreted in terms of both electronic and dihedral angular effects, supporting the model with the geometry (I).

Another steric factors which can affect the solvent sensitivity is the presence of alkyl substituents in the proton acceptor ring. In addition to the dihedral angular effects, an *ortho* methyl group in the proton acceptor ring also hinders the bond dipole of the solvent from approaching the dipole of the OH... π bonded system, as is anticipated from the geometry (I). Furthermore, the introduction of the alkyl group to the *para* position of the proton acceptor ring (I3 and I4) produces little variation in the solvent sensitivity (see Table 2). If the dipolar association exists in the geometry (II), the dipolar association will be made difficult by the presence of the *para* alkyl group, because the *para* alkyl group on the opposite side of the OH... π bond is expected to hinder the approach of the solvent molecule (the positive end of the dipole) to the lone pair electrons on the oxygen atom (the negative end of the dipole). Therefore, the absence of any effects of the *para* alkyl group on the solvent sensitivity agrees with the geometry (I), because the alkyl group at the *para* position is well removed from the site of the dipolar association.

Effects of Temperature on the Solvent Shifts.

According to the Keesom equation, the dipolar association is expected to be affected not only by the steric effects but also by the temperature effects. Table 3 and Fig. 5

Table 3. Temperature effects on the OH... π and OH...O frequencies in CCl₄

1/T(°K)	I	6		8	10	11	12	13	14
		OH...O	OH... π						
3.73	3561.2	3435	3557.3	3550.4	3530.0	3520.7	3512.6	3523.0	3522.1
3.48	3563.0	3438	3559.3	3553.0	3531.1	3523.9	3514.8	3524.5	3524.8
3.24	3564.8	3441	3562.0	3555.7	3532.0	3527.5	3516.6	3527.5	3527.5
3.05	3565.7	3444	3564.4	3556.4	3533.9	3528.1	3517.5	3528.7	3528.4

show the effects of temperature on the frequencies of $\nu_{\text{OH}} \dots \pi$ and $\nu_{\text{OH}} \dots \text{O}$ in CCl_4 .

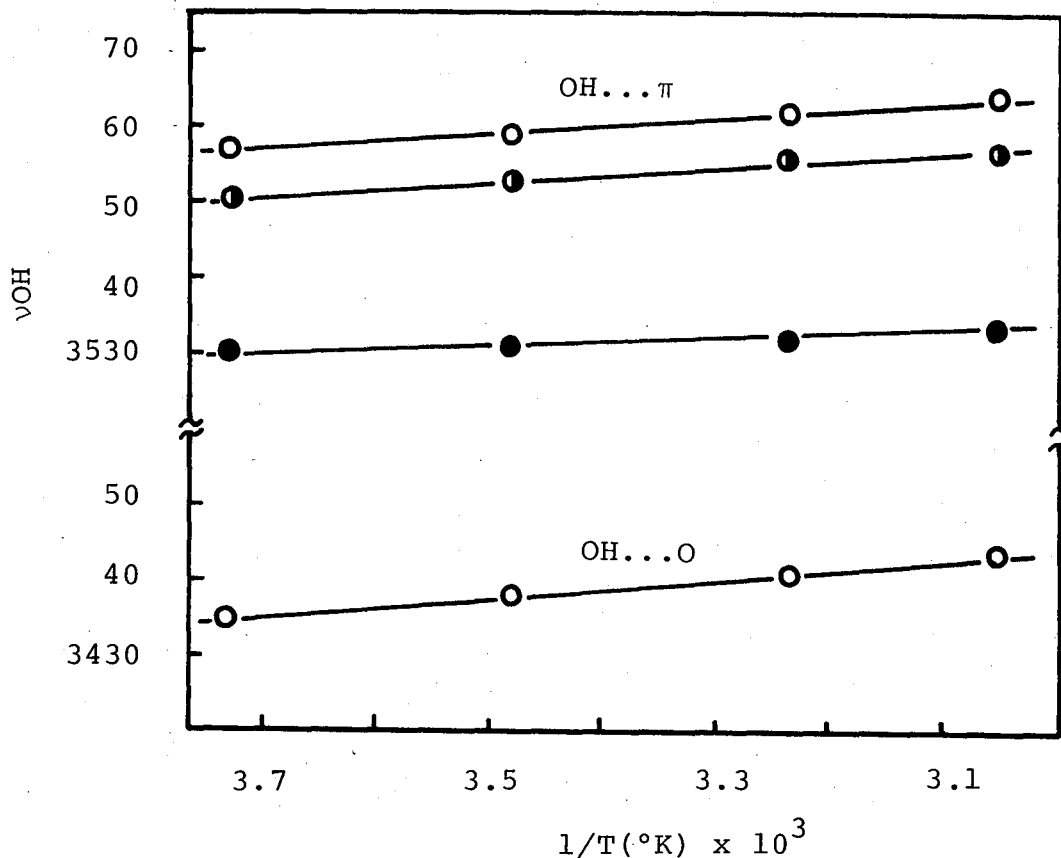


Fig. 5. Plots of $\nu_{\text{OH}} \dots \pi$ and $\nu_{\text{OH}} \dots \text{O}$ vs. $1/T(^{\circ}\text{K})$.

6(○), 8(◐), 10(●).

As the temperature rises, the frequency increases. This phenomenon was often observed in determining the enthalpy for the intermolecular hydrogen bonded system. In the vapor phase measurements, the bonded OH frequencies were found to remain constant with a wide range of temperatures.³⁾

This suggests that the strength of the hydrogen bond itself is not affected by the variation of temperatures. Therefore,

the temperature effects can be interpreted by assuming that the dipolar association is weakened at higher temperature. In other words, the higher temperature causes the desolvation in the hydrogen bonded system arising from the thermal movement. This result again supports the dipolar association theory.

PMR Spectra. The chemical shifts (δ) of the PMR spectra of 2,6-diphenylphenol (8) in CCl_4 , in benzene- d_6 , and hexafluorobenzene and the solvent shifts ($\Delta\delta = \delta_{\text{CCl}_4} - \delta_{\text{C}_6\text{D}_6}$ or C_6F_6) are given in Table 4. These spectra are shown in Fig. 6. For comparison, this Table also includes the IR frequency shifts in these solvents. Compound (8) with a single polar site was selected for this study, because the aromatic solvent-induced shifts (ASIS) become more complex for a compound with multiple polar sites.²⁰⁾ The observed ASIS are due to the dipolar association of the aromatic solvent with the $\text{OH}\dots\pi$ bonded system, not to the intermolecular $\text{OH}\dots\pi$ hydrogen bond formation,²¹⁾ since these IR shifts follow a common pattern obtained for other inert solvents studied here (see Figs. 2 and 3).

It is known²³⁾ that the direction of the ASIS with C_6D_6 is opposed to that with C_6F_6 . As may be seen from Table 3, however, both C_6D_6 and C_6F_6 produced more complex ASIS results. This seeming anomaly can be interpreted by assuming the asymmetric deformation of the geometry for the dipolar association caused by the steric requirement. In order to explain these ASIS results, the schematic representation of the dipolar association between the bond dipoles of C_6D_6 and C_6F_6 molecules

Table 4. Proton chemical shifts (δ) and OH stretching frequencies (ν_{OH}) in CCl_4 , C_6D_6 , and C_6F_6 and solvent shifts ($\Delta\delta$ and $\Delta\nu_{\text{OH}}$) for 2,6-diphenylphenol.

Proton Chemical shifts (ppm)			
	OH proton		
	CCl_4	C_6D_6	C_6F_6
δ	5.12	5.15	5.36
$\Delta\delta$		-0.03	-0.24
2,6-Ring protons ^{a)}			
	CCl_4	C_6D_6	C_6F_6
δ	7.42	7.13	7.43
$\Delta\delta$		0.28	-0.01
OH stretching frequencies (cm^{-1})			
	CCl_4	C_6H_6	C_6F_6
ν_{OH}	3555.7	3549.3	3559.3
$\Delta\nu_{\text{OH}}$		6.4	-3.6

a). Estimated from the δ value of the strongest peak.

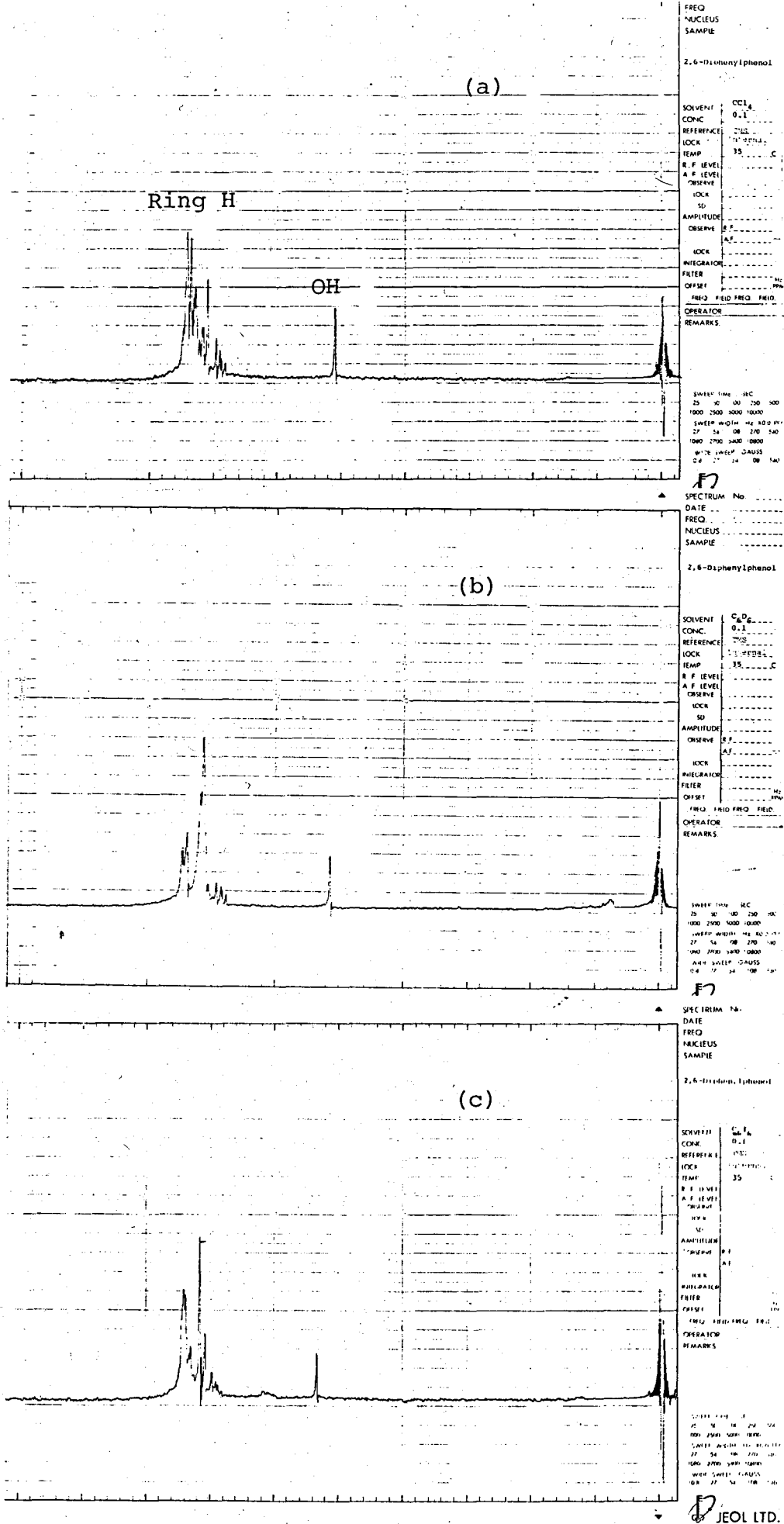


Fig. 6. The PMR spectra of (8) in CCl_4 (a), C_6D_6 (b), and C_6F_6 (c).

and the dipole of the OH... π bonded system is shown in Fig. 7; the direction of the bond dipole of the $\overset{\delta^-}{\text{C}}-\overset{\delta^+}{\text{D}}$ in C_6D_6 shows a sign opposite to that of the $\overset{\delta^+}{\text{C}}-\overset{\delta^-}{\text{F}}$ in C_6F_6 .^{23a)}

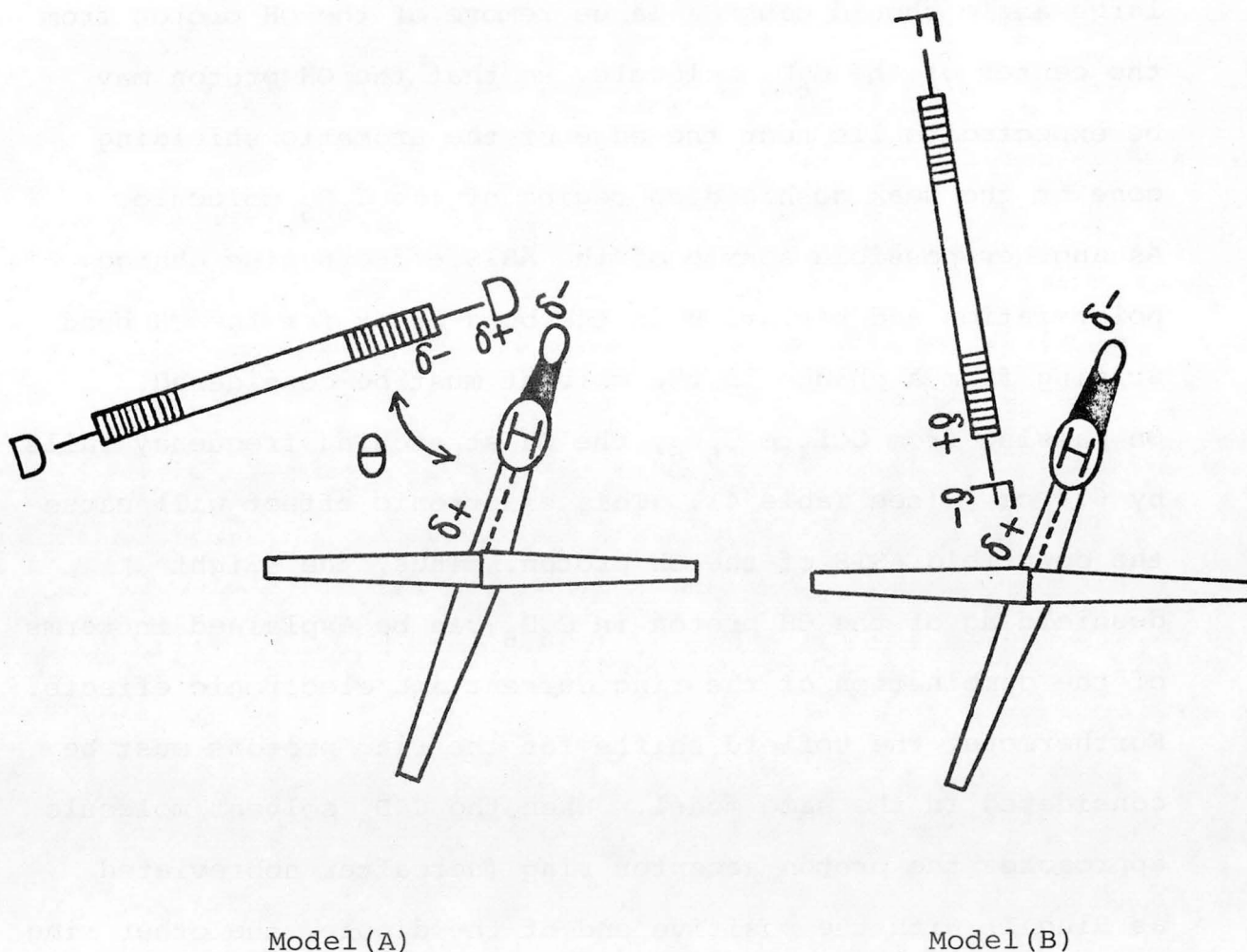


Fig. 7. Schematic representation of the dipolar association between the bond dipoles of benzene- d_6 and hexafluorobenzene and the dipole of the OH... π bonded system.

In C_6D_6 solvent, a slight downfield shift for the OH proton and an upfield shift for the ring protons at the 2,6-positions of the phenol are observed. As is shown in model A,

the π -electron cloud on the C_6D_6 molecule, which is attracted by the dipolar association, will be repelled by the π -electron cloud on the proton acceptor ring, thus increasing the angle, θ , between the dipole of the $OH \dots \pi$ bonded system and the bond dipole of the overlying C_6D_6 solvent molecule. The large angle should cause a large remove of the OH proton from the center of the C_6D_6 molecule, so that the OH proton may be expected to lie near the edge of the aromatic shielding cone or the weak deshielding region of the C_6D_6 molecule. As another possible source of the ASIS effects, the charge polarization and variation in the bond order for the OH bond arising from a change in the solvent must be considered. On passing from CCl_4 to C_6H_6 , the OH stretching frequency falls by 6.4 cm^{-1} (see Table 4). This electronic effect will cause the downfield ASIS of the OH proton. Thus, the slight deshielding of the OH proton in C_6D_6 can be explained in terms of the combination of the ring current and electronic effects. Furthermore, the upfield shifts for the ring protons must be considered in the same model. When the C_6D_6 solvent molecule approaches the proton acceptor ring (hereafter abbreviated as Ring I) with the positive end of the dipole, the other ring (hereafter Ring II) will be further removed from the same C_6D_6 solvent molecule. Therefore, the protons on Ring I will be strongly shielded, and those on Ring II, weakly deshielded. As the average ASIS effects, therefore, the upfield shift was observed in C_6D_6 solvent, supporting the model A.²⁴⁾

On the other hand, C_6F_6 gives a downfield shift in the OH proton and little variation in the ASIS of the ring protons.

It is possible to expect the approach of the fluorine of the C_6F_6 periphery to the positive end of the dipole of the $OH...π$ bonded system, since the van der Waals radius for fluorine (1.35 Å) is almost equal to that for hydrogen (1.2 Å). As is to be anticipated from the model B, the OH proton will be in the deshielding region of the C_6F_6 ring, in spite of the repulsion of the $π$ -electron cloud on the C_6F_6 solvent molecule and the oxygen lone pair electrons. Accordingly, the OH proton should have a downfield shift, although the OH stretching frequency rises by 3.6 cm^{-1} . At the same time, this model shows that the protons on Ring I and Ring II are in the deshielding and shielding region of the C_6F_6 solvent molecule respectively, since the C_6F_6 could be situated along the dipole of the $OH...π$ bonded system. These ASIS, therefore, should cancel each other. In short, the direction of the ASIS can be nicely explained in terms of the model B.

Consequently, it is found that these ASIS results support the model derived from the IR study .

Experimental

Measurement of the Spectra. The infrared spectra were recorded on a JASCO DS-701G grating spectrometer. The spectral slit width under high resolution conditions was 2 cm^{-1} in the region $3200 - 3700\text{ cm}^{-1}$. Sodium chloride cells of 1 and 2 mm thicknesses were used. The concentration of phenols was about 5×10^{-3} M. The frequencies were calibrated by the standard absorption line of water vapor (3568.5 and

3447.2 cm^{-1}). The precision of the measurements on ν_{OH} was about 2 cm^{-1} for the $\text{OH}\dots\pi$ band and about 5 cm^{-1} for the broader $\text{OH}\dots\text{O}$ band. All the measurements were carried out at 35°C. Proton chemical shifts were measured on a JEOL PS-100 spectrometer operating at 100 MHz by using TMS as the internal standard at normal probe temperature (ca. 35°C). Frequency calibration was provided by the use of standard side-band techniques employing an audio-frequency counter. The measured relative chemical shifts are believed accurate to ± 0.1 Hz. The ultraviolet absorption was obtained with a Hitachi 124 automatic recording spectrophotometer in 1.0 cm quartz cells at room temperature. The concentration of the samples in heptane was 10^{-5} - 10^{-4} M.

Materials. Most of the solvents for spectra measurements were spectro-grade solvents and were used without further purification. Bromoform and decalin were purified by known methods.²⁶⁾ Compound (I) was a commercial sample, recrystallized before used. Compounds (2),⁷⁾ (3),⁷⁾ (4),²⁷⁾ (5),²⁸⁾ (6),²⁷⁾ (7),^{6a)} (10),²⁹⁾ (11),³⁰⁾ and (13)³⁰⁾ were prepared according to the published procedures.

2,6-Di-o-tolylphenol (9). Diazotization of 4-amino-2,6-di-o-tolylphenol³⁰⁾ (2.0 g, 6.9 mmol) in a mixture of glacial acetic acid (40 ml) and water (30 ml) at -5 to -10°C afforded 4-diazo-2,6-di-o-tolylcyclohexa-2,5-dienone (1.0 g, 3.9 mmol); mp 137°C (decomp) (from acetone). Reduction of the diazo-ketone (1.0 g) in 2 N hydrochloric acid (40 ml) with hypophosphorous acid (50 ml) gave the phenol (9). Recrystallization from 70% ethanol gave colorless needles;

yield 0.7 g (2.5 mmol); mp 61–63°C. Found: C, 87.4; H, 6.8%.
Calcd for $C_{20}H_{18}O$: C, 87.5; H, 6.6%.

2,6-Diphenylphenol (8). This compound was prepared by a different method from that described in the literature.³¹⁾ The phenol (8) was given by the reduction of 4-diazo-2,6-diphenylcyclohexa-2,5-dienone (mp 130°C (decomp)) according to the procedure described for the phenol (9); mp 101.5–102.5°C (lit,³¹⁾ mp 101°C) (from hexane).

4-Nitro-2,6-bis(2',6'-dimethylphenyl)phenol (I2). 1-Acetoxy-2,6-diiodo-4-nitrobenzene (5.0 g, 12 mmol), 2,6-dimethylbromobenzene (10.8 g, 58 mmol), and copper bronze (15.0 g) were mixed and heated at 200°C for 1 to 2 hr. The reaction mixture was cooled to room temperature and extracted with acetone. The extract was concentrated and chromatographed on alumina to give 1-acetoxy-2,6-bis(2',6'-dimethylphenyl)-4-nitrobenzene. Deacetylation of this product with aqueous hydrogen bromide gave the phenol (I2). Repeated recrystallization from CCl_4 -hexane afforded yellow columns; yield 0.72 g; mp 180–182°C. Found: C, 76.11; H, 6.13; N, 4.01%. Calcd for $C_{22}H_{21}O_3N$: C, 76.06; H, 6.09; N, 4.03%.

4-Nitro-2,6-bis(4'-t-butylphenyl)phenol (I4). To a mixture of *t*-butylchloride (4.3 g, 46.5 mmol) and (I0) (2.0 g, 6.7 mmol) was added powdered aluminium chloride (0.4g, 3 mmol) at 40°C. The mixture was then stirred for 5 hr. A subsequent in the usual way gave a brown solid which was chromatographed on silica gel; elution with benzene-hexane (5:1) afforded the phenol (I4) (1.4 g, 3.5 mmol). Recrystallization from benzene-hexane gave yellow plates; mp 162–164°C. Found:

C, 77.49; H, 7.29; N, 3.50%. Calcd for C₂₆H₂₉O₃N: C, 77.39; H, 7.24; N, 3.47%.

References

- 1) A. Allerhand and P. von R. Schleyer, *J. Am. Chem. Soc.*, 85, 371 (1963).
- 2) L. J. Bellamy, K. J. Morgan, and R. J. Pace, *Spectrochim. Acta*, 22, 535 (1966).
- 3) a) Z. Yoshida and E. Ōsawa, *Nippon Kogyo Kagaku Zasshi*, 69, 23 (1966); b) E. Ōsawa and Z. Yoshida, *Spectrochim. Acta, Part A*, 23, 2029 (1967).
- 4) P. V. Huong and J. C. Lassegues, *Spectrochim. Acta, Part A*, 26, 269 (1970).
- 5) L. J. Bellamy and R. J. Pace, *Spectrochim. Acta, Part A*, 27, 705 (1971).
- 6) a) M. Ōki, H. Hosoya, and H. Iwamura, *Bull. Chem. Soc. Jpn.*, 34, 1391 (1961); M. Ōki and H. Iwamura, *ibid.*, 34, 1395 (1961); b) W. F. Baitinger, Jr., P. von R. Schleyer, and K. Mislow, *J. Am. Chem. Soc.*, 87, 3168 (1965); c) H. Musso and G. Sandrobk, *Ber.*, 97, 2076 (1964).
- 7) M. Ōki and H. Iwamura, *J. Am. Chem. Soc.*, 89, 576 (1967).
- 8) L. J. Bellamy and R. L. Williams, *Trans. Faraday Soc.*, 55, 14 (1959). $\Delta\nu/\nu = [\nu(\text{vapor}) - \nu(\text{solvent})] \times 10^3 / \nu(\text{vapor})$.
- 9) See chapter II
- 10) The dipolar association mechanism in the carbonyl carbon system was found in the correlation between the *G* value and the ¹³C chemical shift of the carbonyl carbon; see chapter IV.
- 11) a) E. A. Cutmore and H. E. Hallam, *Trans. Faraday Soc.*,

58, 40 (1962); b) H. E. Hallam and T. C. Ray, *ibid.*, 58, 1299 (1962).

12) G. C. Pimentel and A. L. McClellan, "The Hydrogen Bond," Freeman, San Fransisco (1960), pp. 82-102.

13) For example, the ν_{max} value was used as a measure of the strength of the OH... π bonding; H. Iwamura and K. Hanaya, *Bull. Chem. Soc. Jpn.*, 43, 3901 (1970).

14) H. Suzuki, *Bull. Chem. Soc. Jpn.*, 32, 1340, 1350, 1357, (1959); 33, 109 (1960).

15) a) Z. Yoshida and N. Ishibe, *Bull. Chem. Soc. Jpn.*, 42, 3254 (1969); b) M. Basila, E. L. Saier, and L. R. Cousins, *J. Am. Chem. Soc.*, 87, 1665 (1965).

16) According to Keesom equation, the association energy E of a pair of dipoles in the vapor state is given by

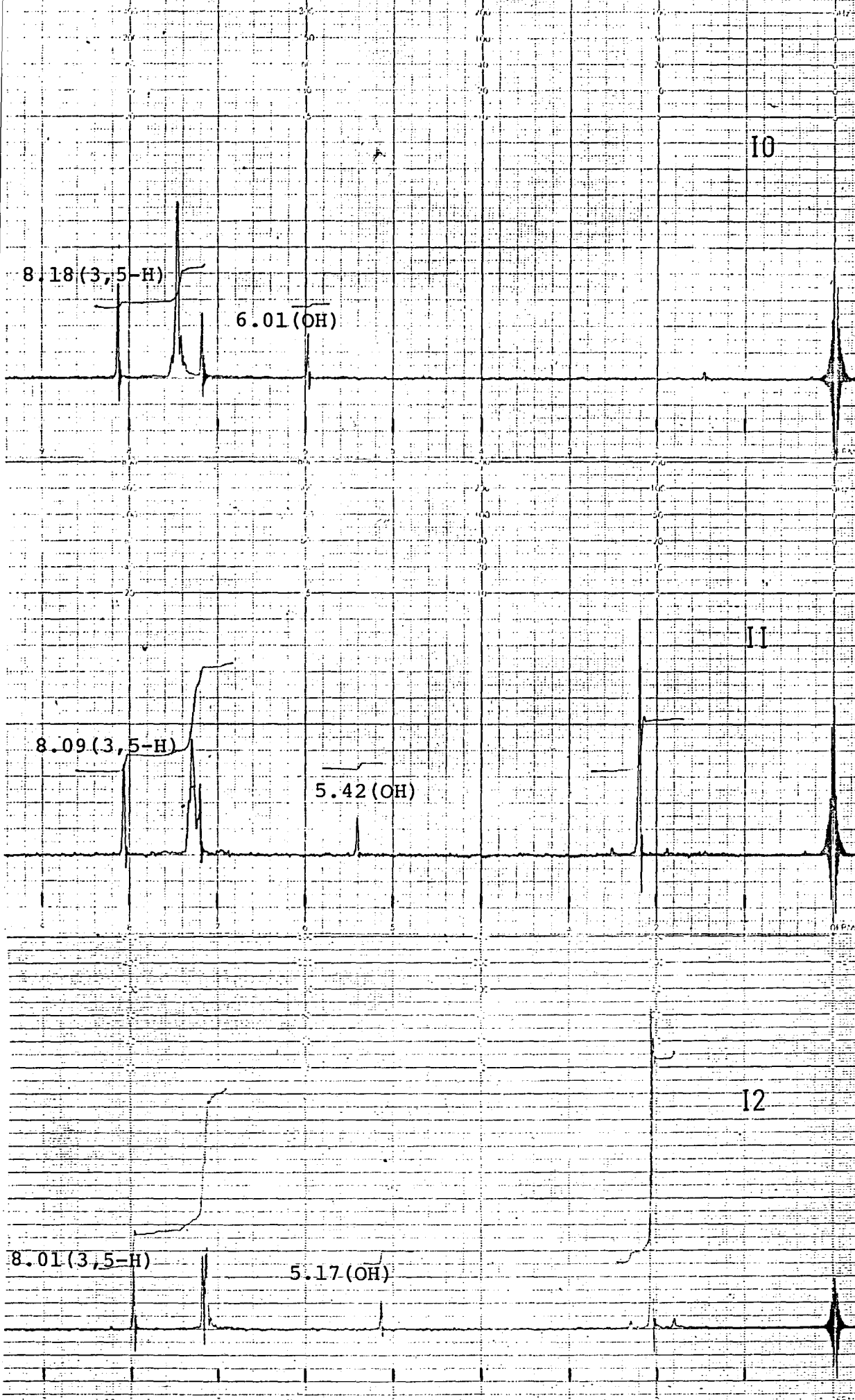
$$E = -2/3 \mu_1^2 \mu_2^2 / R^6 k T$$

where μ_1 and μ_2 are the dipole moment of dipoles 1 and 2, R is the interdipolar distance, k is Boltzman constant and T is absolute temperature; W. H. Keesom, *Z. Physik.* 22, 129 (1921).

17) Similar model of type XH...O-H...OR₂ was found in alcohol/ether complexes in proton donating solvents.^{2,5)}

18) See chapter VI.

19) In the PMR spectra of these phenols in CDCl₃, the upfield shifts for 3,5-protons in the phenol ring and OH proton are observed in going from I0 to I2 (see Fig. 8). This is interpreted in terms of steric interactions between the methyl group(s) and the phenol ring. As the dihedral angle increases, 3,5-protons and OH proton are more deeply



SOLVENT	CDCl ₃			
CONC.	0.1			
REFERENCE	TMS			
LOCK	Internal			
TEMP.	35			
R. F. LEVEL				
A. F. LEVEL				
OBSERVE				
LOCK				
SD				
AMPLITUDE				
OBSERVE	R.F.			
	A.F.			
LOCK				
INTEGRATOR				
FILTER				
OFFSET				
FREQ. FIELD FREQ. FIELD				
OPERATOR				
REMARKS				
SWEEP TIME SEC				
25	50	100	250	500
1000	2500	5000	10000	
SWEEP WIDTH Hz X 0.01 Hz				
27	54	108	270	540
1080	2700	5400	10800	

SOLVENT	CDCl ₃			
CONC.	0.1			
REFERENCE	TMS			
LOCK	Internal			
TEMP.	35			
R. F. LEVEL				
A. F. LEVEL				
OBSERVE				
LOCK				
SD				
AMPLITUDE				
OBSERVE	R.F.			
	A.F.			
LOCK				
INTEGRATOR				
FILTER				
OFFSET				
FREQ. FIELD FREQ. FIELD				
OPERATOR				
REMARKS				
SWEEP TIME SEC				
25	50	100	250	500
1000	2500	5000	10000	
SWEEP WIDTH Hz X 0.01 Hz				
27	54	108	270	540
1080	2700	5400	10800	

SOLVENT	CDCl ₃			
CONC.	0.1			
REFERENCE	TMS			
LOCK	Internal			
TEMP.	35			
R. F. LEVEL				
A. F. LEVEL				
OBSERVE				
LOCK				
SD				
AMPLITUDE				
OBSERVE	R.F.			
	A.F.			
LOCK				
INTEGRATOR				
FILTER				
OFFSET				
FREQ. FIELD FREQ. FIELD				
OPERATOR				
REMARKS				
SWEEP TIME SEC				
25	50	100	250	500
1000	2500	5000	10000	
SWEEP WIDTH Hz X 0.01 Hz				
27	54	108	270	540
1080	2700	5400	10800	

Fig. 8. The PMR spectra of 10, 11, and 12 in CDCl₃.

immersed in the shielding region of 2,6-aryl rings.

20) The orientation of aromatic solvent to alkyl and nitro groups attached to aromatic ring was found in literatures;

a) J. Ronayne and D. H. Williams, *J. Chem. Soc., B*, 540 (1967);

b) Y. Nomura and Y. Takeuchi, *Tetrahedron*, 25, 3839 (1969).

21) Giles' refractive index measurement²²⁾ for detecting intermolecular hydrogen bonding pairs in solution shows no possibility of an intermolecular OH... π bond formation, presumably because the presence of the 2- and 6-phenyl groups of the phenol hinders the approach of aromatic solvent to the OH group. The detail of this refractometric result will be published elsewhere.

22) C. H. Giles and R. B. McKay, *J. Biol. Chem.*, 237 3388 (1962). This method is a well established, simple and sensitive one. (For example, see: Z. Yoshida, E. Ōsawa, and R. Oda, *J. Phys. Chem.*, 68, 2895 (1964).)

23) a) R. D. Bertrand, R. D. Compton, and J. G. Verkade, *J. Am. Chem. Soc.*, 92, 2702 (1970); b) R. S. Armstrong, M. J. Aroney, R. K. Duffin, H. J. Stootman, and R. J. LeFevre, *J. Chem. Soc., Perkin Trans 2*, 3811 (1975); c) K. Nikki, N. Nakahata, and N. Nakagawa, *Tetrahedron Lett.*, 3811 (1975).

24) This model seems to be consistent with the generally accepted model^{20,25)} in which the π -electron cloud on the C_6H_6 solvent molecule orients with the electron deficient center on a solute molecule.

25) J. Ronayne and D. H. Williams, *Annu. Rev. NMR Spectrosc.*, 2, 83 (1969).

26) A. Weissberger, ed, "Techniques of Chemistry,"

Vol 2; "Organic Solvents," 3rd Ed, Wiley-Interscience,
New York (1970).

27) H. Musso and H. G. Matthies, *Chem. Ber.*, 94, 336 (1961).

28) H. Musso and W. Steckelberg, *Ann. Chem.*, 693, 187
(1966).

29) H. B. Hill, *Amer. Chem. J.*, 24, 5 (1900).

30) E. C. S. Jones and J. Kenner, *J. Chem. Soc.*, 1842 (1931).

31) A. Luttringhans and D. Ambros, *Chem. Ber.*, 89, 463
(1956).

CHAPTER II. Effects of Basic Solvents on Intramolecular
OH... π Hydrogen Bonded System. Steric Effects
on Intermolecular Hydrogen Bond Formation of
2,6-Diarylphenols with Base

Abstract. Using a series of 2,6-diarylphenols as the proton donors, the thermodynamics of the competitive hydrogen bond formation between intramolecular OH... π and intermolecular OH...(Base) systems has been studied by examining the OH stretching IR absorption spectra in the presence of proton acceptor bases in CCl₄ solution. The steric effects on intermolecular hydrogen bond formation suggested that the hydrogen bonding-OH group is approximately coplanar with the phenol ring, even in these sterically hindered hydrogen bonded systems. This is also supported by the PMR result. The probable geometry for hydrogen bonding is discussed in relation to the stereochemical environment around the OH... π bonding. It was found that the steric effects on hydrogen bonding can affect not only the enthalpy but also the entropy changes accompanying the formation of intermolecular hydrogen bond.

• Introduction

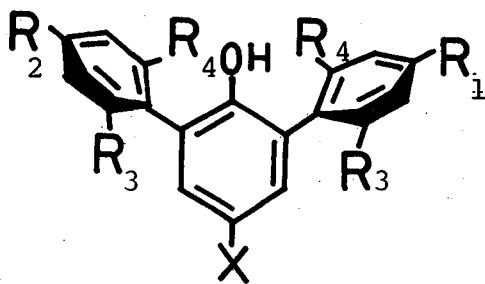
In contrast to the extensive investigation of hydrogen bonding between simple phenols and proton acceptors, much less attention has been paid to the hydrogen bonded systems for the sterically hindered phenols. The quantitative thermodynamic study on the hindered system is even more limited.

Concerning the steric effects on the hindered hydrogen

bonded systems, serious discrepancies have appeared in the literature. Bellamy *et al.*¹⁾ and Rao *et al.*²⁾ reported that the enthalpies of hydrogen bonding are nearly equal for both unhindered and hindered systems, and that the low equilibrium constants in the hindered systems are mainly due to the entropy factors.

On the other hand, Yoshida *et al.*³⁾ found that the steric effects on hydrogen bonding could influence not only the enthalpy but also the entropy changes. In these studies, 2,6-dialkylphenols were used as the sterically hindered proton donors.

In order to reveal the steric effects on hydrogen bonding in the hindered systems, 2,6-diarylphenols (I - I0), in which only intramolecular OH... π hydrogen bonding is possible in CCl_4 , are selected for this study as the sterically hindered phenols. These phenols are expected to cause a marked steric hindrance to the formation of the intermolecular hydrogen bond, owing to the presence of 2,6-diaryl rings.



- | | |
|----|--|
| I | $R^1=R^2=R^3=R^4=H, X=NO_2$ |
| 2 | $R^1=R^2=CH_3, R^3=R^4=H, X=NO_2$ |
| 3 | $R^1=R^2=C(CH_3)_3, R^3=R^4=H, X=NO_2$ |
| 4 | $R^1=R^2=R^3=H, R^4=CH_3, X=NO_2$ |
| 5 | $R^1=R^2=H, R^3=R^4=CH_3, X=NO_2$ |
| 6 | $R^1=C(CH_3)_3, R^2=R^3=R^4=H, X=NO_2$ |
| 7 | $R^1=R^2=R^3=R^4=H, X=H$ |
| 8 | $R^1=R^2=R^3=R^4=H, X=OCH_3$ |
| 9 | $R^1=R^2=R^3=H, R^4=CH_3, X=H$ |
| I0 | $R^1=R^2=R^3=H, R^4=CH_3, X=OCH_3$ |

In this chapter, the thermodynamic parameters, $-\Delta G$, $-\Delta H$, and $-\Delta S$ for the hydrogen bond formation of these phenols to proton acceptors are determined by the use of IR spectroscopy. The steric effects on these hindered hydrogen bonded systems are discussed on the basis of the variation of thermodynamic parameters caused by the structural factors. The probable geometry for these hydrogen bonding is deduced from the IR and PMR results, and the distance and angle of hydrogen bond are roughly estimated using a Dreiding model. Furthermore, the substituent effects on the free energy changes for hydrogen bond formation are briefly discussed.

Experimental

Materials. Most of the solvents were spectrograde reagents and were distilled from calcium hydride immediately before use. Cyclohexanone, benzonitrile, and alkyl nitriles were purified by known methods.⁴⁾

Compounds (1), (2), (3), (4), (5), (7), and (9) have been already identified in Chapter I.

4-Nitro-2-phenyl-6-(4'-t-butyl)phenol (6). This phenol was formed as a by-product in the preparation of (3) (see Chapter I). mp 140–141°C (from benzene). Found: C, 76.14; H, 6.05; N, 4.00%. Calcd for $C_{22}H_{21}O_3N$: C, 76.06; H, 6.09; N, 4.03%.

4-Methoxy-2,6-diphenylphenol (8). Methyl iodide (3g, 0.021 mol) and anhydrous potassium carbonate (3g) were added to a solution of 2,6-phenylhydroquinone⁵⁾ (5.5g, 0.021 mol).

in acetone (40 ml) and the mixture was refluxed at 60–70°C for *ca.* 6h. Work-up gave a viscous oil which was purified by chromatography on silica gel to give the phenol (8) (3.0g, 0.01 mol). Found: C, 82.45; H, 6.00%. Calcd for $C_{19}H_{16}O_2$: C, 82.58; H, 5.84%.

4-Methoxy-2,6-di-o-tolylphenol (10). Reduction of 2,6-di-*o*-tolylbenzoquinone⁵⁾ (2g, 0.007 mol) in glacial acetic acid (120 ml) with zinc powder (4g) afforded 2,6-di-*o*-tolyl hydroquinone (1.4g, 0.005 mol), mp 135–137°C (from benzene). This hydroquinone (1g, 0.004 mol) was treated as described for (8) to give the phenol (10) (0.6g, 0.002 mol), mp 64–66°C (from hexane). Found: C, 82.91; H, 6.55%. Calcd for $C_{21}H_{20}O_2$: C, 82.85; H, 6.62%.

These methoxyphenols 8 and 10 are also obtained in the following procedure. The photolysis with a low-pressure mercury lamp of 4-diazo-2,6-diphenylcyclohexa-2,5-dienone (see Chapter I) and 4-diazo-2,6-di-*o*-tolylcyclohexa-2,5-dienone (see Chapter I) in methanol lead principally to the formations of (8) and (10), with little formations of (7) and (9), respectively. Their physical constants and spectra agreed with those obtained from the ordinary method.

Measurement of the spectra. All the IR spectra were recorded on a JASCO DS-701G grating IR spectrometer, except for the case of the data listed in Table 5, which were obtained with a JASCO DS-402G spectrometer. The conditions for determination of the spectra were the same as in Chapter I. Concentration ranged from 0.003 to 0.008 M for the proton donors and from 0.07 to 0.4 M for the proton acceptors.

The cells (2 mm, CaF₂) were placed in a thermostated air-bath and were permitted to stand for at least 15 min. It was possible to control the temperature in the sample and the air-box within $\pm 1.0^\circ\text{C}$ in the range 5.5–20.0°C and within $\pm 0.5^\circ\text{C}$ in the range 28.5–55.0°C. The PMR spectra were obtained with a JEOL PS-100 spectrometer (100 MHz) in the same conditions described in Chapter I.

Analysis of the spectra. The equilibrium constants are defined by

$$K = C_1 / C_2 \cdot C_3$$

in which C_1 , C_2 , and C_3 are the concentrations of intermolecular hydrogen bonded complex, free donor (intramolecular OH... π bonded complex), and unbonded acceptor base, respectively.

Also, $C_1 = C'_2 - C_2$ in which C'_2 is the initial concentration of donor, and C_2 can be calculated from the plots of absorbance against concentration for each donor, at temperatures chosen for determination of K (Fig. 1) (5.5°C, 14.0°C, 20.0°C, 28.5°C, 36.0°C, 45.5°C, and 55.0°C). Further, $C_3 = C'_3 - C_1$ in which C'_3 is the initial concentration of acceptor.

In this way, the equilibrium constants were determined, and $-\Delta H$ was obtained from the plots of $\log K$ against $1/T$ (Fig. 2). Using the relations, $-\Delta G = RT \ln K$ and $-\Delta G = -\Delta H + T\Delta S$, the values of $-\Delta G$ and $-\Delta S$ were also obtained. The values of $-\Delta G$ and $-\Delta H$ are probably accurate to $\pm 5\%$ and $-\Delta S$ to ± 1 cal/mol/deg.

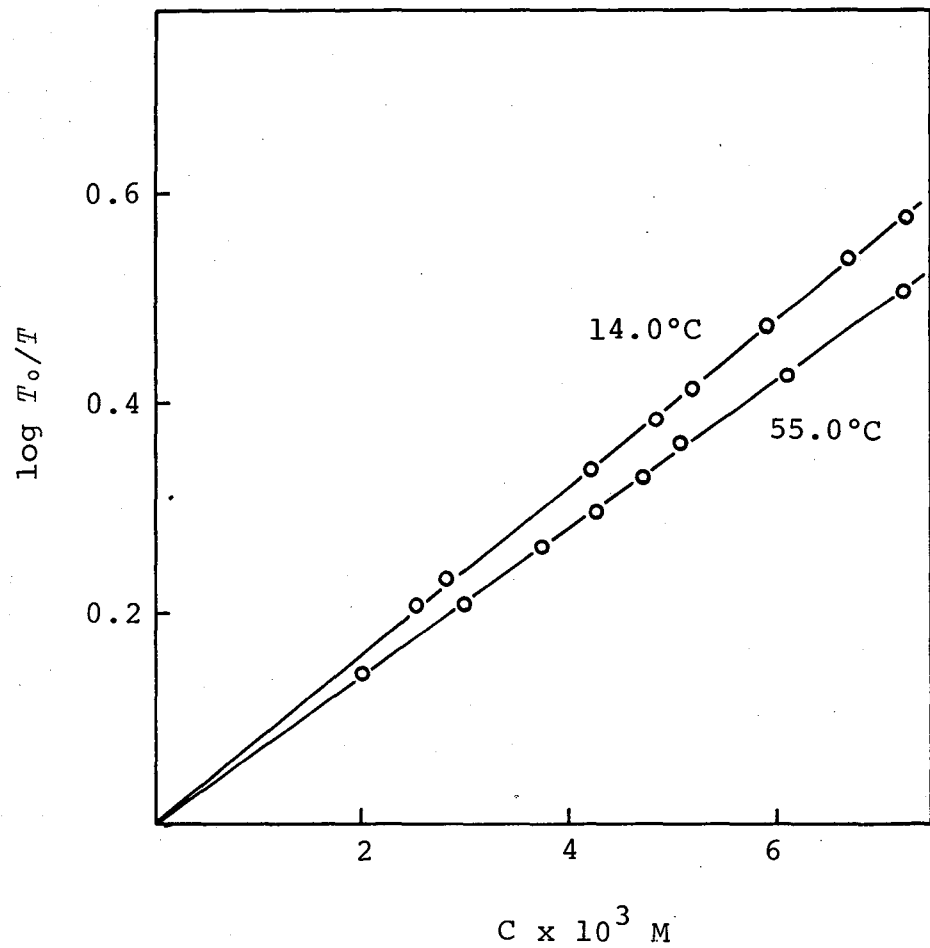


Fig. 1. Plots of absorbance against concentration for (I) at 14.0°C and 55.0°C .

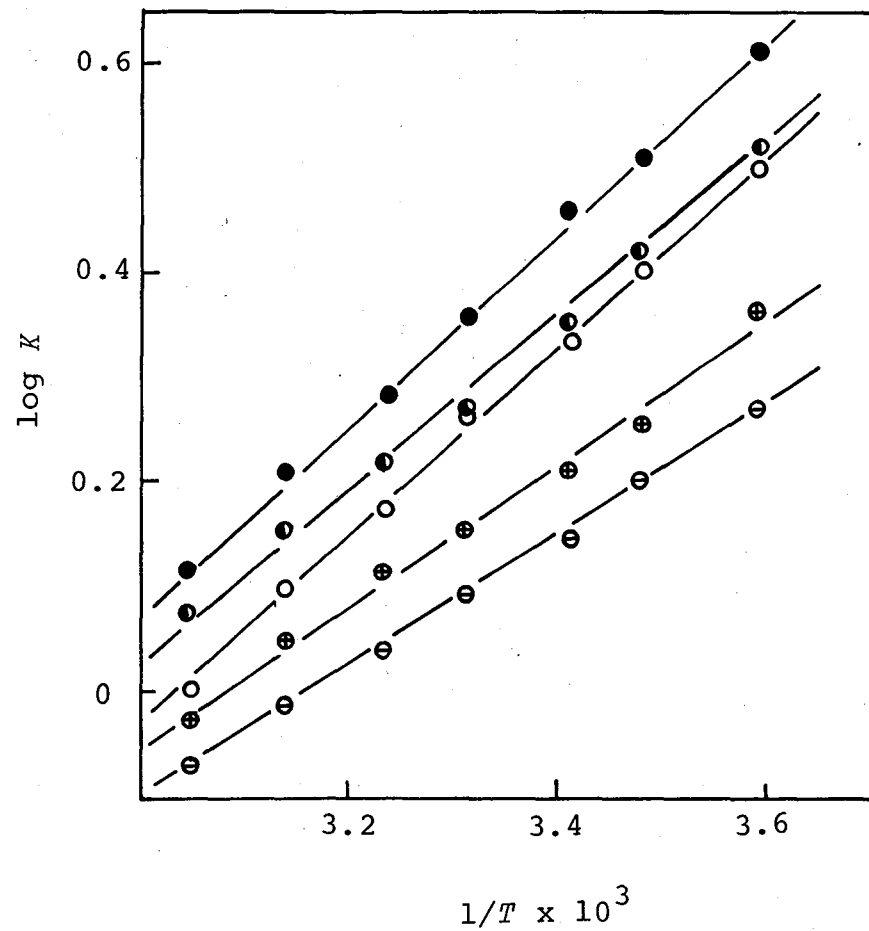


Fig. 2. Plots of $\log K$ against $1/T$ for intermolecular hydrogen bonding of (I)-(5) with dioxane. ○: (1), ⊕: (2), ⊖: (3), ●: (4), ● (with dot): (5).

Results and Discussion

Steric Effects on Hydrogen Bonding. In the presence of proton acceptor base, the OH stretching IR absorption spectra of (I)–(5) in CCl_4 solution, were all doublets, as shown in Fig. 3. The IR spectra show that there is a competition between intramolecular $\text{OH}\cdots\pi$ and intermolecular $\text{OH}\cdots\text{B}(\text{Base})$ hydrogen bonds.

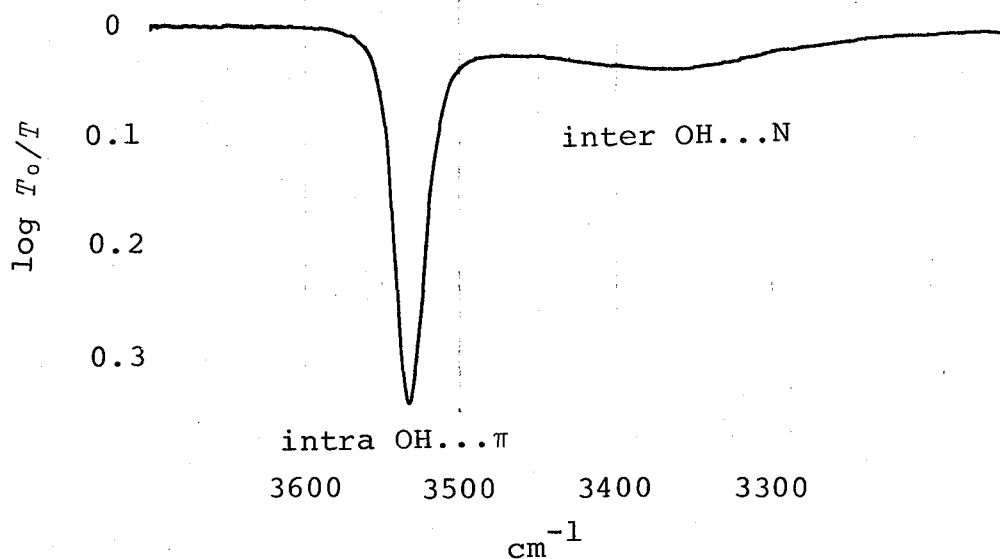


Fig. 3. OH stretching absorption spectrum (ABS measurement) of 4-nitro-2,6-diphenylphenol (I) (0.00604 M) in the presence of benzonitrile (0.347 M) in CCl_4 .

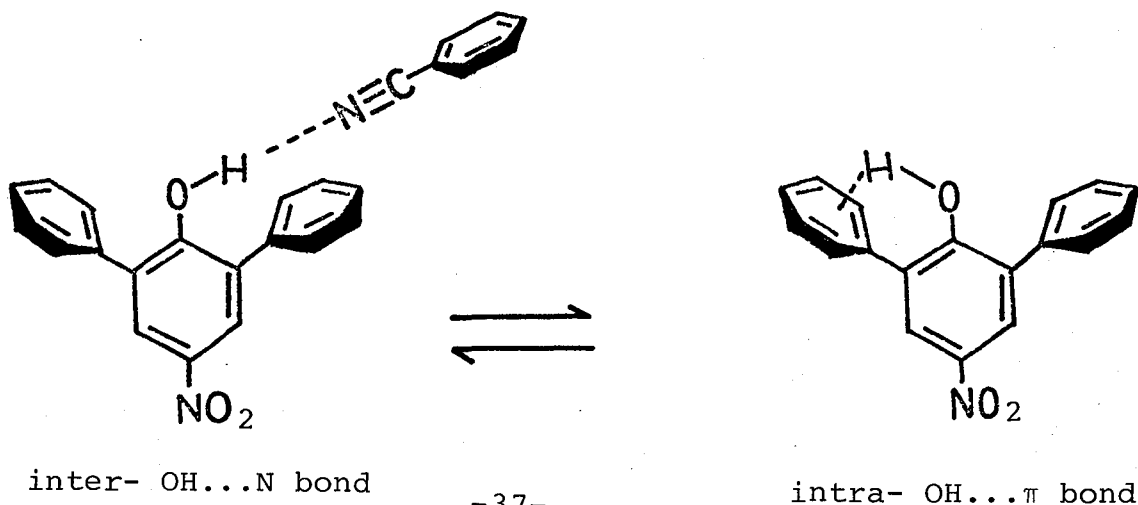


Table 1 lists the measured values of $-\Delta G$, $-\Delta H$, and $-\Delta S$ for the intermolecular hydrogen bond formation of (1)-(5) with the proton acceptors. The OH stretching frequencies, $\nu_{\text{OH...B}}$, and the frequency shifts, $\Delta\nu_{\text{OH}}(\nu_{\text{OH...}\pi} - \nu_{\text{OH...B}})$, are given in Table 2.

From the comparison with a recent thermodynamic data⁶⁾ ($-\Delta G = 1.96$, $-\Delta H = 6.54$, and $-\Delta S = 15.4$) for 4-nitrophenol - benzonitrile system, it is found that the introduction of aryl groups to the 2 and 6 positions of 4-nitrophenol causes a marked decrease of the thermodynamic values. These phenols, therefore, can be considered as a poor proton donors. As can be seen from Table 1, the thermodynamic parameters vary widely from compound to compound. In Series I (1-3), the values of $-\Delta G$, $-\Delta H$, and $-\Delta S$ decrease in going from 1 to 3, while 2 and 3 give the high $\nu_{\text{OH...B}}$ frequencies and the small $\Delta\nu_{\text{OH}}$ shifts as compared with 1. It seems that the thermodynamic values decrease with the increasing bulkiness of the 4'-alkyl group. This suggests that the presence of 4'-alkyl group hinders the approach of the proton acceptor molecule to the hydroxyl group and that the hydrogen bonding-OH group is coplanar with the phenol ring, or at least close to it, even in these hindered hydrogen bonded systems. If the OH bond is markedly twisted away from the plane of the phenol ring, the steric effects of 4'-alkyl group on the hydrogen bond formation become insignificant, because the proton acceptor molecule is further removed from the 4'-alkyl group. Furthermore, the ν_{OH} spectrum of 4-nitro-2-phenyl-6-(4'-*t*-butylphenyl)phenol (6), unsymmetrical 2,6-diarylphenol, splits into a triplet with the bonded $\nu_{\text{OH...N}}$ peak unusually flat-topped, in the

Table 1. Thermodynamic values for hydrogen bond formation of
I - 5 with proton acceptors

Proton acceptor		1	2	3	4	5
DMSO	$-\Delta G$ ^{a)}	2.00	1.53	1.45	2.10	2.00
	$-\Delta H$ ^{b)}	5.98	4.79	4.69	5.51	5.30
	$-\Delta S$ ^{c)}	13.2	10.8	10.7	11.3	10.9
Benzonitrile	$-\Delta G$	0.12	0.09	-0.06	0.19	0.15
	$-\Delta H$	4.11	3.04	2.65	4.07	4.00
	$-\Delta S$	13.2	9.8	9.0	13.0	13.0
THF	$-\Delta G$	0.57	0.36	0.32	0.62	0.60
	$-\Delta H$	5.10	4.47	4.26	4.73	3.83
	$-\Delta S$	15.0	13.6	13.1	13.6	10.7
Dioxane	$-\Delta G$	0.39	0.22	0.13	0.49	0.42
	$-\Delta H$	4.37	3.17	2.93	4.25	3.55
	$-\Delta S$	13.2	9.8	9.3	12.5	10.4
Cyclohexanone	$-\Delta G$	0.57	0.34	0.24	0.69	0.71
	$-\Delta H$	4.76	3.11	2.84	4.33	3.87
	$-\Delta S$	13.9	9.2	8.6	12.1	10.5

a) Kcal/mol. b) Kcal/mol. c) cal/mol/deg.

Table 2. Frequencies^{a)} and frequency shifts due to hydrogen bond formation at 28.5°C.

Compound	Dioxane	THF	Benzonitrile	
1	$\nu_{\text{OH...B}}/\text{cm}^{-1}$	3285	3210	3360
	$\Delta\nu_{\text{OH}}/\text{cm}^{-1}$	247	322	172
2	$\nu_{\text{OH...B}}/\text{cm}^{-1}$	3305	3235	3375
	$\Delta\nu_{\text{OH}}/\text{cm}^{-1}$	223	293	153
3	$\nu_{\text{OH...B}}/\text{cm}^{-1}$	3295	3225	3390
	$\Delta\nu_{\text{OH}}/\text{cm}^{-1}$	233	303	138
4	$\nu_{\text{OH...B}}/\text{cm}^{-1}$	3310	3230	3355
	$\Delta\nu_{\text{OH}}/\text{cm}^{-1}$	218	298	173
5	$\nu_{\text{OH...B}}/\text{cm}^{-1}$	3310	3220	3355
	$\Delta\nu_{\text{OH}}/\text{cm}^{-1}$	207	297	162

a) The $\nu_{\text{OH...B}}$ frequencies in DMSO and cyclohexanone were omitted from the Table. In DMSO, the $\nu_{\text{OH...O}}$ component so overlap with ν_{CH} that it is not easy to separate them. The $\nu_{\text{OH...O}}$ in cyclohexanone is too asymmetric to obtain reliable values, although this has been also observed in simple phenol.⁷⁾

presence of benzonitrile in CCl_4 , as shown in Fig. 4.

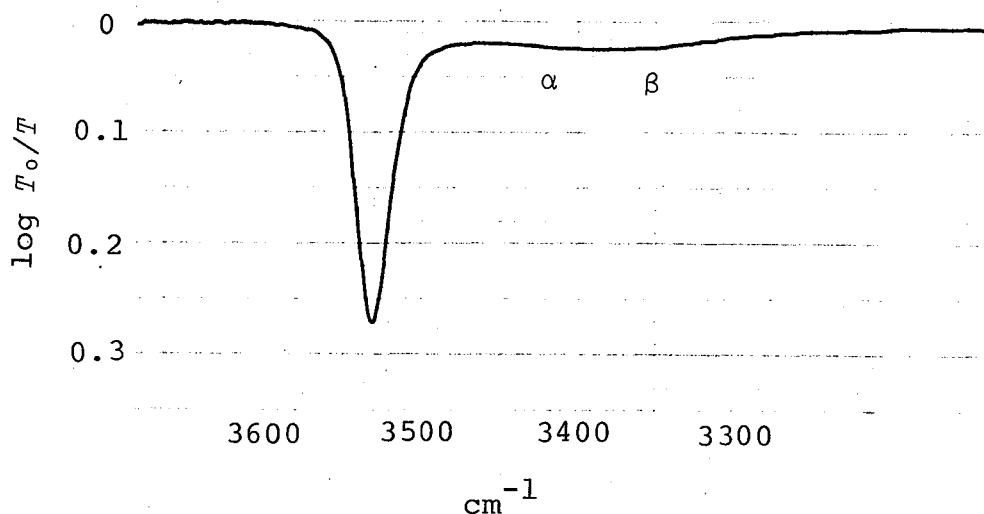
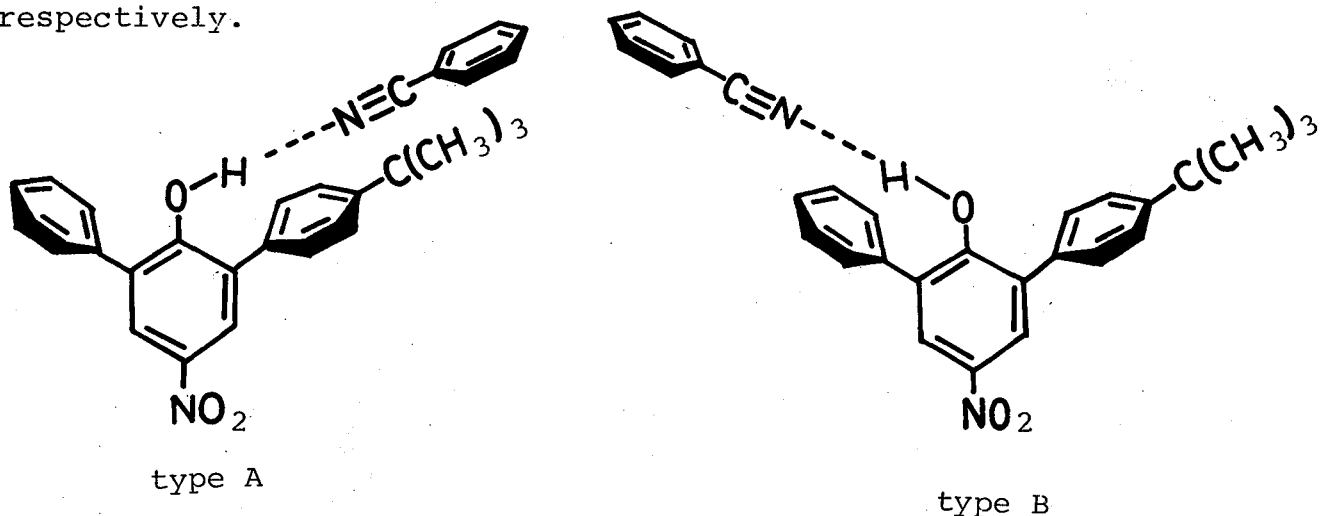


Fig. 4. OH stretching absorption spectrum (ABS measurement) of 4-nitro-2-phenyl-6-(4'-*t*-butylphenyl)phenol (6) (0.00489 M) in the presence of benzonitrile (0.347 M) in CCl_4 .

The close doublet (α and β) in the bonded $\nu\text{OH}\dots\text{N}$ may be taken as due to two kinds of $\text{OH}\dots\text{N}$ hydrogen bonds, again supporting the coplanarity of the OH group. On the basis of the $\nu\text{OH}\dots\text{N}$ frequencies of 1 and 3 listed in Table 2, the α and β bands can be assigned to the OH group associated in type A and type B, respectively.



In the hindered hydrogen bonded systems, the result of the coplanarity of the OH group with the phenol ring is consistent with those of Yoshida *et al.*³⁾ and Tsuno *et al.*⁸⁾ who studied the substituent effect on the hydrogen bonding in 4-substituted 2,6-xylenols by the use of Hammett equation.

In order to investigate the probable geometry for the intermolecular hydrogen bonded system now being studied, the PMR spectra of 2 - 5 were determined in CDCl_3 and benzonitrile with TMS as an internal standard. The chemical shifts of methyl and *t*-butyl protons of these phenols and solvent shifts are tabulated in Table 3.

Table 3. Chemical shifts (δ)^{a)} of methyl and *t*-butyl protons in CDCl_3 and benzonitrile and solvent shifts (Δ) of 2 - 5

Compound	CDCl_3	Benzonitrile	Δ ($\delta_{\text{CDCl}_3} - \delta_{\text{BZ}}$)
2 4'-Me;	2.41	2.29	0.13
3 4'- <i>t</i> -Bu;	1.35	1.28	0.07
4 2'-Me;	2.19	2.25	-0.06
5 2',6'-Me;	2.06	2.11	-0.05

a) In ppm relative to TMS. The error is within $\pm 0.1\text{Hz}$.

In benzonitrile solvent, the upfield shifts for methyl and *t*-butyl protons in 2 and 3 and the downfield shifts for methyl protons in 4 and 5 are observed. The geometrical model for the intermolecular hydrogen bonded system between benzonitrile and these phenols is discussed, assuming that all of these solvent effect on chemical shifts are due to the anisotropy of benzonitrile molecule which is attracted by the intermolecular hydrogen bond formation. In the light of the anisotropy of benzonitrile molecule, the direction of these solvent shifts can be understood by reference to the simplified model for the hydrogen bonding(see Fig. 5).

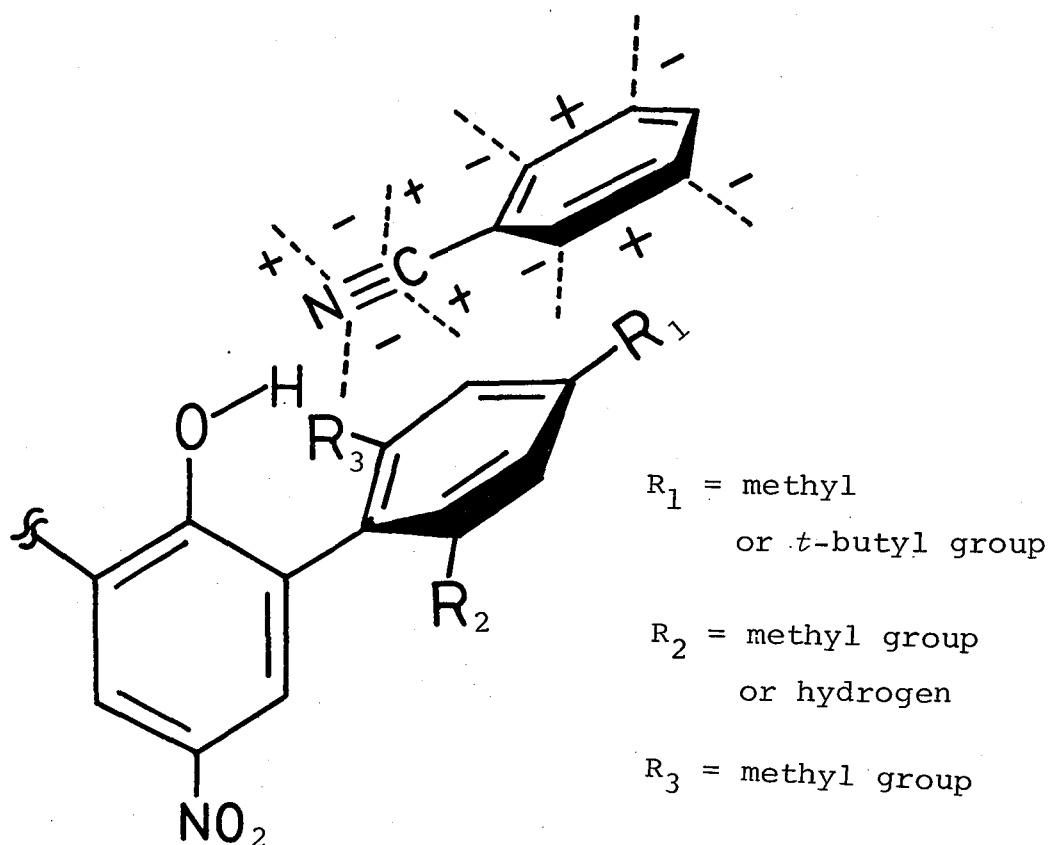
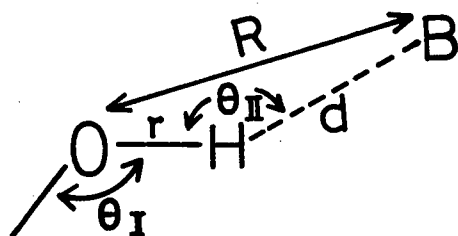


Fig. 5. Schematic representation of the shielding (+) and deshielding (-) regions of benzonitrile molecule which is attracted by the intermolecular hydrogen bond formation.

Thus, the methyl and *t*-butyl groups in 2 and 3 are immersed in the shielding region of the phenyl portion in benzonitrile molecule, while the methyl groups in 4 and 5 lie in the deshielding region of the nitrile portion in benzonitrile molecule. The PMR data, therefore, can be regarded as additional evidence in support of the steric interaction between the 4'-alkyl group and the proton acceptor molecule. Furthermore, the coplanarity of the OH group can also be rationalized in terms of this model.

The hydrogen bonding can be characterized geometrically by the parameters, r , d , R , θ_I , and θ_{II} .



In the intermolecular hydrogen bonding of 1, 2, and 3 with benzonitrile, the parameters were measured on a Dreiding model. This study requires that five important conditions be fulfilled. i) The angle $\theta_I = 109^\circ$ and the distance $r = 0.75 \text{ \AA}$ obtained from the X-ray result of 1 (see Chapter VI) were used. ii) The dihedral angle between the 2 or 6-aryl group and the phenol ring was assumed to be about the same for 2,6-diphenylphenol (7) ($\theta = ca. 60^\circ$; see Chapter I), because the 4-nitro and 4'-alkyl groups will not extremely alter the conformational environment around the $\text{OH} \dots \pi$ bond.

iii) It is reasonable to presume that the closest approach of the benzonitrile molecule to the 2 or 6- aryl ring is van der Waals contacts for interacting groups (or atoms) (van der Waals radius,⁹⁾ H-; 1.20 Å, N^oE; 1.60 Å, average half-width of aromatic rings; 1.77 Å, CH₃-; 1.70 Å, (CH₃)₃C-; *ca.* 3.0 Å¹⁰⁾). iv) Hamilton's equation¹¹⁾ was applied to obtain a reasonable limiting OH...N≡C- distance,

$$d < W_H + W_B - 0.2 \text{ \AA}^{\circ}$$

where W_H and W_B are the van der Waals radii of hydrogen and nitrogen, respectively; $d < 1.20 + 1.60 - 0.2 = 2.60 \text{ \AA}^{\circ}$.

v) The limiting distance for the shortest O...N is $2.50 \pm 0.05 \text{ \AA}^{\circ}$ ¹¹⁾

On the basis of these important conditions, the parameters, d , R , and θ_{II} were estimated (Table 4).

Table 4. Hydrogen bond parameters for OH...N≡C- system

Parameter	(1) and (2)	(3)
At $d = 2.6 \text{ \AA}^{\circ}$,		
$d(\text{H}\dots\text{N})$	2.6 \AA°	2.6 \AA°
$R(\text{O}\dots\text{N})$	$3.0\text{--}3.2 \text{ \AA}^{\circ}$	$3.4\text{--}3.6 \text{ \AA}^{\circ}$
Angle θ_{II}	$140\text{--}150^{\circ}$	$130\text{--}135^{\circ}$
At $d = 2.0 \text{ \AA}^{\circ}$,		
$d(\text{H}\dots\text{N})$	2.0 \AA°	2.0 \AA°
$R(\text{O}\dots\text{N})$	$2.6\text{--}2.8 \text{ \AA}^{\circ}$	$2.6\text{--}2.8 \text{ \AA}^{\circ}$
Angle θ_{II}	$135\text{--}130^{\circ}$	$115\text{--}120^{\circ}$

As is seen from Table 4, when the parameter, $d(\text{H}\dots\text{N}$ distance), is changed from 2.6 \AA to 2.0 \AA , the parameter R becomes the limitation of the shortest $\text{O}\dots\text{N}$ distance (2.5 \AA) (see condition V). In this range of the $\text{H}\dots\text{N}$ distance, the model is consistent with the PMR result (see Table 3). For these hydrogen bonded systems, therefore, the $\text{H}\dots\text{N}$ distance is assumed to be about $2.0 - 2.6 \text{ \AA}$. The values of parameters thus derived may have considerable uncertainty, but the relative values are adopted in the following discussion.

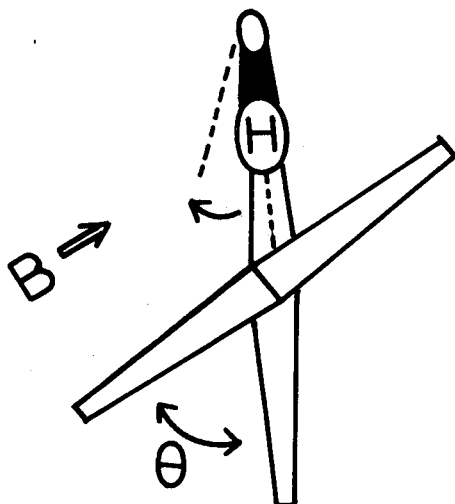
In cases of 1 and 2, the plane of phenyl ring of the overlying benzonitrile molecule is almost parallel to the 2 or 6-aryl ring, while 3 does not present the parallel geometry, because the 4'-*t*-butyl group pushes up the overlying benzonitrile molecule, causing the angle (*ca.* 20°) between two planes of benzonitrile and the 2 or 6-aryl ring. In the result, it is found that the hydrogen bonded system in 3 is more bent than those in 1 and 2, although the marked difference in the $\text{O}\dots\text{N}$ distance is not observed (see Table 4). Clearly, the large angle θ_{II} caused by the steric repulsion between the *t*-butyl group and the 2 or 6-aryl ring weakens the intermolecular hydrogen bonding and produces the marked decrease of $-\Delta G$ and $-\Delta H$ and the increase of $\nu_{\text{OH}\dots\text{B}}$. Furthermore, the decrease of $-\Delta S$ can be mainly attributed to the less restricted rotational and vibrational movement in a weak hydrogen bonded system, owing to the steric effect.

In this model, the differences in the $\text{O}\dots\text{N}$ distance and angle θ_{II} between 1 and 2 are within the error of measurements, but, actually, there is a noticeable steric hindrance of 4'-methyl group in 2 to the hydrogen bond formation, as is

seen from the decrease of the thermodynamic values (see Table 1); in other words, the observed steric effect partly supports the model in which the interacting molecules (benzonitrile and the 2 or 6- aryl ring) oriente in the parallel geometry as closely as their geometry allows, because the van der Waals radius for methyl group (1.70 \AA) is about the same for that of half-width of aromatic ring (1.77 \AA).

On the other hand, Series II (1, 4, and 5) shows the more complex trend of the thermodynamic parameters. The values of $-\Delta H$ and $-\Delta S$ decrease in the order $1 < 4 < 5$, while the values of $-\Delta G$ becomes maximum for 4, although the variation in the thermodynamic parameter is small as compared with Series I (see Table 1). The $\nu_{\text{OH}} \dots \text{B}$ and $\Delta \nu_{\text{OH}}$ do not show a clear trend.

One of the possibilities which reasonably explains the observed trends is shown as follows. In this Series, introduction of methyl group(s) to the 2' and/or 6' positions of proton acceptor ring produces an increase of the dihedral angle between the 2 or 6-aryl ring and the phenol ring (see Chapter I). Taking the above discussed model into consideration, the facility in the proximity of the proton acceptor molecule to the site is supposed to remain unaltered with the change of dihedral angle ($\theta > 60^\circ$). However, the more favorable approach is possible for the smaller dihedral angle, if the OH group is slightly twisted away from the phenol plane, as shown in Fig. 6. The accuracy of the experimental results does not preclude this possibility of the slight twist. At the same time, the strength of intramolecular OH... π bond



B; Proton acceptor base

θ ; Dihedral angle

Fig. 6. Schematic representation of the approach of the proton acceptor base to the OH group.

should also be considered, because the strength of the OH... π bond increases with the increasing of dihedral angle (see Chapter I). It seems that the stronger OH... π bond prevents the formation of intermolecular hydrogen bond. However, the experimental result shows the reverse trend. This electronic effect, therefore, is negligibly small. Furthermore, the approach of the proton acceptor to the OH group will be difficult by the bulkiness of the 2 or 6-aryl group ($\angle 4 < 5$) arising from an internal rotation about the pivot bond of the biphenyl skeleton. Therefore, these steric restriction of approach of the proton acceptor to the OH group should be sufficient to cause a decrease of the $-\Delta G$, $-\Delta H$, and $-\Delta S$ values. The observed trend of $-\Delta G$, however, can not be explained in terms of this steric effect. This trend may best be understood when the competitive effect working in opposition is considered. In addition to the steric effects caused by the 2 or 6-aryl group, the rate and energy of

activation for internal rotation about the pivot bond of the biphenyl skeleton should be considered, because the intermolecular hydrogen bonded system is destroyed by the internal rotation. It is generally accepted that the presence of bulky substituent at *ortho* position(s) of the biphenyl skeleton produces a decrease in rate for the internal rotation, owing to higher energy barrier caused by the bulky substituent. Therefore, the values of $-\Delta G$ will increase in the order $5 > 4 > 1$, if the rate for the internal rotation can only be operative in determining the $-\Delta G$ value. In short, the experimental results could be explained in terms of the combination of the above mentioned factors.

From these considerations of the thermodynamic study in Series I and II, it is thus concluded that for the sterically hindered hydrogen bonded system studied here the steric effects on hydrogen bonding can clearly influence not only the enthalpy but also the entropy changes accompanying the formation of the intermolecular hydrogen bond.

Thermodynamic Parameter Correlations. Pimentel *et al.*¹²⁾ have recently reviewed the linear relationship between $-\Delta H$ and $-\Delta S$ for intermolecular hydrogen bonding of phenols with proton acceptors. The lack of correlation, however, has also been reported for phenol¹³⁾ and *p*-fluorophenol¹⁴⁾ adducts. In the present data, when the values of $-\Delta H$ are plotted against the values of $-\Delta S$, a linear correlation is obtained, except for the case of DMSO (Fig. 7). This suggests that for minor structural changes the stronger hydrogen bonded system with a higher value of $-\Delta H$ requires a more restricted complex

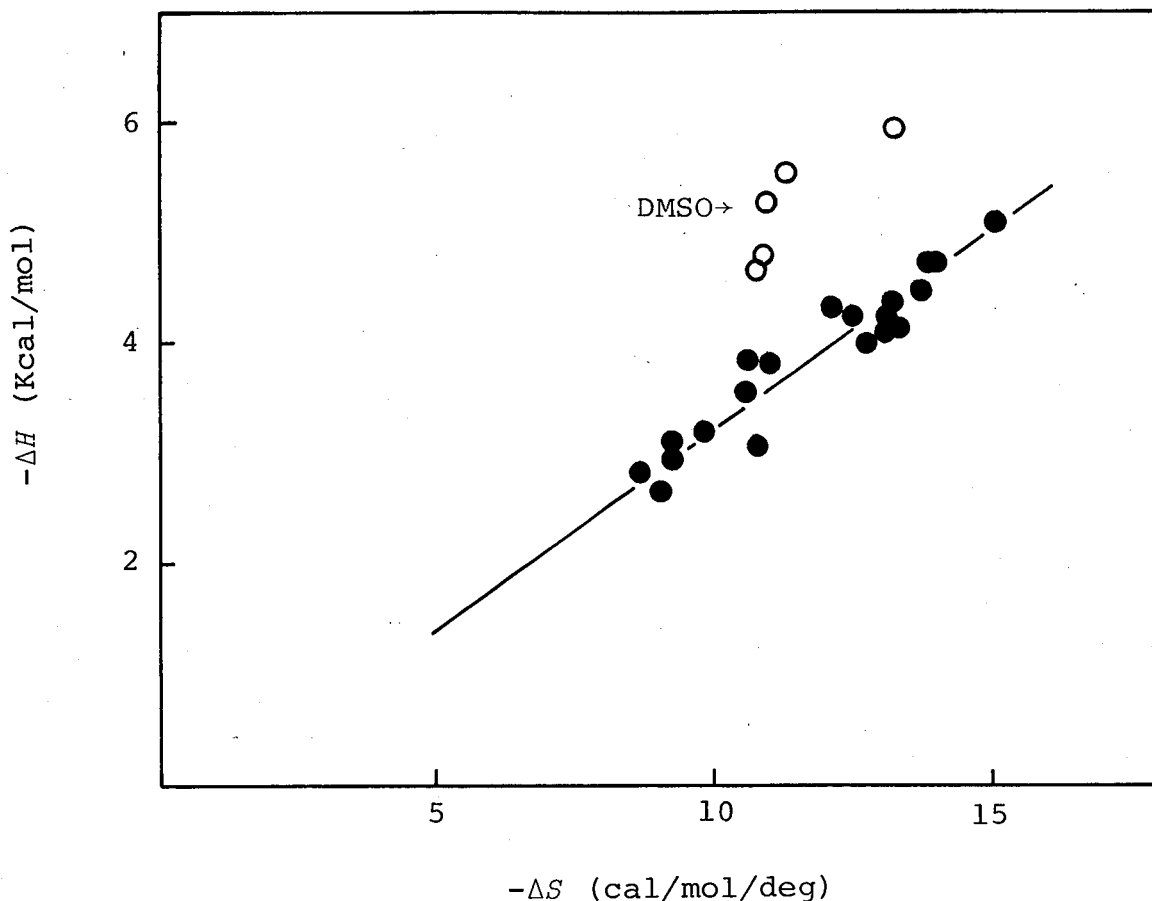
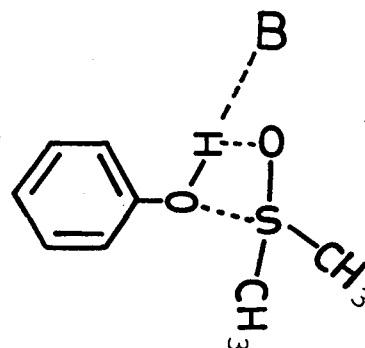


Fig. 7. Correlation between $-\Delta H$ and $-\Delta S$.

configuration so that a larger value of $-\Delta S$ is expected. As anticipated from a β -scale of HBA (hydrogen bond acceptor basicities) proposed by Taft *et al.*,¹⁵⁾ DMSO should produce a largest value of $-\Delta H$ in the bases selected for this study, assuming that the steric effects on the hydrogen bonding are a negligible small. The values of β -scale increase in the order: DMSO(0.752) > cyclohexanone(0.534) > THF(0.523) > benzonitrile(0.409) > dioxane(0.386). Therefore, the deviation from this correlation implies that the values of $-\Delta S$ is smaller than expected from the larger value of $-\Delta H$. Taft *et al.*^{15,16)} also found that DMSO shows the anomalous behavior in plot of $\log K$ vs. ^{19}F chemical shifts for the *p*-fluorophenol - base system and suggested that the dipolar complex between

DMSO and the OH group may exist. If this dipolar complex is true, the entropy change should decrease, owing to more restricted hydrogen bonded system. However, author's experimental results seem not to be consistent with Taft's model.



Furthermore, an examination of Arnett's data on $-\Delta H$ shows that a linear relation between $-\Delta H$ and a β -scale of HBA is found for hydrogen bonding of *p*-fluorophenol with bases (Fig. 8).

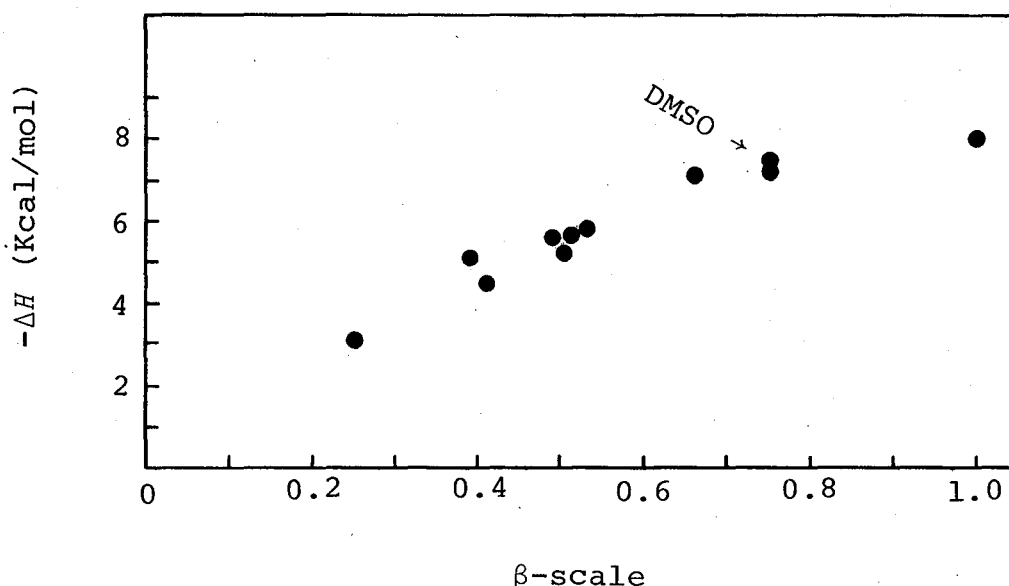


Fig. 8. Plots of $-\Delta H$ vs. β -scale for *p*-fluorophenol - proton acceptors.

In this plot, DMSO fits the correlation line. Therefore, the observed anomaly should be again ascribed to the entropy term, but no satisfactory interpretation of smaller values in $-\Delta S$ can be given. For a limited number of the present data,

a linear correlation between $-\Delta H$ and β -scale does not exist. This can be attributed to the steric effects on the enthalpy term.

Drago *et al.* have shown a general enthalpy - spectral shifts $\Delta\nu_{OH}[\nu_{OH}(\text{free}) - \nu_{OH}\dots B]$ relationship for unhindered hydrogen bonded system.¹⁷⁾ The plot of $-\Delta H$ vs. $\Delta\nu_{OH}$ is shown in Fig. 9. It seems to be no general relationship for the sterically hindered system studied here. Drago's $\Delta H - \Delta\nu$ relationship should be applied to the unhindered system.

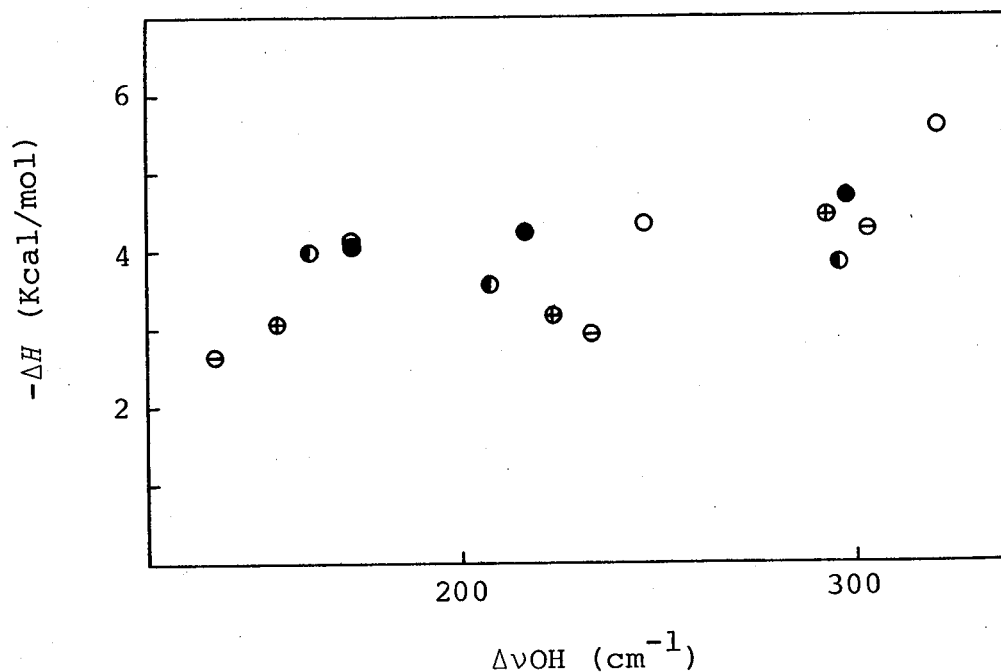


Fig. 9. Plots of $-\Delta H$ vs. $\Delta\nu_{OH}$. ○: 1, ⊕: 2, ⊖: 3, ●: 4, ●: 5.

Effect of Substituents on Free Energy Changes for Intermolecular Hydrogen Bond Formation. Table 5 lists the values of $-\Delta G$ and $\nu_{OH}\dots N$ frequencies for the intermolecular

Table 5. Free energy changes and frequencies^{a)} for hydrogen bonding of 4-substituted 2,6-diarylphenols with alkyl nitriles

Compound		CH ₃ CN	(CH ₃) ₂ CHCN	(CH ₃) ₃ CCN
1	-ΔG Kcal/mol	0.00	0.09	0.14
	νOH..N/cm ⁻¹	3369	3351	3340
7	-ΔG Kcal/mol	-0.60	-0.55	-0.43
	νOH..N/cm ⁻¹	3436	3423	3416
8	-ΔG Kcal/mol	-0.67	-0.58	-0.51
	νOH..N/cm ⁻¹	3442	3428	3422
4	-ΔG Kcal/mol	0.08	0.18	0.26
	νOH..N/cm ⁻¹	3363	3347	3336
9	-ΔG Kcal/mol	-0.43	-0.42	-0.37
	νOH..N/cm ⁻¹	3434	3419	3416
10	-ΔG Kcal/mol	-0.44	-0.57	-0.37
	νOH..N/cm ⁻¹	3440	3431	3419

a) νOH...N at infinite dilution of CCl₄.

hydrogen bonding of 4-substituted 2,6-diarylphenols (I, 4, 7, 8, 9, and 10) with alkyl nitriles. By comparing the values of $-\Delta G$ for the compound pairs of I and 4, 7 and 9, and 8 and 10, it is found that the phenols (4, 9, and 10) with a larger dihedral angle produce a large $-\Delta G$ value as compared with the corresponding phenols (I, 7, and 8). The same trend is observed as was discussed in Series II (see Table 1). As to the 4-substituent effect on the free energy changes, the $-\Delta G$ values increase with the increasing electron-attracting power of the substituent, while the $\nu_{OH \cdots N}$ frequencies decrease. At the same time, the intra-molecular $OH \cdots \pi$ bond should be strengthened. The experimental result shows that the substituent effects play a important role in the inter- rather than the intra-molecular hydrogen bond formation. In general, the π electron systems are considered to be weak proton acceptor as compared with the lone pair electrons (in nitrogen atom of alkyl nitrile).

There is a difference in the entropy term between intra- and inter-molecular hydrogen bond formation. The intermolecular hydrogen bond formation appears to be disfavorable, because of the loss of the degrees of freedom in the rotational and vibrational movement arising from the intermolecular association. Therefore, these two factors should be considered.

Comparison of $-\Delta G$ with $\nu_{OH \cdots N}$ reveals linear correlations for a group of phenols (Fig. 10). This indicates that the $\nu_{OH \cdots N}$ frequency at infinite dilution of CCl_4 is a convenient measure of the stability of the intermolecular $OH \cdots N$ bond. The slopes of the lines are virtually the same

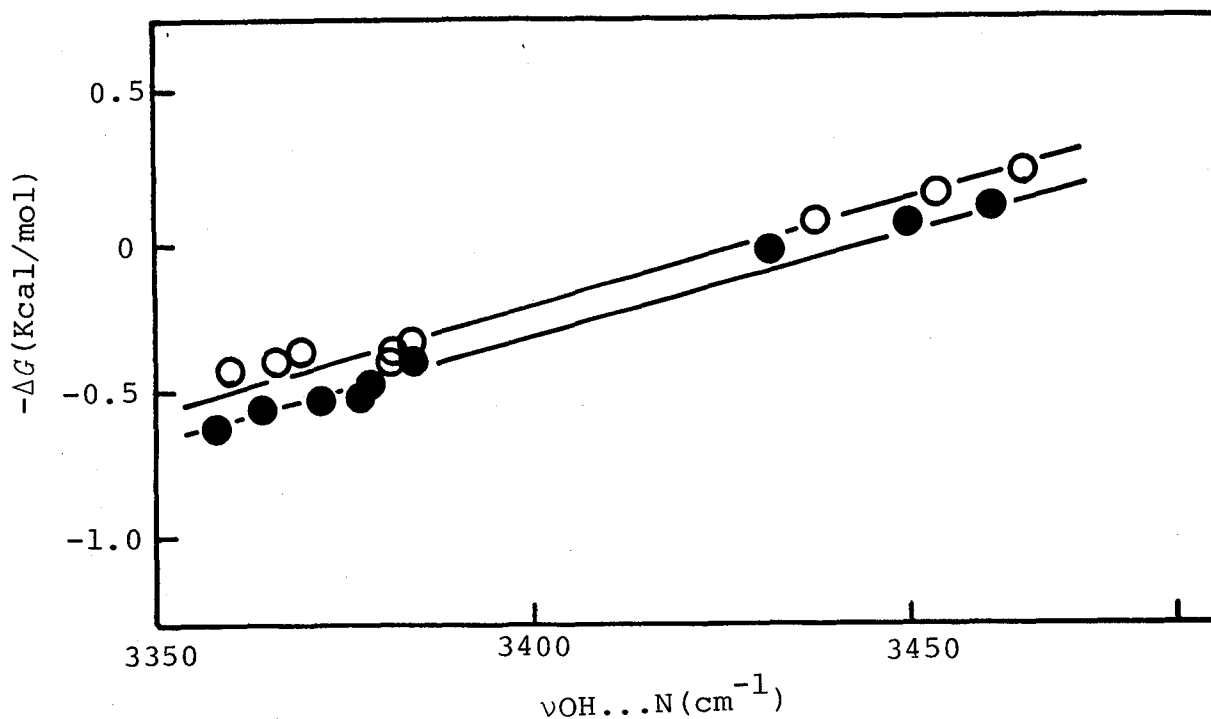


Fig. 10. Relation between $-\Delta G$ and $\nu_{\text{OH}\dots\text{N}}$. ●: (1, 4, and 7)
○: (4, 9, and 10).

and the difference in free energy change between two set of phenols is *ca.* 0.1 kcal/mol. Furthermore, the success of this correlation means that the changes of $-\Delta G$ are attributed to the electronic factors produced by the change of substituent, and there seem to be no extreme steric hindrance to the hydrogen bond formation. In fact, the values of $-\Delta G$ for the different nitriles increase with the base strength of alkyl nitriles. This suggests that the inductive effect of alkyl group in nitrile outweighs the small steric effect. On the assumption that the alkyl group in nitrile is situated outside the π electron cloud of the 2 or 6-aryl ring and that the O-H bond is collinear with the $\text{N}\equiv\text{C}$ - bond, it could be estimated that the H...N distance is longer than 2.0–2.2 Å. This distance is consistent with the proposed model for benzonitrile.

References

- 1) a) Bellamy and Williams, *Proc. Roy. Soc., A* 224, 119 (1960); b) Bellamy, Eglinton, and Morman, *J. Chem. Soc.*, 4762 (1961).
- 2) S. Singth and C. N. R. Rao, *J. Am. Chem. Soc.*, 88, 2142 (1966).
- 3) Z. Yoshida and N. Ishibe, *Bull. Chem. Soc. Jpn.*, 42, 3259 (1969).
- 4) A. Weissberger, ed, "Techniques of Chemistry," Vol 2; "Organic Solvents," 3rd Ed, Wiley-Interscience, New York (1970).
- 5) E. Charles, S. Jones, and J. Kenner, *J. Chem. Soc.*, 1842 (1931).
- 6) I. Jawed, *Bull. Chem. Soc. Jpn.*, 50, 2602 (1977).
- 7) a) Fritzche, *Spectrochim. Acta*, 21, 799 (1965); b) Whetsel and Kagarise, *Spectrochim. Acta*, 18, 315 (1962); c) L. J. Bellamy and R. J. Pace, *Spectrochim. Acta*, 27A, 705 (1971).
- 8) M. Fujio, M. Mishima, Y. Tsuno, Y. Yukawa, and Y. Takai, *Bull. Chem. Soc. Jpn.* 48, 2127 (1975).
- 9) J. Hine, ed, "Structural Effects on Equilibria in Organic Chemistry," Wiley-Interscience, New York (1975), p 47.
- 10) This van der Waals radius was estimated on the basis of that of methyl group.
- 11) P. Schuster, G. Zundel, and C. Sandory, ed, "The Hydrogen Bond," Vol 2, North-Holland Publ., Amsterdam. New York. Oxford (1976). p. 402 and p. 433.
- 12) G. C. Pimentel and A. L. McClellan, *Ann. Revs. Phys. Chem.*, 22, 347 (1971).

- 13) S. Ghersetti and A. Lusa, *Spectrochim. Acta*, 21, 1067 (1965).
- 14) T. S. S. R. Murty, T. M. Gorrie, and P. von R. Schelyer, *J. Am. Chem. Soc.*, 92, 2365 (1970).
- 15) M. J. Kamlet and R. W. Taft, *J. Am. Chem. Soc.*, 98, 377 (1976).
- 16) L. Joris, J. Mitsky, and R. W. Taft, *J. Am. Chem. Soc.*, 94, 3438 (1972); 94, 3442 (1972); G. Gurka and R. W. Taft, *ibid.*, 91, 4794 (1969).
- 17) K. F. Purcell and R. S. Drago, *J. Am. Chem. Soc.*, 89, 2874 (1967); R. S. Drago and T. D. Eply, *ibid.*, 91, 2883 (1969); R. S. Drago, L. B. Parr, and C. S. Chamberlain, *ibid.*, 99, 3204 (1977).

on the effect of basic solvents which produced only the *trans*-form of biphenyl-ols (I - 4). The *cis*-percentage was estimated by application of the Hammett equation to 4-substituted 2,6-diphenylphenols (5 - 9) in which only the *cis*-form is possible in CCl_4 .

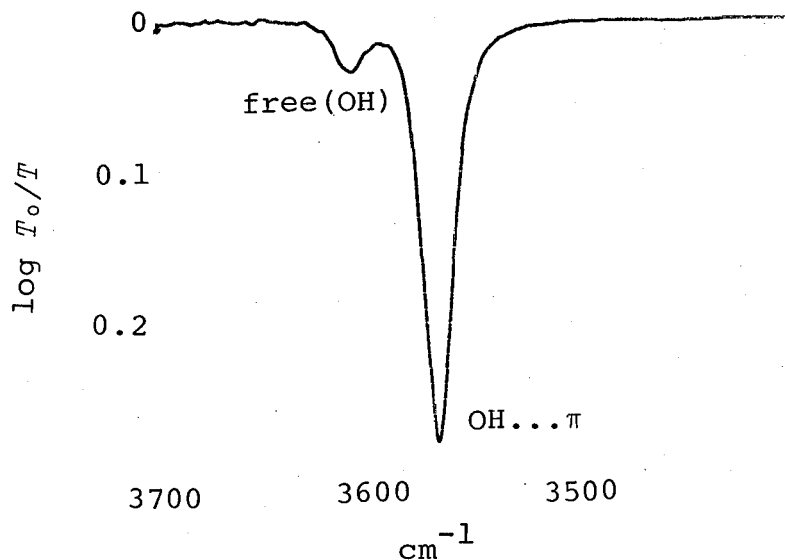
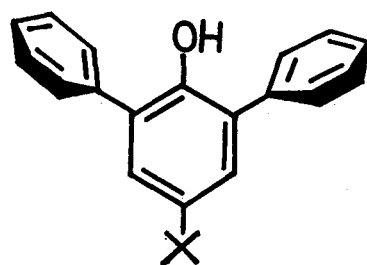
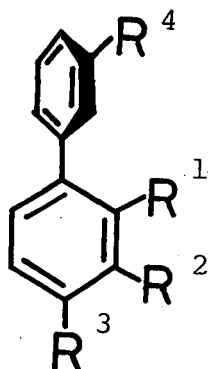


Fig. 1. OH stretching absorption (ABS measurement) of I (0.00497 M) in CCl_4 .



- I
- | | |
|---|---|
| 1 | $R^1 = \text{OH}, R^2 = R^3 = R^4 = \text{H}$ |
| 2 | $R^2 = \text{OH}, R^1 = R^3 = R^4 = \text{H}$ |
| 3 | $R^3 = \text{OH}, R^1 = R^2 = R^4 = \text{H}$ |
| 4 | $R^2 = R^4 = \text{OH}, R^1 = R^3 = \text{H}$ |

- | | |
|---|---------------------------|
| 5 | $\text{X} = \text{NO}_2$ |
| 6 | $\text{X} = \text{CN}$ |
| 7 | $\text{X} = \text{H}$ |
| 8 | $\text{X} = \text{OCH}_3$ |
| 9 | $\text{X} = \text{NH}_2$ |

Results and Discussion

Application of Solvent Effect to the Equilibrium Study.

The integrated intensities of the hydroxyl group of the biphenylols (I - 4) were measured in CCl_4 and in basic solvents as proton acceptors (Table 1). In these basic solvents, the hydroxyl group of the biphenylols is considered to fully interact with the lone pair electrons of the proton acceptor molecules, because the biphenylols (I - 4) exhibit only the single broad band attributed to intermolecular hydrogen bond formation.

Table 1. Integrated intensities and intensity ratios of biphenylols in CCl_4 and basic solvents

Compound	Integrated intensity $A \times 10^{-4} (\text{l mol}^{-1} \text{cm}^{-2})$					
	CCl_4		Solvents			
	<i>trans</i>	<i>cis</i>	$\text{CH}_3\text{C}\equiv\text{N}$	THF	Dioxane	Acetone
I	0.18	1.25	6.83	7.16	7.22	7.57
2	1.37		7.90	8.77	8.32	8.90
3	1.12		7.24	7.52	7.79	7.71
4	2.29		14.58	14.98	15.84	15.74

Compound pair	Integrated intensity ratio				
	$\text{CH}_3\text{C}\equiv\text{N}$	THF	Dioxane	Acetone	Average
A(I)/A(2)	0.86	0.82	0.87	0.85	0.85
A(I)/A(3)	0.94	0.95	0.93	0.98	0.95
A(I)/A(4)	0.47	0.48	0.46	0.48	0.47

Therefore, biphenyl-2-ol is forced into the *trans*-form in these basic solvents.

It is found from Table 1 that the integrated intensity ratios for the compound pairs remain constant regardless of the change of solvent. This trend is consistent with that obtained by Cole *et al.*²⁾ The constancy of integrated intensity ratios for other compounds having a hydroxyl group was tested using data reported in the literature^{3,4)} (Table 2), thus establishing the utility of the method. From this, a calculated integrated intensity due to the *trans*-form of biphenyl-2-ol in CCl_4 , $A'([\text{I}]_{t(\text{trans})})$, can be estimated by the interpolation of the K value in equation (1) into (2), assuming the constancy of the integrated intensity ratios with the change from basic solvent to CCl_4 .

$$[A([\text{I}])/A(n)] = K \text{ (constant), } n = 2 - 4 \quad (1)$$

$$[A(n)]_{\text{CCl}_4} \times K = A'([\text{I}]_t) \quad (2)$$

Thus, equation (3) affords the average percentage of *trans*-isomer.

$$\% \text{ trans} = 100 \times [A([\text{I}]_t)/A'([\text{I}]_t)] = \text{ca. } 16\text{--}17\%, \quad (3)$$

where $A([\text{I}]_t)$ is 0.18 (see Table 1).

In short, application of the solvent effect shows that the percentage of *trans*-isomer results in *ca.* 16–17%.

Table 2. Integrated intensities and intensity ratios of silanols

Compound	Integrated intensity $A \times 10^{-4}$ ($1 \text{ mol}^{-1} \text{cm}^{-2}$)			
	Solvent			
	CHCl_3	CCl_4	C_6H_{12} ^{a)}	CS_2
Ph_2MeSiOH (I)	1.72	1.28	1.09	1.51
PhMe_2SiOH (II)	1.59	1.17	1.03	1.30
Me_3SiOH (III)	1.37	1.00	0.97	1.07
Et_3SiOH (IV)	1.31	0.98	0.83	1.03
Pr^n_3SiOH (V)	1.28	0.96	0.81	0.99
Bu^n_3SiOH (VI)	1.11	0.93	0.79	0.97

Compound pair	Integrated intensity ratio			
	Solvent			
	CHCl_3	CCl_4	C_6H_{12} ^{a)}	CS_2
A (I)/A (II)	1.08	1.09	1.06	1.16
A (I)/A (III)	1.26	1.28	1.24	1.41
A (I)/A (IV)	1.31	1.31	1.31	1.47
A (I)/A (V)	1.34	1.33	1.35	1.53
A (I)/A (VI)	1.55	1.38	1.38	1.56

a) Cyclohexane.

Application of Hammett Treatment to the Equilibrium Study.
 Since 2,6-diphenylphenol (7) possesses only an $\text{OH} \dots \pi$ hydrogen bonded hydroxyl group in CCl_4 ,^{5,6)} an estimate of the integrated intensity due to the hydroxyl group of the *cis*-only

form of biphenyl-2-ol can be obtained from the measured intensity for 2,6-diphenylphenol by applying a correction for the polar effect of an *ortho*-phenyl substituent. Therefore, the σ_o (*ortho*) value for the phenyl substituent was estimated by the use of the Hammett equation.

The values for the OH stretching frequencies of 3- and 4-substituted phenols⁷⁾ were satisfactorily correlated by the Yukawa-Tsuno equation⁸⁾ (equation 4) where (x) is the substituent and the σ constants were taken from ref. 9.

$$\nu_{\text{OH}}(\text{x}) - \nu_{\text{OH}}(\text{H}) = -13.97\sigma - 10.62(\sigma^- - \sigma) + 0.02 \quad (4)$$

(s 0.81 cm^{-1} , corr coeff 0.993)

Also, the results obtained by Ōki *et al.*¹⁾ show that a good Yukawa-Tsuno correlation can be obtained for 2-phenyl-4(or-5)-substituted phenols (equation 5)

$$\nu_{\text{OH}}(\text{x}) - \nu_{\text{OH}}(\text{H}) = -13.62\sigma - 15.45(\sigma^- - \sigma) + 0.356 \quad (5)$$

(s 1.40 cm^{-1} , corr coeff 0.996)

Equation (5) has ρ and r values sufficiently close to those of equation (4) to suggest that the *o*-phenyl substituent has an effectively constant effect. This can justify the interpolation of $\nu_{\text{OH}}(\text{free})$ for biphenyl-2-ol into equation (4) in order to estimate the σ_o value for the *o*-phenyl substituent.

On the assumption that the $(\sigma^- - \sigma)$ term is small compared to σ value, the σ_o value for the *o*-phenyl substituent can be estimated by use of equation (6) ($\sigma_o = ca. 0.2$).

$$3607.4 - 3610.1 = -13.97\sigma - 10.62(\sigma^- - \sigma) + 0.02 \quad (6)$$

Furthermore, a Yukawa-Tsuno equation is applied to the integrated intensities (Table 3) for 4-substituted 2,6-diphenylphenols (equation 7 and Fig. 2). Therefore, multiplication of this slope(0.47) by the σ_o value yields the integrated

intensity, A' , for one *o*-phenyl group (equation 8).

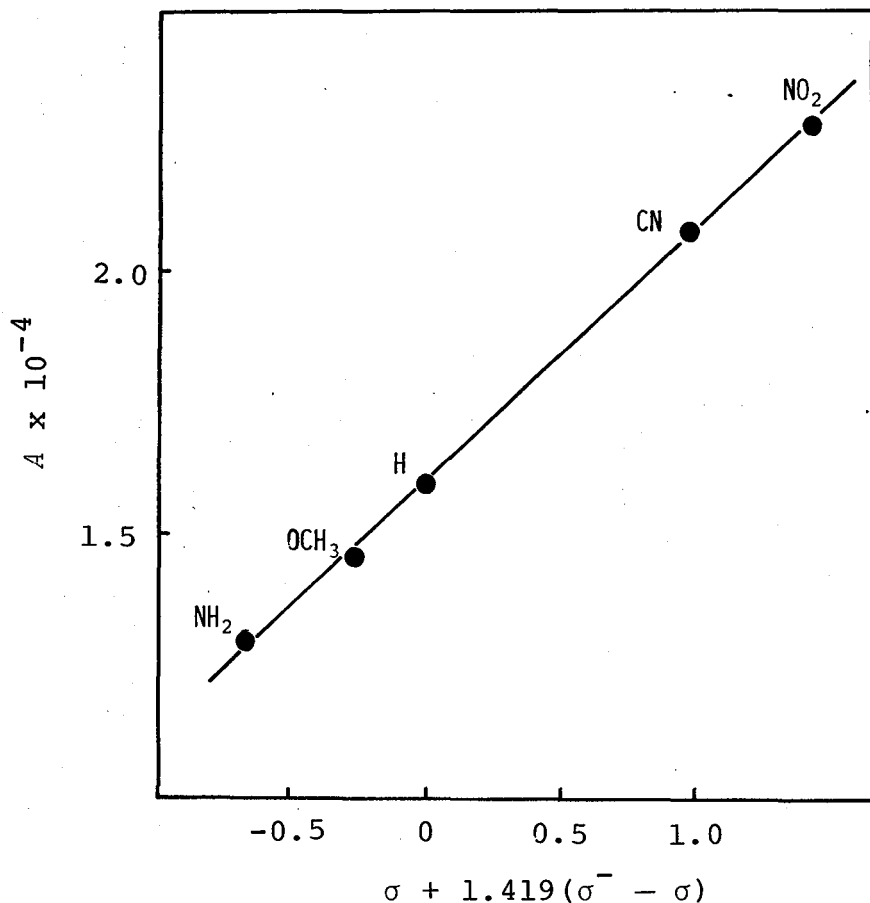


Fig. 2. Yukawa-Tsuno plot for the integrated intensities of 4-substituted 2,6-diphenylphenols.

Table 3. Integrated intensities of 4-substituted 2,6-diphenylphenols

	5	6	7	8	9
$A \times 10^{-4} (1 \text{ mol}^{-1} \text{ cm}^{-2})$	2.28	2.08	1.60	1.46	1.30

$$A_{(x)} - A_{(H)} = 0.47\sigma + 0.667 (\sigma^- - \sigma) + 0.002 \quad (7)$$

$$(\text{ } s \text{ } 0.015A \times 10^{-4} \text{ } 1 \text{ mol}^{-1} \text{ cm}^{-2}, \text{ corr coeff } 1.000)$$

$$A' = 0.47 \times 0.2 = 0.094 \quad (8)$$

From this, it is possible to obtain the percentage of the *cis*-isomer of biphenyl-2-ol according to equation (9).

$$\% \text{ cis} = A(I)_{\text{cis}} \times 100 / [A(7) - A'] = \text{ca. } 83\%. \quad (9)$$

Thus, the percentage of *cis*-isomer was estimated from the Hammett treatment to be *ca.* 83%.

It is concluded that the results of two different methods lead to satisfactory agreement, *i.e.*, the *trans*-isomer is present in *ca.* 16–17% with the *cis*-isomer in *ca.* 83% for biphenyl-2-ol in CCl₄.

Experimental

Measurement of the Spectra. The IR spectra were measured with a JASCO DS-402G grating spectrometer at a spectral slit width of 2 cm⁻¹ at 29°C. Other experimental conditions for recording spectra were the same in Chapters I and II.

Materials. Compounds (1 – 3) were commercial samples, recrystallized before use. Compounds (4)¹⁰ and (9)¹¹ are known. Compounds (5), (7), and (8) have been already identified in the previous chapter.

4-Cyano-2,6-diphenylphenol (6). To a solution of 4-diazo-2,6-diphenylcyclohexa-2,5-dienone⁶ (2.0 g, 7.3 mmol) in acetic acid (40 ml) and hydrochloric acid (1.8 ml) was added potassium iodide (2.6 g, 16 mmol) at room temperature. Work-up in the usual way gave a viscous oil which was purified by chromatography on silica gel to give 4-iodo-2,6-diphenylphenol (1.8 g, 4.8 mmol). The iodo-compound (1.0 g, 2.7 mmol)

was treated with copper(I) cyanide-pyridine [with copper(II) sulphate and *p*-cyanotoluene as a catalyst] under reflux for 9 hr. The usual work-up afforded the phenol (6) (0.5g, 1.8 mmol). mp 159.5–160.5°C (from methanol). Found: C, 84.04; H, 4.91; N, 5.23%. Calcd for C₁₉H₁₃ON: C, 84.11; H, 4.83; N, 5.16%.

References

- 1) M. Ōki and H. Iwamura, *Bull. Chem. Soc. Jpn.*, 34, 1395 (1961).
- 2) A. R. H. Cole, L. H. Little, and A. J. Michell, *Spectrochim. Acta*, 21, 1169 (1965).
- 3) L. J. Bellamy, G. Eglinton, and J. F. Morman, *J. Chem. Soc.*, 4762 (1961).
- 4) O. Nillius and H. Kriegsmann, *Spectrochim. Acta*, 26A, 121 (1970).
- 5) M. Ōki, H. Hosoya, and H. Iwamura, *Bull. Chem. Soc. Jpn.*, 34, 1391 (1961).
- 6) See Chapter I.
- 7) L. L. Ingraham, J. Corse, G. F. Bailey, and F. Stitt, *J. Am. Chem. Soc.*, 74, 2297 (1952).
- 8) Y. Yukawa and Y. Tsuno, *Bull. Chem. Soc. Jpn.*, 32, 971 (1959).
- 9) J. A. Gordon and R. A. Ford, ed, "The Chemist's Companion. A Handbook of Practical Data, Techniques, and References," Wiley, New York (1972), pp. 152–153.
- 10) C. Häussermann and H. Teichmann, *Ber.*, 27, 2108 (1894).
- 11) E. Charles, S. Jones, and J. Kenner, *J. Chem. Soc.*, 1842 (1931).

CHAPTER IV. Effects of Solvents on Carbon-13 Chemical
 Shifts of Carbonyl Carbon Systems

Abstract. Carbon-13 chemical shifts of carbonyl carbons were determined in aprotic solvents having the solvent polarity parameter G . The ^{13}C chemical shifts as a function of solvent are found to be correlated with the G value, except for the case of acetonitrile. The unusual behavior of acetonitrile in the solvent shifts can be interpreted by the anisotropy effect of $\text{C}\equiv\text{N}$ bond arising from the dipolar complex between acetonitrile solvent and a carbonyl-containing solute.

Introduction

Concerning the effects of solvents on carbon-13 chemical shifts of carbonyl carbons, extensive discussions have been done in the literature.¹⁻³⁾ The ^{13}C chemical shifts of carbonyl carbons are sensitive to the change of solvent, particularly for solvents capable of hydrogen bonding toward the lone pair electrons of the carbonyl oxygen. The causative factors for ^{13}C chemical shifts have been separated into three independent terms,

$$\sigma = \sigma_d + \sigma_p + \sigma'$$

where σ_d is the diamagnetic shielding term, σ_p the paramagnetic term, and σ' the contributions from anisotropy in the magnetic susceptibility of neighboring atoms and groups.

In the present work the ^{13}C chemical shift changes of

the carbonyl carbon systems have been studied in a range of aprotic solvents having the G values. The G value is the solvent polarity parameter empirically assigned to the solvents by Allerhand and Schleyer⁴⁾ in order to explain the solvent-induced IR frequency shifts. Some correlation between the ^{13}C chemical shifts and the G value is expected to be found, because the paramagnetic contribution is the dominate factor in producing most ^{13}C chemical shift changes.

Results and Discussion

Table summarizes the changes in ^{13}C chemical shift, together with IR frequency shift, of the carbonyl carbon systems (I) - (III) as a function of solvent. The ^{13}C chemical shifts listed in Table appear to become greater with an increase in the G value. As shown in Figure, when the ^{13}C chemical shifts are plotted against the G value, a linear correlation is obtained, except for the case of acetonitrile. The success of G correlation means that the G value becomes a convenient measure of solvent dependence of ^{13}C chemical shifts and that the ^{13}C chemical shifts are related to the IR frequency shifts [(I) $\delta^{13}\text{C} = 0.24\Delta\nu - 0.02$, (II) $\delta^{13}\text{C} = 0.22\Delta\nu - 0.24$, (III) $\delta^{13}\text{C} = 0.55\Delta\nu - 0.57$, from Table]. Furthermore, this correlation also indicates that the origin of the ^{13}C chemical shifts is mainly due to the paramagnetic term, supporting theoretical argument of ^{13}C chemical shifts,⁵⁾ because the principal factors affecting paramagnetic term are the charge polarization, variation in bond order, and average

Table. The ^{13}C chemical shifts^{a)} and IR frequency shifts^{b)} for carbonyl carbon systems as a function of solvent

Solvents	G value	Acetophenone (I)		Cyclohexanone (II)		Acetone (III) ^{c)}	
		$\delta^{13}\text{C}$	$\Delta\nu$	$\delta^{13}\text{C}$	$\Delta\nu$	$\delta^{13}\text{C}$	$\Delta\nu$
(1) Hexane	44	0.00	0.0	0.00	0.0		
(2) Cyclohexane	49	0.31	1.2	0.13	1.7		
(3) Diethyl ether	64					0.0	0.0
(4) Carbon tetrachloride	69					0.7	2.0
(5) Toluene	74	1.20	6.1	1.58	7.3		
(6) Benzene	80	1.75	7.2	1.64	10.1	1.2	3.8
(7) Dioxane	86	2.54	8.9	2.61	10.6	2.0	5.9
(8) Methyl iodide	89					2.0	5.9
(9) Acetonitrile	93	3.76	10.2	4.07	17.4	4.1	6.0
(10) Dichloromethane	100	2.97	12.0	3.88	18.2		
(11) Chloroform	106	3.40	14.3	4.19	21.0	4.3	9.0

a) $\delta^{13}\text{C}$ (p.p.m.) corresponds to downfield shift from hexane. b) $\Delta\nu$ (cm^{-1}) = $\nu(\text{hexane}) - \nu(\text{solvent})$. c) The ^{13}C chemical shifts taken from Ref.1; $\delta^{13}\text{C}$ and $\Delta\nu$ relative to diethyl ether.

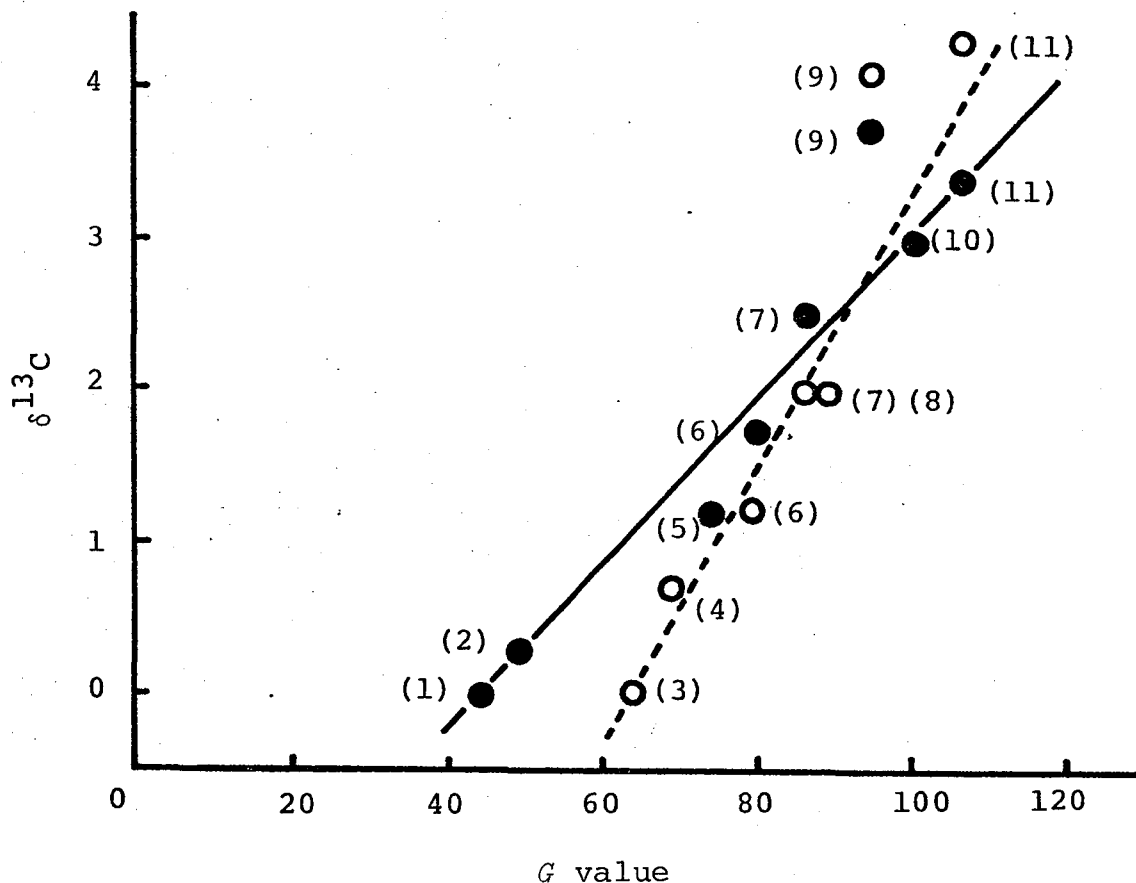
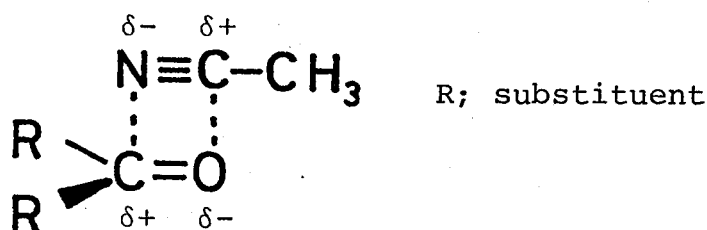


Figure. Correlation between ^{13}C chemical shifts and G value of the solvents (●, acetophenone; ○, acetone).

excitation energy.

As can be seen in Figure, acetonitrile solvent shows a significant deviation. This suggests that the effects other than the paramagnetic contribution might be operative in determining the ^{13}C chemical shift in acetonitrile solvent. In cases where the strong solvent-solute interaction such as local association due to hydrogen bonding or dipolar complex is expected, the ^{13}C chemical shifts may be strongly affected by the magnetic anisotropy of solvent molecule. For this reason, the deviation from the G plot appears to arise from

the anisotropy effect of C≡N bond due to local ordering of acetonitrile molecule around the carbonyl group. This possibility can be interpreted by assuming a dipolar complex as shown in Scheme.



Scheme

The direction of deviation in the ^{13}C chemical shift is consistent with the anisotropy effect of C≡N bond as anticipated from the assumed dipolar association model. A similar geometry for the dipolar complex was found in the association of polar group such as benzonitrile - dimethyl sulfoxide complex⁶⁾ or acetonitrile dimer.⁷⁾

Both benzene and toluene molecules also contain strong anisotropy effect, but these solvents show no marked deviation in contrast to acetonitrile solvent. In these aromatic solvents, since the solvation is mainly due to relatively weak association such as dipole - (induced) dipole⁸⁾ or dipole - quadrupole⁹⁾ type, one possible explanation is that these solvent molecule remote from the carbonyl group may be disfavorable for the anisotropy effect on the ^{13}C chemical shift.

From the correlation between the ^{13}C chemical shift and the G value, it was found that the G value can explain

the paramagnetic contribution, but not the characteristic anisotropy effects in NMR solvent shift. The marked deviation, therefore, may be important. It is thus concluded that for the carbonyl carbon systems studied here the G value becomes a convenient measure of the solvent dependence of ^{13}C chemical shift except for special case.

Experimental

The ^{13}C FT NMR spectra were obtained by a JNM PS-100 spectrometer operating at 25.03 MHz by using TMS as an internal standard. Spectral reproducibility was 0.05 ppm in individual solvents. The concentration of the sample was *ca.* 10 mol%. IR spectra were recorded on a JASCO DS-402G grating spectrometer. The uncertainty in $\nu_{\text{C=O}}$ frequency was $\pm 0.5 \text{ cm}^{-1}$.

References

- 1) G. E. Maciel and J. J. Natterstad, *J. Chem. Phys.*, 42, 2752 (1965).
- 2) G. L. Nelson, G. C. Levy and J. P. Neilan, *J. Am. Chem. Soc.*, 94, 3089 (1972).
- 3) T. H. Whitesides and J. P. Neilan, *J. Am. Chem. Soc.*, 97, 908 (1975).
- 4) A. Allerhand and P. von R. Schleyer, *J. Am. Chem. Soc.*, 85, 371 (1963).
- 5) For example, T. D. Alger, D. M. Grant, and E. G. Paul, *J. Am. Chem. Soc.*, 88, 5397 (1966); A. J. Jones, D. M. Grant,

J. R. Russell, and G. Fraenckel, *J. Phys. Chem.*, 73, 1624 (1969).

6) C. D. Ritchie and A. L. Pratt, *J. Am. Chem. Soc.*, 86, 1571 (1964).

7) R. Yamdagni and P. Kebarle, *J. Am. Chem. Soc.*, 94, 2940 (1972).

8) For example, W. G. Schneider, *J. Phys. Chem.*, 66, 2653 (1962); see also Chapter I in this thesis.

9) K. Nikki, N. Nakahata and N. Nakagawa, *Tetrahedron Lett.*, 3811 (1975).

CHAPTER V. Effects of Solvents on the Electronic
Absorption Spectrum of Sodium 4-Nitro-
phenoxide in the Presence of 15-Crown-
5 Ether

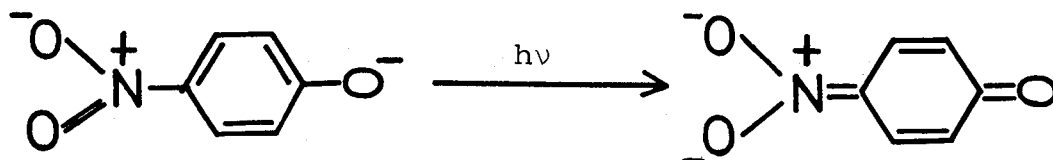
Abstract. The electronic absorption spectrum of sodium 4-nitrophenoxide was determined in 21 solvents of varying polarities by the aid of the ability of 15-crown-5 ether to solubilize the salt in nonpolar solvents. These spectra showed a marked difference between hydroxylic solvents and nonhydroxylic solvents. A possible interpretation for this difference is presented.

Introduction

In polar solvents, solvent effects on phenoxides and carbanions have been investigated extensively,¹⁾ and discussed in connection with several reaction rates and mechanisms.²⁾ In contrast to polar solvent effects, the behavior of the ion pair system in nonpolar solvents has not been described, because of less solubility. In this chapter the effects of solvents in the presence of 15-crown-5 ether upon the electronic absorption spectrum of sodium 4-nitrophenoxide are discussed on the basis of the correlation between the solvent shifts and Dimroth's solvent polarity parameter, E_t (hereafter abbreviated as D's E_t), values.³⁾

Results and Discussion

The Table summarizes the solvent-induced spectral shifts for sodium 4-nitrophenoxide (I) relative to 4-nitroanisole (II) in a range of solvents. The appropriate compound (II) was used as a reference standard, because the solvation effects on 4-nitrophenyl portion are assumed to be similar in both compounds. In certain nonpolar solvents, in order to obtain a sufficient solubility of the salt for the measurement of the λ_{\max} value, a large excess of the sodium chelating agent, 15-crown-5 ether, was used. Since it is desirable that solvent shifts be compared under the same conditions, all the spectra were measured in the presence of a large excess of the crown ether. The λ_{\max} value is attributed to a $\pi \rightarrow \pi^*$ transition with the character of an intramolecular charge transfer from the oxygen anion to the hydrocarbon portion.



The crown ether's effects on the spectra are also given in the Table.

It is found that the enhanced red shifts ($-\Delta\nu_{\max}$ values in the Table) are correlated well by the D's E_t values (see Figure). As can be seen in the Figure, however, the correlation is separated into two set of straight lines, one for hydroxylic solvents and the other for nonhydroxylic solvents. Furthermore, it should be noted that the slopes of the two

Table. Electronic spectral shifts for sodium 4-nitrophenoxide (I) relative to 4-nitroanisole (II) in the presence of 15-crown-5 ether in a range of solvents^{a)}

Solvents	$\lambda_{\max}^{(I)}/\text{nm}^{b)}$	$\lambda_{\max}^{(II)}/\text{nm}$	$-\Delta\nu_{\max}/\text{kK}^{c)}$	D's E_t value
(1) <i>t</i> -Butyl alcohol	421.0(+1)	307.0	8.82	43.9
(2) Isopropyl alcohol	414.5(0)	307.0	8.44	48.6
(3) <i>n</i> -Propyl alcohol	407.0(0)	308.0	7.90	50.7
(4) Ethanol	406.0(0)	308.0	7.84	51.9
(5) Methanol	389.0(0)	309.0	6.65	55.5
(6) Ethylene glycol	407.5(0)	316.0	7.11	56.3
(7) Water	403.5	317.0	6.77	63.1
(8) CCl ₄	385.0 ^{d)}	302.0	7.14	32.5
(9) Toluene	391.0 ^{d)}	308.0	6.89	33.9
(10) Benzene	393.0 ^{d)}	308.5	6.96	34.5
(11) Diethyl ether	391.0 ^{d)}	302.5	7.48	34.6
(12) Dioxane	407.5(+1)	307.5	7.98	36.0
(13) THF	404.0 ^{d)}	309.0	7.61	37.4
(14) Bromobenzene	406.0 ^{d)}	313.0	7.32	37.5
(15) 1,2-Dimethoxyethane	410.0(+3)	308.5	8.02	38.2
(16) CHCl ₃	417.5 ^{d)}	312.0	8.10	39.1
(17) Dichloromethane	420.0 ^{d)}	313.0	8.14	41.4
(18) Dichloroethane	416.0 ^{d)}	312.5	7.98	41.9
(19) DMF	435.5(0)	319.0	8.36	43.8
(20) DMSO	438.0(0)	318.0	8.62	45.0
(21) Acetonitrile	429.0(0)	311.5	8.79	46.0

a) Reproducibility < 1 nm. b) The value in parentheses represents the magnitude of the crown ether effect on the λ_{\max} value; positive numbers indicate red shifts. c) Enhanced red shifts for compound (I) as compared with compound (II); $-\Delta\nu_{\max}$, kK = $[1/\lambda(I) - 1/\lambda(II)] \times 10^4$. d) Not sufficiently soluble in the absence of 15-crown-5 ether.

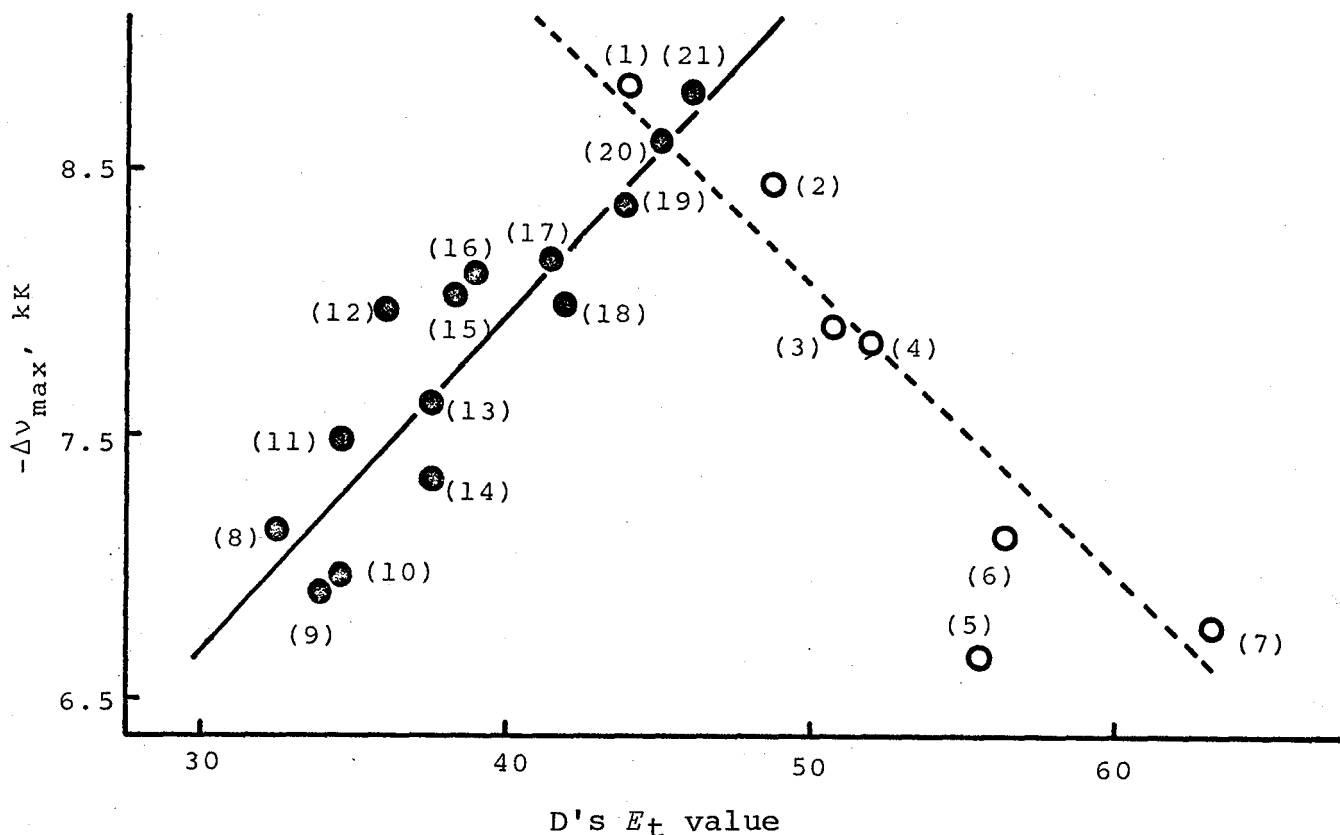


Figure. Correlation between $-\Delta\nu_{\max}$ value and D's E_t value.

(○): Hydroxylic solvents, (●): nonhydroxylic solvents.

straight lines show opposite signs.

In the hydroxylic solvents, the phenoxide anion is presumably present as a cation-free anion rather than as sufficiently tight ion aggregates, because the anion is supposed to be strongly solvated by hydrogen bonding. Indeed, the addition of crown ether produces essentially no effect on the λ_{\max} value (see Table). Therefore, it seems reasonable to assume that the hydroxylic solvent-induced shifts are mainly due to the direct H-bonding solvation of the phenoxide anion. A stronger H-bonding solvation should produce a larger blue shift, because the oxygen of phenoxide is more negative in

the ground state than in the excited state. In fact, the decreasing order of the $-\Delta\nu_{\max}$ value is consistent with the α -scale of solvent H-bond donor acidities (HBD)⁴⁾ reported by Taft and Kamlet, except for methanol and ethylene glycol. Furthermore, the parallelism between the $-\Delta\nu_{\max}$ value and the D's E_t value (see Figure) suggests the operation of similar H-bonding solvation mechanisms, because the D's E_t value is based on the electronic transition of the pyridinium betain with the phenoxide anion site.

On the other hand, the nonhydroxylic solvents are presumed to be poor anion solvators, so that direct solvations of the phenoxide anion can be neglected. The nonhydroxylic solvent shifts can be interpreted by assuming an interaction between the sodium cation bound by the crown ether and the phenoxide anion. It is known⁵⁾ that the D's E_t value is correlated with such measures of the ionizing power of solvents as Winstein's Y value⁶⁾ and Kosower's Z value.⁷⁾ Therefore, the increasing D's E_t value may be expected to cause a larger charge separation between the sodium cation bound by the crown ether and the phenoxide anion, and in general the charge separation should produce red shift.¹⁾ Indeed, the observed red shifts are found to be proportional to the D's E_t value (see Figure). As to the crown ether effects, the absence of any effect in the dipolar aprotic solvents suggests that the salt is a relatively free ion.

Consequently, the $-\Delta\nu_{\max}$ - D's E_t value correlation revealed a difference in the solvation mechanism of sodium 4-nitrophenoxide between the hydroxylic solvents and the

nonhydroxylic solvents. This result is analogous to the chemical result with regard to the alkylation of phenoxides, naphthoxides and oximates.²⁾

Experimental

The electronic spectra were obtained using a Hitachi 124 automatic recording spectrophotometer. A quartz cell 1.0 cm in length was employed, and the concentration of the sample was of the order of 10^{-4} M.

Sodium 4-nitrophenoxide was dried *in vacuo* at 110°C overnight. The solvent were freshly distilled before use, and the spectro-grade solvents were used without further purification, except for chloroform, which was chromatographed on alumina. The 15-crown-5 ether was a commercial sample (Aldrich Chemical Company, Inc.).

References

1) H. E. Haugg and A. D. Schaefer, *J. Am. Chem. Soc.*, 87, 1587 (1965); J. F. Garst, R. A. Klein, D. Walmsley, and E. R. Zabolotny, *ibid.*, 87, 4087 (1965); R. C. Kerber and A. Porter, *ibid.*, 91, 366 (1969); W. Martir, A. E. Alegria, and G. R. Stevenson, *ibid.*, 98, 7955 (1976).

2) N. Kornblum, P. J. Berrigan, and J. le Noble, *J. Am. Chem. Soc.*, 82, 1257 (1960); 85, 1141 (1963); N. Kornblum, R. Selzer, and Phaberfield, *ibid.*, 85, 1148 (1963); A. J. Parker, *J. Chem. Soc.*, 1328 (1963); J. le Noble, T. Hayakawa, A. R. Sen, and Y. Tatukami, *J. Org. Chem.*, 36, 193 (1971);

S. G. Smith and M. P. Hanson, *ibid.*, 36, 1931 (1971).

3) K. Dimroth, C. Reichardt, T. Spiepmann, and F. Bohlmann, *Ann.*, 661, 1 (1963).

4) R. W. Taft and M. J. Kamlet, *J. Am. Chem. Soc.*, 98, 2886 (1976). The α -scale of HBD increases in the order: [Solvents (1)<(2)<(3)<(6)<(4)<(5)<(7)].

5) E. M. Kosower, "Physical Organic Chemistry," John-Wiley & Sons, New York (1968), p. 303.

6) E. Grunwald and S. Winstein, *J. Am. Chem. Soc.*, 73, 2700 (1951).

7) E. M. Kosower, *J. Am. Chem. Soc.*, 80, 3253, 3261, 3267 (1958).

CHAPTER VI. Crystal Structures and IR Spectra of 4-Substituted 2,6-Diphenylphenols Containing Intramolecular OH... π Hydrogen Bonding¹⁾

Abstract. The crystal structures of 4-substituted (NO_2 , H, and OC_2H_5) 2,6-diphenylphenols have been determined by single-crystal X-ray analysis. These three-dimensional structures around the O-H group closely resemble one another. The intramolecular OH... π hydrogen bond is found between the hydroxyl H atom and the π electrons on two carbon atoms of the *ortho* phenyl group for each crystal structure. In addition to the intramolecular OH... π bonding, the weak intermolecular OH... π bond is observed in the crystals of 4-nitro-2,6-diphenylphenol. The structure of 4-ethoxy-2,6-diphenylphenol contains the intra- and inter-molecular OH... π bonds, and the intermolecular OH...O bond. The crystal and molecular structures well explain the OH stretching bands appeared in the IR spectra of these phenols in the solid state.

Introduction

Hitherto many spectroscopic studies have been carried out on the hydrogen bonding in which π electrons are involved as the proton acceptor base. As far as we know, however, only a few unequivocal X-ray studies have been reported.^{2,3)}

In order to elucidate the stereochemistry of the intramolecular OH... π bond, the structures of 4-substituted (H; 1, NO_2 ; 2 and OC_2H_5 ; 3) have been studied by X-ray diffraction.

The IR spectra in the solid state are examined to interpret

on the basis of the crystal structures determined, and the discussion on the stereochemistry around the OH group is given in this chapter.

Experimental

X-Ray Crystallographic Analysis. The crystal data, number of reflections, and final residuals are listed in Table 1.

Table 1. Crystallographic data, number of reflections, and final residuals for 1, 2, and 3

	1	2	3
Mol formula	$C_{18}H_{14}O$	$C_{18}H_{13}NO_3$	$C_{20}H_{18}O_2$
Mol weight	246.3	291.3	290.4
Size (mm ³)	0.28x0.14x0.12	0.22x0.28x0.11	0.4x0.2x0.1
Crystal system	orthorhombic	monoclinic	triclinic
Space group	$P2_12_12_1$	$C2/c$	$P\bar{1}$
Lattice constants			
a (Å)	11.165(1)	21.983(3)	10.857(1)
b	18.399(1)	9.259(1)	14.593(2)
c	6.368(1)	14.208(2)	10.467(1)
α (°)	90	90	104.80(1)
β	90	95.32(2)	96.96(1)
γ	90	90	84.05(1)
D_x (g·cm ⁻³)	1.251	1.344	1.215
Z	4	8	4
Unique data	1754	3328	5587
$ F > 3\sigma(F)$	1271	2040	3598
Final R	0.052	0.051	0.057

The X-ray intensity data were collected by the θ - 2θ scan technique on a computer-controlled four-circle diffractometer, using a graphite-monochromatized $\text{MoK}\alpha$ radiation. The structures were solved by applications of the symbolic addition procedure,⁴⁾ and refined by the block-diagonal least-squares method. Anisotropic thermal vibrations were assumed for the non-hydrogen atoms. All the H atoms, including the hydroxyl H atom, were clearly found from difference Fourier maps and their positional and isotropic thermal parameters were refined.

Measurement of the IR Spectra. The IR spectra were obtained with a JASCO DS-701G grating spectrometer. The conditions for determination of the spectra were the same as in Chapter I.

Materials. The preparations of compounds (1) and (2) were described in Chapter I.

4-Ethoxy-2,6-diphenylphenol (3). A solution of 4-diazo-2,6-diphenylcyclohexa-2,5-dienone (2g, 6.8 mmol) (see Chapter I) in ethanol (500 ml) was irradiated with a low-pressure mercury lamp under bubbling nitrogen. Evaporation of the solvent gave a slightly yellow residue which was dissolved in benzene and chromatographed on a silica gel column. Elution with benzene gave **3** (1g, 3.4 mmol), and as a by-product 2,6-diphenylphenol (0.3g, 1.2 mmol). mp 92–94°C (from benzene). Found; C, 82.81, H, 6.20%. Calcd for $\text{C}_{20}\text{H}_{18}\text{O}_2$: C, 82.73; H, 6.25%.

Results and Discussion

In CCl_4 solution, 4-substituted 2,6-diphenylphenols (1-3) show only a singlet OH stretching IR absorption spectra due to the intramolecular OH... π hydrogen bonding. On the other hand, more complex νOH spectra are observed in the solid state (CsI disk), as shown in Fig. 1. Deuteration of the OH group produces a quite similar νOH spectral pattern and the frequencies fall by $907\text{--}924\text{ cm}^{-1}$, owing to the heavy atom effect (band a \rightarrow 2608.9, b \rightarrow 2607.9, c \rightarrow 2588.6, d \rightarrow 2636.0, e \rightarrow 2620.0, f \rightarrow 2608.6, g \rightarrow 2604.6 cm^{-1}). This result shows that these observed bands (a-g in Fig. 1) can be assigned to the OH stretching vibrations.

Figs. 2, 3, and 4 show the molecular structures of 1, 2, and 3 with the atom-labelling schemes, respectively. The important distances and angles are given in Table 2. It is found from Figs. 2-4 and Table 2 that the geometrical structures around the OH group closely resemble one another. The OH group is almost coplanar with the phenol ring (I), and the *ortho* phenyl rings, (II) and (III), are twisted about the ring (I) in opposite directions. The hydroxyl H(1) atom approaches the π electron cloud on both C(7) and C(12) carbon atoms. The distances, H(1)...C(7) and H(1)...C(12), are almost the same (2.40-2.59 \AA).⁵⁾ The H(1)...C(7) or C(12) distance is considerably shorter than 2.9 \AA , the sum of the van der Waals radii for hydrogen (1.2 \AA) and carbon (1.7 \AA). Thus, the OH group seems to be favorably located to interact equally with the π electrons on both C(7) and C(12) atoms in the crystals.

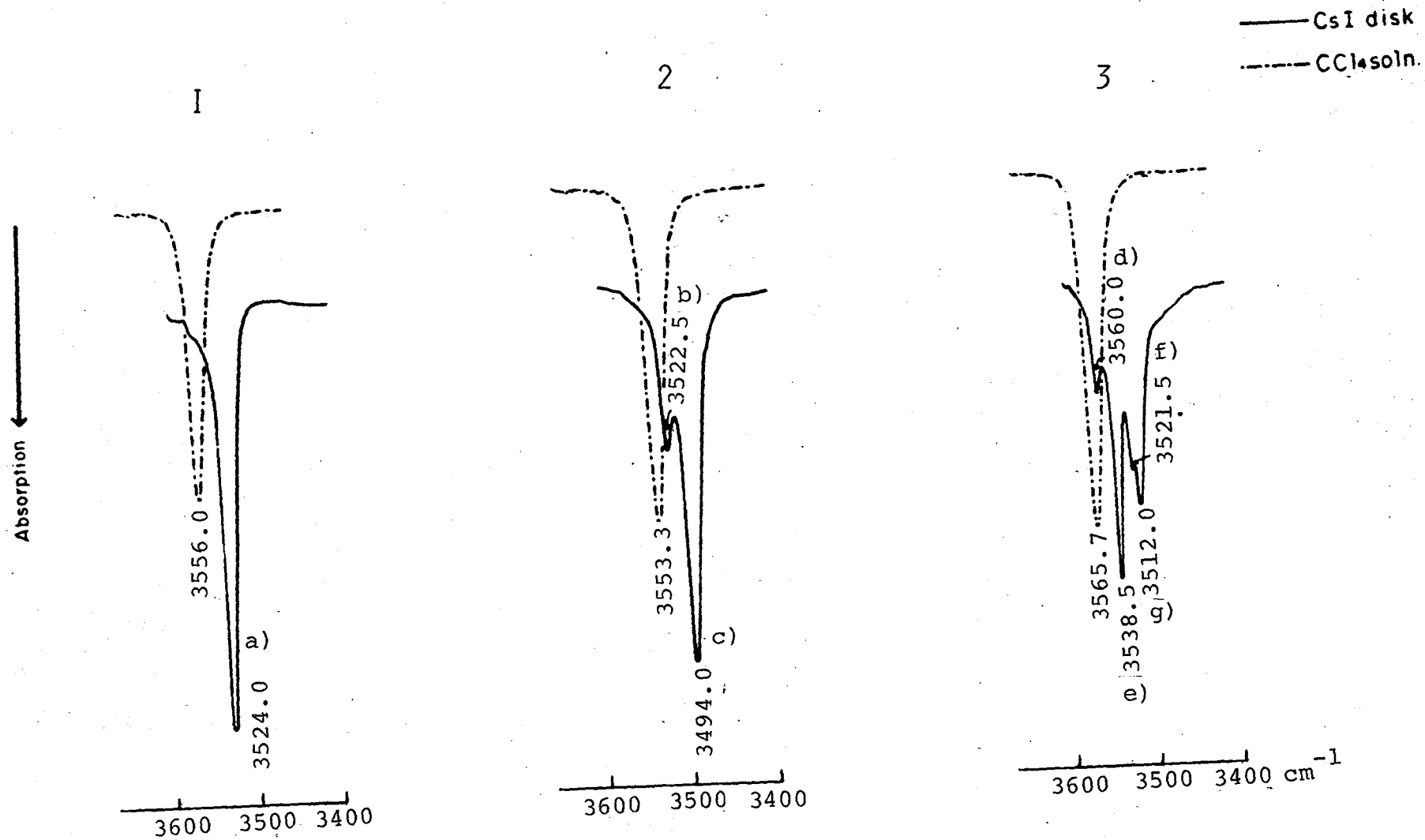


Fig. 1. The ν_{OH} spectra of 1, 2, and 3 in CCl_4 and in solid (CsI disk) state.

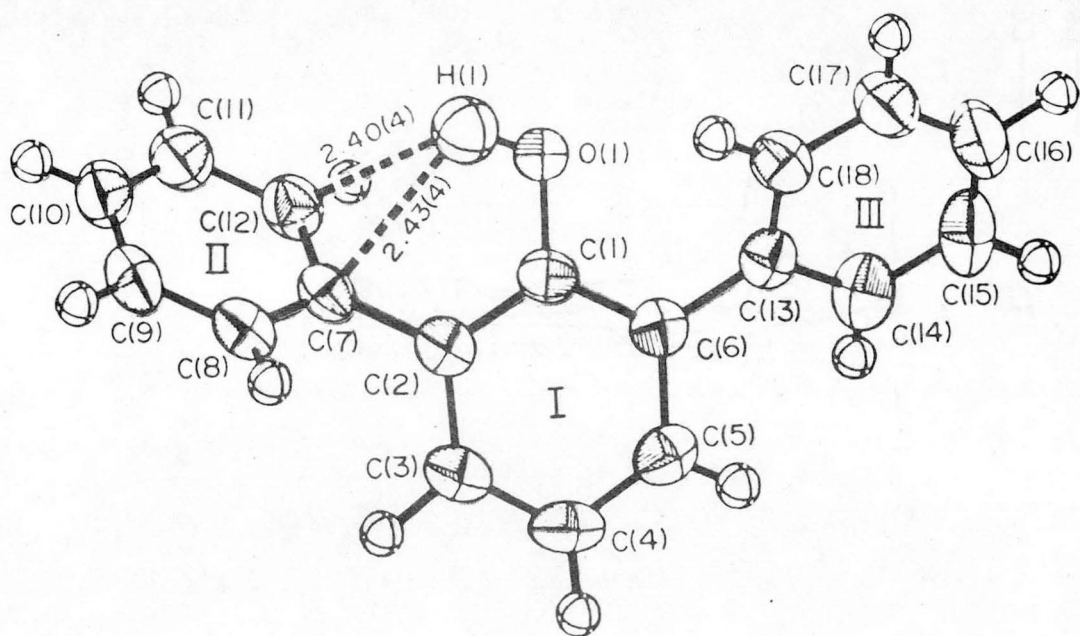


Fig. 2. Molecular structure of **1** viewed perpendicular to ring (I).

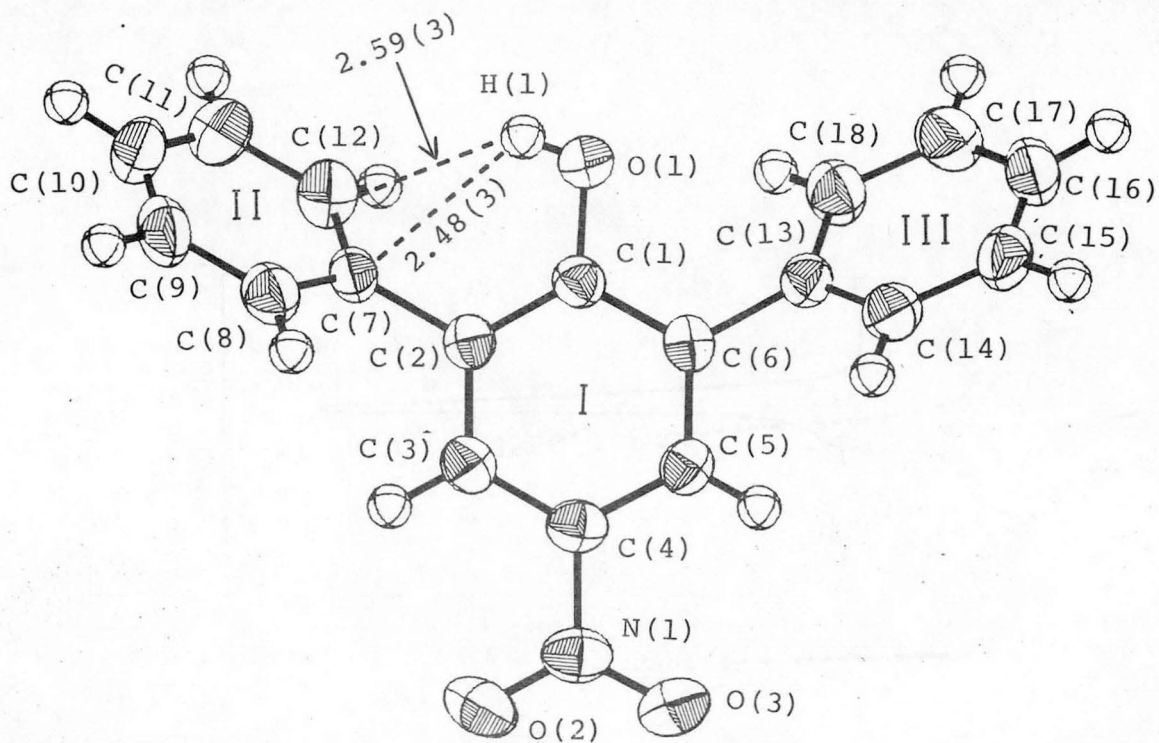


Fig. 3. Molecular structure of **2** viewed perpendicular to ring (I).

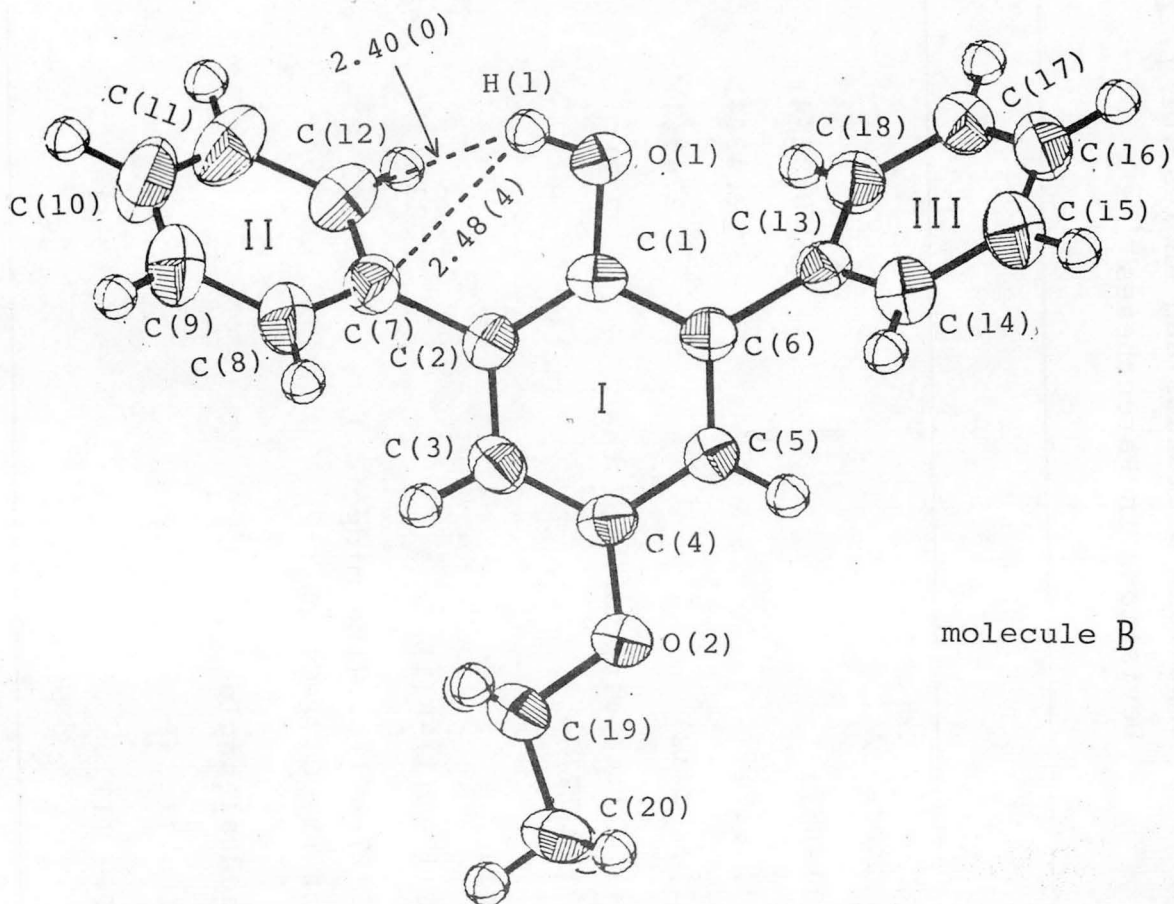
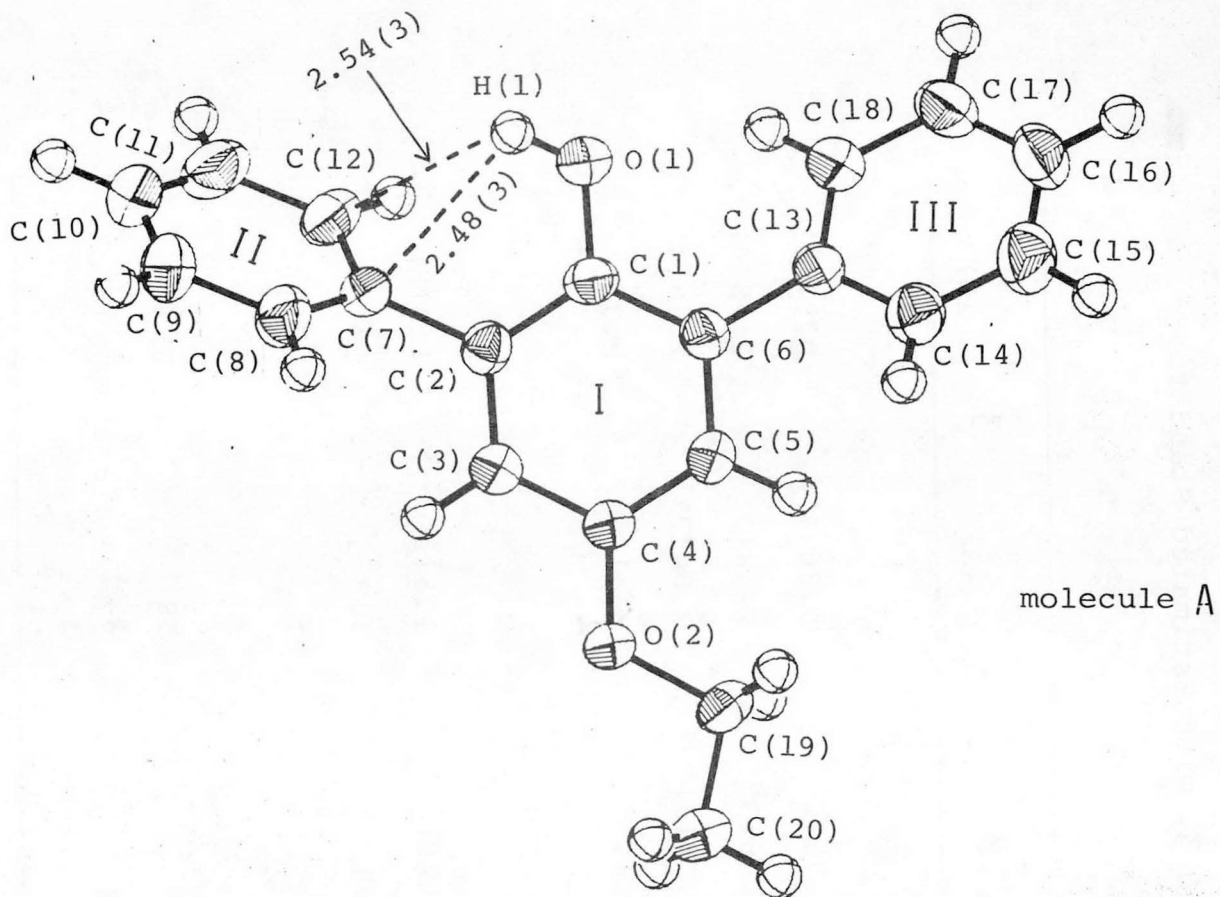


Fig. 4. Molecular structure of **3** (A and B) viewed perpendicular to ring (I).

Table 2. Important Distances and Angles for I, 2, and 3, with Estimated Standard Deviations in Parentheses^{a)}

	I	2	(A)	3	(B)
Distance Å					
O(1)-H(1)	0.92(4)	0.75(2)	0.86(4)	0.87(4)	
H(1)...C(7)	2.43(4)	2.48(3)	2.48(3)	2.48(4)	
H(1)...C(12)	2.40(4)	2.59(3)	2.54(3)	2.40(4)	
H(1)...(the midpoint) of the C(7)-C(12)	2.31	2.44	$\bar{2}.41$ $\bar{2}$	2.31	
angle °					
C(1)-O(1)-H(1)	111(3)	110(2)	115(2)	110(2)	
O(1)-H(1)...(the midpoint) of the C(7)-C(12)	122	104	117	123	
Dihedral angle °					
I - II	52	58	58	51	
I - III	44	52	37	56	

a) Detailed bond lengths and angles are given in Appendix.

In molecule I, the ν_{OH} spectrum in the solid state, as well as that in CCl_4 , shows only one peak, at 3524.0 cm^{-1} (see Fig. 1), which falls by 88 cm^{-1} from 3512 cm^{-1} of ordinary phenol in CCl_4 . This strongly suggests the presence of intramolecular $OH \dots \pi$ hydrogen bonding in the crystals of molecule I. Furthermore, no close intermolecular contact involving the OH group was found in the packing in the crystal lattice, as shown in Fig 5.

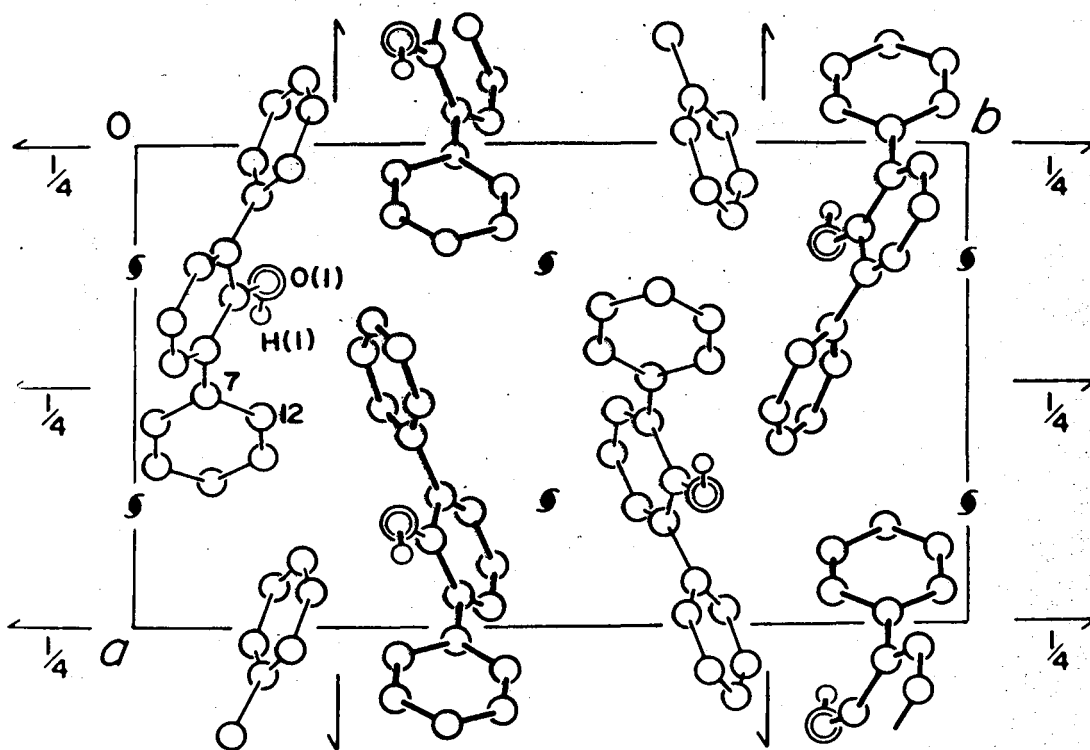


Fig. 5. Projection of the crystal structure of I along the c axis.

Therefore, the observed single ν_{OH} spectrum in the solid state can be assigned to the OH group in the intramolecular $OH \dots \pi$ bonding between H(1) and the π electrons on both

C(7) and C(12) carbon atoms. This result is consistent with that deduced from the IR data on 2-hydroxybiphenyls in CCl_4 solution.⁶⁾

The phenol (2) is also expected to possess the intramolecular $\text{OH}\dots\pi$ bonding in the crystals, because the stereochemistry around the OH group is similar to that of the phenol (1) (see Fig. 3 and Table 2). The νOH spectrum of 2 in the solid state is observed as a doublet (b and c bands in Fig. 1). In order to establish the assignments of the b and c bands, in view of the crystal-structure results, two factors should be considered; one is the dihedral angle between the phenol ring (I) and the proton acceptor ring (II), and the other a substituent effect. That is, a large dihedral angle and/or an electron-attracting substituent in the phenol ring produce a stronger $\text{OH}\dots\pi$ bond,⁶⁾ resulting in a decrease of the $\nu\text{OH}\dots\pi$ frequency. The νOH frequency due to the intramolecular $\text{OH}\dots\pi$ bonding of 2 should occur at a much lower frequency than that of 1, because 2 has a strong electron-attracting substituent, nitro group, and the large dihedral angle (see Table 2) as compared with 1. From this, the c band at 3494.0 cm^{-1} can be attributed to the intramolecular $\text{OH}\dots\pi$ bonding between H(1) and both C(7) and C(12). In this $\text{OH}\dots\pi$ bonding, as can be seen from Table 2 and Fig. 3, the angle $\text{O}(1)\text{-H}(1)\dots(\text{the midpoint})$ of the C(7) and C(12) bond is 104° , which is fairly small compared with the other systems (1 and 3), although no marked change is observed in the distance $\text{H}(1)\dots(\text{the midpoint})$. The $\text{OH}\dots\pi$ bond seems to be strengthened by the smaller angle, because the overlap between

the two orbitals concerned [the π electrons ($2p\sigma$) and hydroxyl H atom ($1s$)] becomes more favorable.

The crystal structure of **2** projected along the *b* axis is shown in Fig. 6.

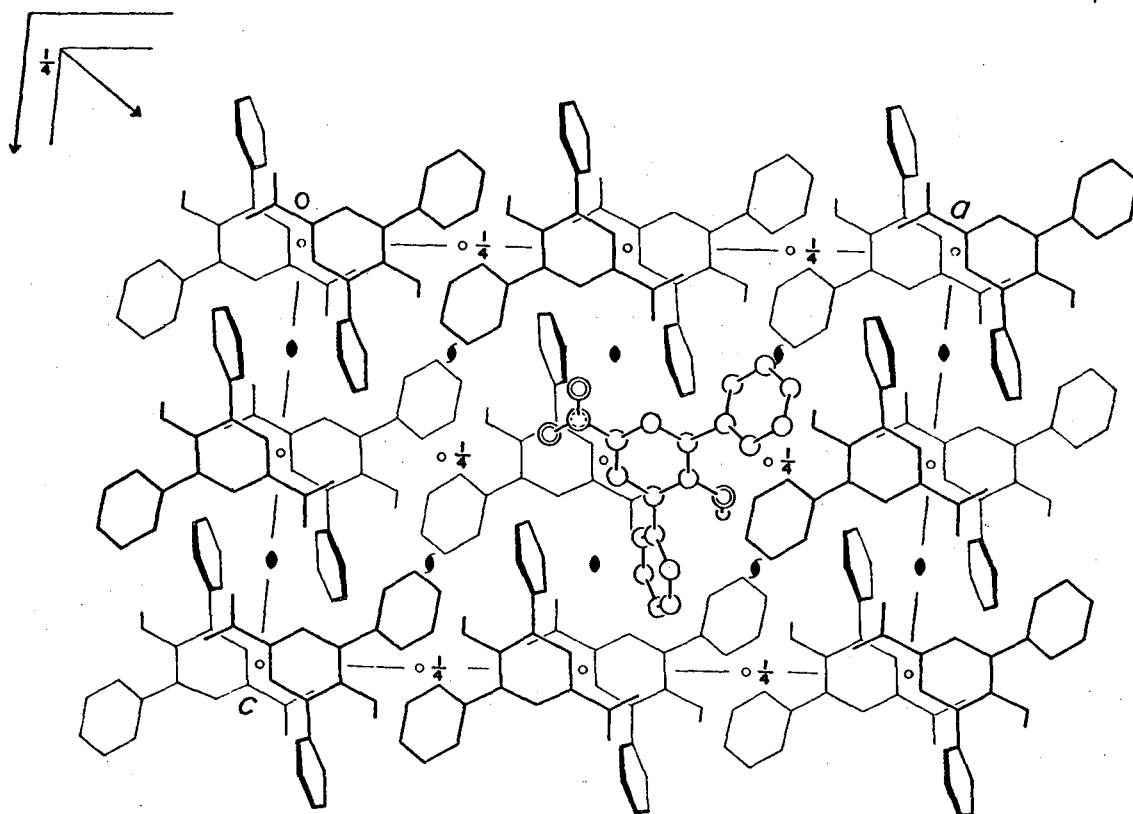


Fig. 6. Projection of the crystal structure of **2** along the *b* axis.

The intermolecular weak contacts are found between H(1) and both C(15) and C(16) atoms. The intermolecular distances H(1)...C(15) and H(1)...C(16) are 2.88(2) and 2.92(2) Å, respectively. These values are almost equal to the sum of the van der Waals radii (2.9 Å), and the occurrence of the weak intermolecular OH... π bonding can be expected. From this, the *b* band at 3522.5 cm^{-1} must be due to this OH... π

bonding. Also, the b band has the less intensity and the high frequency as compared with the c band. This can be ascribed to the longer OH... π distance. Furthermore, it is interesting to note that the H(1) atom approaches from the upper side to the π -electrons on both C(15) and C(16) atoms in order to establish this interaction, but not to the sixfold axis of the phenyl ring (III), as shown in Fig. 7.

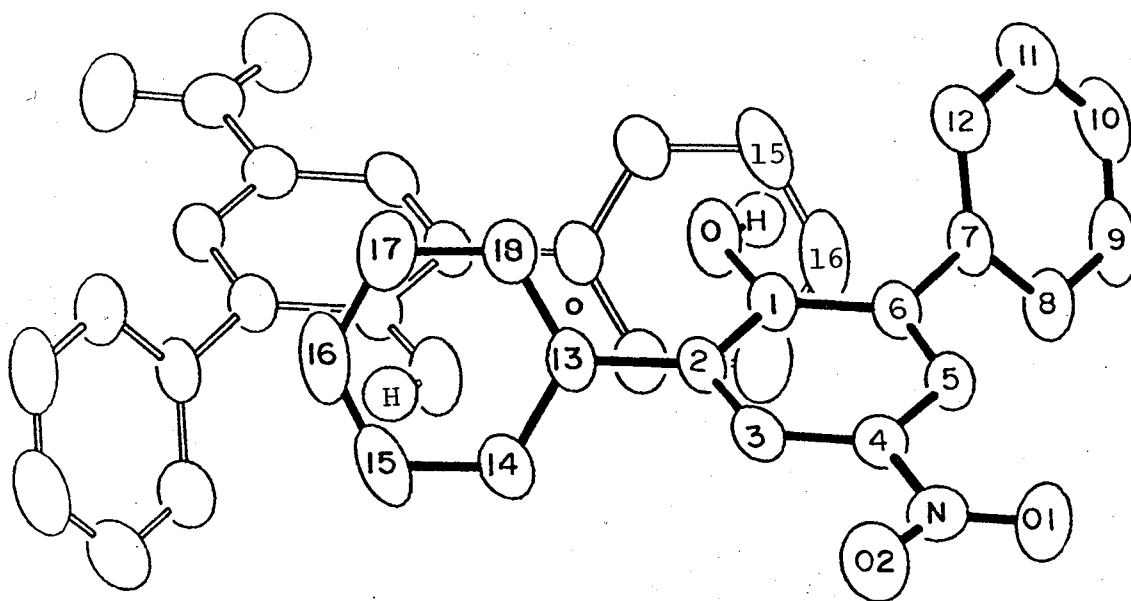


Fig. 7. A portion of the crystal structure of 2 showing the intermolecular approach of H(1) atom to both C(15) and C(16) atoms.

The direction of approach of H(1) to the two carbon atoms is quite similar to that in the intramolecular OH... π bonding of []. This stereochemistry, however, is different from that found in the crystal of tributylammonium tetraphenylborate monohydrate,³⁾ where each water H atom is located almost immediately above the center of a phenyl ring to form the

intermolecular OH... π bonding, the H...C(aromatic) distances ranging 2.49(3) – 2.91(3) Å.

In molecule **3**, the crystal structure consists of two crystallographically independent molecules (A and B), as shown in Fig. 4. The corresponding bond lengths and angles in the two independent molecules with the opposite orientation of the ethoxy group agree closely with each other. As with the crystal structures of **1** and **2**, the intramolecular OH... π bond is also found in either molecule (A and B). The arrangement of the molecule **3** viewed along the *c* axis is shown in Fig. 8.

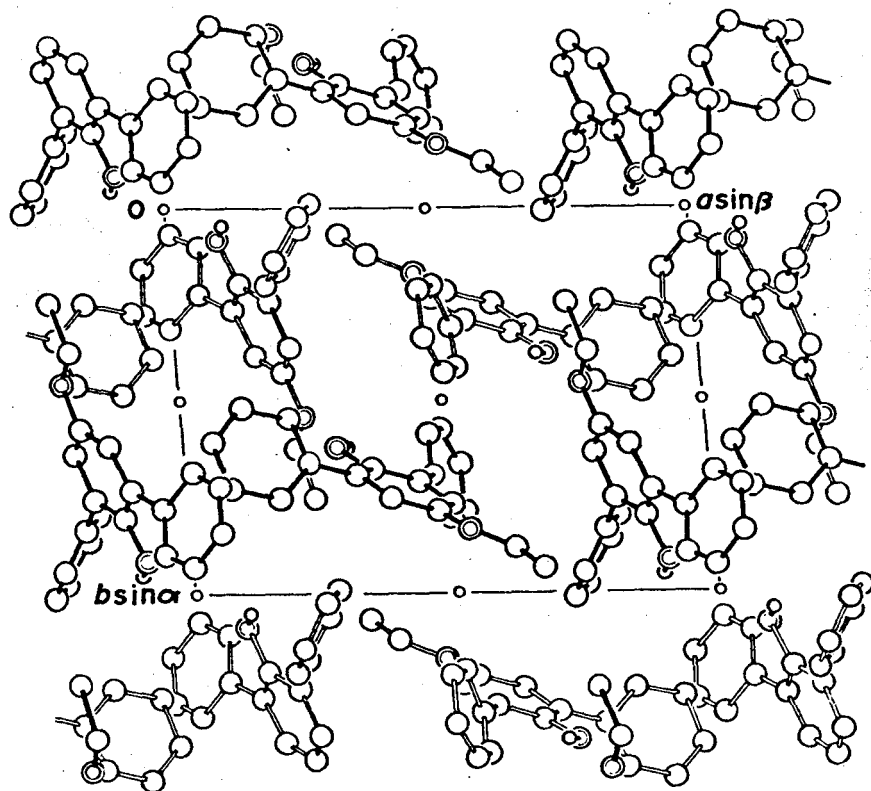


Fig. 8. Projection of the crystal structure of **3** along the *c* axis.

The most interesting feature is the possibility of the presence of the intermolecular OH... π bonding between A and its inverted molecule A' and the intermolecular OH...O bonding between A and B. Figs 9 and 10 show the relevant molecular arrangements. In Fig. 9, the intermolecular distances H(1)...C(17) and H(1)...C(18) are 2.80(3) and 2.98(3) Å, respectively, which are close to the values found in the weak intermolecular OH... π bond of **2** (2.88(2) and 2.92(2) Å). The stereochemistry of this OH... π bond is also quite similar to that in **2**. This suggests the presence of the intermolecular OH... π bonding between A and A' in **3**.

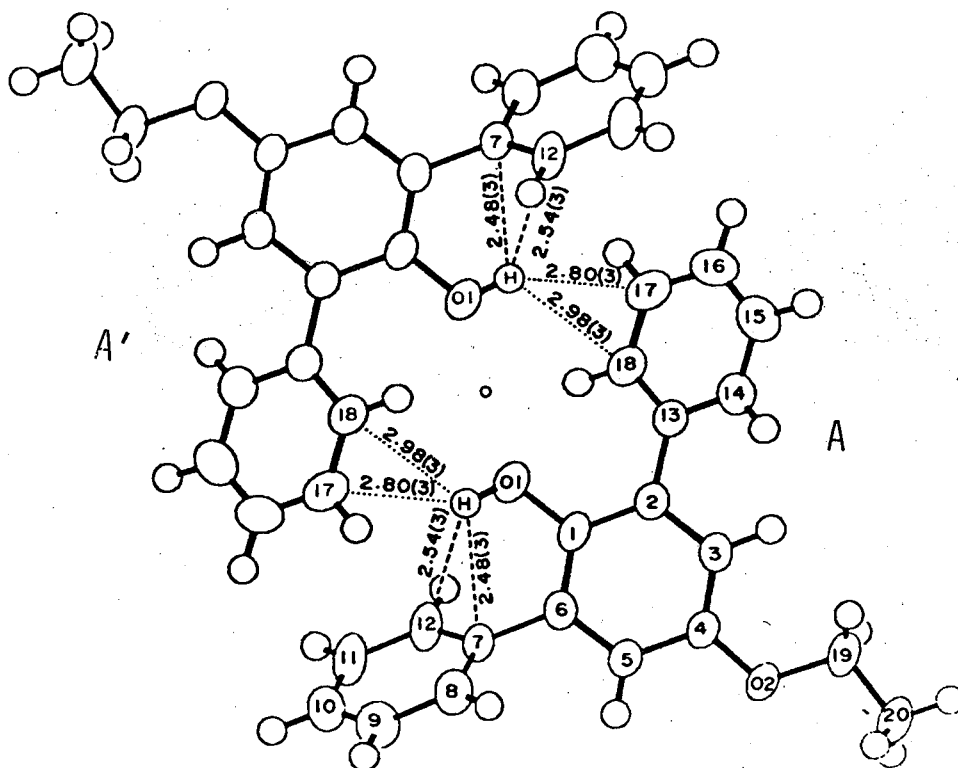


Fig. 9. A portion of the crystal structure of **3** showing the intermolecular weak contacts between H(1) atom and both C(17) and C(18) atoms. The weak contacts and the intramolecular OH... π bonding are shown by the dotted lines.

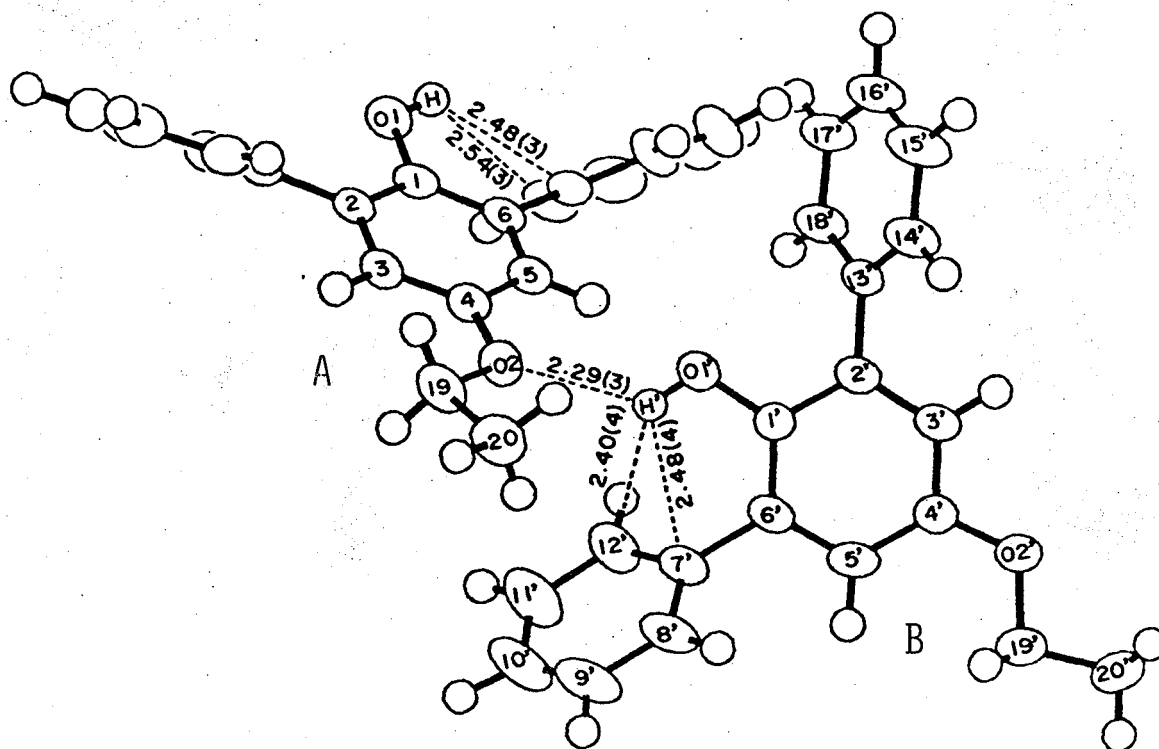


Fig. 10. A portion of the crystal structure of 3 showing the intermolecular close contact between H(1) atom and O(2) atom. The close contact and the intramolecular OH... π bonding are shown by the dotted lines.

In Fig. 10, the intermolecular H(1)...O(2) distance is 2.29(3) Å, which is about 0.3 Å less than the sum of the van der Waals radii of 2.6 Å. Baur⁷⁾ has proposed that the OH...O distance shorter than 2.4 Å can be taken as a possible indication of OH...O hydrogen bonding. This limiting distance, 2.4 Å, agrees with the value estimated from Hamilton's equation (see Chapter II); distance $< 1.2 + 1.4 - 0.2 = 2.4$ Å. Also, the angle O(1)-H(1)...O(2) is 128°, indicating the bent hydrogen bonded system. Recently, a very bent OH...O hydrogen bond has been found by neutron diffraction study;⁸⁾ the angle O-H...O is 116.6°, distance OH...O being 2.31 Å. From these considerations, it can be rationalized that the intermolecular OH...O

hydrogen bond exists between A and B.

The ν_{OH} spectrum of **3** in the solid state splits into a quadruplet, as shown in Fig. 1. These bands (d, e, f, and g) can be attributed to the four kinds of hydrogen bonded species, on the following basis. i) The frequency of the intermolecular OH...O hydrogen bonded species is supposed to be lower than those of the inter- and intra-molecular OH... π species, because the basicity of the lone pair electrons on oxygen atom is larger than that of the π electrons. ii) The band due to the weak intermolecular OH... π bonding should have a less intensity and a high frequency as compared with that of the intramolecular one, as was observed for the b band in the molecule **2**. iii) The intramolecularly OH... π bonded OH frequency in the A molecule should be located at a lower frequency than that in the B molecule, because the dihedral angle between the rings (I) and (II) in the A molecule is larger by 7° than that in the B molecule (see Table 2). iv) The ν_{OH} frequency due to the intramolecular OH... π bonding of the B molecule should occur at a higher frequency than that of **1**, because for the molecules **3**(B) and **1** having the almost same dihedral angle (52° and 51°) the ethoxy substituent (electron-releasing one) of **3**(B) can be operative in determining the ν_{OH} ... π frequency.

From the consideration of i), it is found that the band g at the lowest frequency, 3512.0 cm^{-1} , is most probably assignable to the intermolecular OH...O hydrogen bond. Novak⁹⁾ has reported an empirical correlation curve of the ν_{OH} vs. O...O distance in the OH...O hydrogen bonded systems.

In this correlation, the frequency corresponding to the O(1)...O(2) distance (2.875 \AA) in the A-B pair falls near 3500 cm^{-1} , supporting this assignment, although the O-H...O angle should be considered in this correlation. The consideration of ii) shows that the d band with the small intensity at the highest frequency, 3560.0 cm^{-1} , can be assigned to the intermolecularly OH... π bonded species in the A-A' pair. The remainder of the band should correspond to the intramolecular OH... π bonding. On the basis of iii)¹⁰⁾ and iv)¹¹⁾, the e and f bands can be assigned to the OH species in the intramolecular OH... π bonding in the B and A molecules, respectively.

Consequently, the crystal structures of these phenols revealed by the X-ray study nicely explain the results of the IR study on the solid state.

References

- 1) This study has been carried out in cooperation with Professor Kazumi Nakatsu of Kwansai Gakuin University. The author wishes to thank Professor K. Nakatsu for his invaluable advice on this study and to all the members of his research group for their useful discussions.
- 2) A. D. U. Hardy and D. D. MacNicol, *J. Chem. Soc., Perkin Trans. 2*, 1140 (1976).
- 3) A. Aubry, J. Protas, E. Moreno-Gonzales, and M. Marraud, *Acta Crystallogr.*, B33, 2572 (1977).
- 4) J. Karle and I. L. Karle, *Acta Crystallogr.*, 21, 849 (1966).

5) The corresponding distances found in 2,2-bis-(2-hydroxy-5-methyl-3-*t*-butylphenyl)propane are 2.13, 2.19, 2.49, and 2.52 Å.

6) M. Ōki and H. Iwamura, *J. Am. Chem. Soc.*, 89, 576 (1967).

7) W. H. Baur, *Acta Crystallogr.*, B28, 1456 (1972).

8) G. M. Brown and H. A. Levy, *Acta Crystallogr.*, B29, 790 (1973).

9) A. Novak, *Struct. and Bond.*, 18, 177 (1974).

10) The dihedral angular effect on the $\nu_{\text{OH}} \dots \pi$ frequency could be roughly estimated from the correlation in 2-hydroxybiphenyls between $\Delta \nu_{\text{max}}$ and dihedral angle.⁶⁾ The difference (7°) in the dihedral angle between A and B molecules results in *ca.* 5 – 10 cm^{-1} , assuming that the angular effect on ν_{OH} for the phenol (3) is the same as that for 2-hydroxybiphenyls.

11) In case of the molecular structures having the same dihedral angle, the $\nu_{\text{OH}} \dots \pi$ frequency can be attributed to the electronic effect arising from the changes of the substituent; in other words, the frequency shifts due to the electronic effect in the solid state should parallel those in CCl_4 solution. In the compound pairs with the almost same dihedral angle of [(51°) and 3(B) (52°), and 2 (58°) and 3(A) (58°), the frequency shifts in the solid state [$\nu(3\text{B}) - (1)$; 14.5 cm^{-1} and $\nu(3\text{A}) - \nu(2)$; 27.5 cm^{-1}] well correspond to 9.7 cm^{-1} and 32.4 cm^{-1} in CCl_4 , respectively, again supporting these assignments.

APPENDIX

Bond lengths (in Å) and bond angles (in °) for molecule I

Bond	Length	Bond	Length
O(1)-H(1)	0.92(4)	C(10)-C(11)	1.377(5)
C(1)-O(1)	1.381(4)	C(11)-C(12)	1.390(5)
C(1)-C(2)	1.412(4)	C(12)-C(7)	1.397(5)
C(2)-C(3)	1.400(5)	C(6)-C(13)	1.486(4)
C(3)-C(4)	1.372(5)	C(13)-C(14)	1.396(5)
C(4)-C(5)	1.374(5)	C(14)-C(15)	1.376(5)
C(5)-C(6)	1.397(5)	C(15)-C(16)	1.376(7)
C(6)-C(1)	1.389(4)	C(16)-C(17)	1.382(6)
C(2)-C(7)	1.480(4)	C(17)-C(18)	1.390(5)
C(7)-C(8)	1.394(4)	C(18)-C(13)	1.396(5)
C(8)-C(9)	1.386(5)		
C(9)-C(10)	1.371(5)		

Bond	Angle	Bond	Angle
C(1)-O(1)-H(1)	111(3)	C(7)-C(8)-C(9)	121.2(3)
C(2)-C(1)-O(1)	120.4(3)	C(8)-C(9)-C(10)	120.2(3)
C(6)-C(1)-O(1)	117.3(3)	C(9)-C(10)-C(11)	120.1(3)
C(2)-C(1)-C(6)	122.3(3)	C(10)-C(11)-C(12)	120.0(3)
C(1)-C(2)-C(3)	117.1(3)	C(7)-C(12)-C(11)	120.9(3)
C(1)-C(2)-C(7)	122.7(3)	C(6)-C(13)-C(14)	120.7(3)
C(3)-C(2)-C(7)	120.2(3)	C(6)-C(13)-C(18)	121.3(3)
C(2)-C(3)-C(4)	121.5(3)	C(14)-C(13)-C(18)	117.9(3)
C(3)-C(4)-C(5)	119.8(3)	C(13)-C(14)-C(15)	121.3(4)
C(4)-C(5)-C(6)	121.9(3)	C(14)-C(15)-C(16)	120.3(4)
C(1)-C(6)-C(5)	117.4(3)	C(15)-C(16)-C(17)	119.6(4)
C(1)-C(6)-C(13)	123.7(3)	C(16)-C(17)-C(18)	120.4(4)
C(5)-C(6)-C(13)	118.9(3)	C(13)-C(18)-C(17)	120.5(3)
C(2)-C(7)-C(8)	120.4(3)		
C(2)-C(7)-C(12)	121.9(3)		
C(8)-C(7)-C(12)	117.6(3)		

Bond lengths(in Å) and bond angles(in °) for molecule 2

Bond	Length	Bond	Length
O(1)-H(1)	0.75(2)	C(10)-C(11)	1.371(4)
C(1)-O(1)	1.357(2)	C(11)-C(12)	1.387(3)
C(1)-C(2)	1.404(3)	C(12)-C(7)	1.385(3)
C(2)-C(3)	1.385(3)	C(6)-C(13)	1.488(3)
C(3)-C(4)	1.381(3)	C(13)-C(14)	1.386(3)
C(4)-C(5)	1.382(3)	C(14)-C(15)	1.380(3)
C(5)-C(6)	1.388(3)	C(15)-C(16)	1.366(4)
C(6)-C(1)	1.405(3)	C(16)-C(17)	1.381(4)
C(2)-C(7)	1.494(3)	C(17)-C(18)	1.381(4)
C(7)-C(8)	1.383(3)	C(18)-C(13)	1.390(3)
C(8)-C(9)	1.377(3)	C(4)-N(1)	1.464(3)
C(9)-C(10)	1.377(4)	N(1)-O(2)	1.224(3)
		N(1)-O(3)	1.222(3)

Bond	Angle	Bond	Angle
C(1)-O(1)-H(1)	110(2)	C(7)-C(8)-C(9)	120.6(2)
C(2)-C(1)-O(1)	122.0(2)	C(8)-C(9)-C(10)	120.5(2)
C(6)-C(1)-O(1)	116.3(2)	C(9)-C(10)-C(11)	119.7(2)
C(2)-C(1)-C(6)	121.6(2)	C(10)-C(11)-C(12)	120.0(2)
C(1)-C(2)-C(3)	118.5(2)	C(7)-C(12)-C(11)	120.7(2)
C(1)-C(2)-C(7)	120.8(2)	C(6)-C(13)-C(14)	119.9(2)
C(3)-C(2)-C(7)	120.7(2)	C(6)-C(13)-C(18)	121.7(2)
C(2)-C(3)-C(4)	119.9(2)	C(14)-C(13)-C(18)	118.3(2)
C(3)-C(4)-C(5)	121.6(2)	C(13)-C(14)-C(15)	121.1(2)
C(4)-C(5)-C(6)	120.1(2)	C(14)-C(15)-C(16)	119.9(2)
C(1)-C(6)-C(5)	118.2(4)	C(15)-C(16)-C(17)	120.3(2)
C(1)-C(6)-C(13)	122.0(2)	C(16)-C(17)-C(18)	119.9(2)
C(5)-C(6)-C(13)	119.8(2)	C(13)-C(18)-C(17)	120.6(2)
C(2)-C(7)-C(8)	120.1(2)	C(3)-C(4)-N(1)	119.3(2)
C(2)-C(7)-C(12)	121.4(2)	C(5)-C(4)-N(1)	119.1(2)
C(8)-C(7)-C(12)	118.5(2)	C(4)-N(1)-O(2)	118.1(2)
		C(4)-N(1)-O(3)	118.8(2)
		O(2)-N(1)-O(3)	123.1(2)

Bond lengths(in Å) and bond angles(in °) for molecule 3(A)

Bond	Length	Bond	Length
O(1)-H(1)	0.86(4)	C(10)-C(11)	1.378(5)
C(1)-O(1)	1.377(3)	C(11)-C(12)	1.386(5)
C(1)-C(2)	1.398(3)	C(12)-C(7)	1.383(4)
C(2)-C(3)	1.388(4)	C(6)-C(13)	1.494(3)
C(3)-C(4)	1.387(4)	C(13)-C(14)	1.394(3)
C(4)-C(5)	1.381(3)	C(14)-C(15)	1.391(4)
C(5)-C(6)	1.405(4)	C(15)-C(16)	1.371(5)
C(6)-C(1)	1.397(4)	C(16)-C(17)	1.374(4)
C(2)-C(7)	1.492(4)	C(17)-C(18)	1.388(4)
C(7)-C(8)	1.381(4)	C(18)-C(13)	1.390(4)
C(8)-C(9)	1.390(4)	C(4)-O(2)	1.376(3)
C(9)-C(10)	1.364(5)	O(2)-C(19)	1.440(4)
		C(19)-C(20)	1.510(4)

Bond	Angle	Bond	Angle
C(1)-O(1)-H(1)	115(2)	C(7)-C(8)-C(9)	120.5(3)
C(2)-C(1)-O(1)	120.9(2)	C(8)-C(9)-C(10)	120.4(3)
C(6)-C(1)-O(1)	118.0(2)	C(9)-C(10)-C(11)	119.8(3)
C(2)-C(1)-C(6)	121.1(2)	C(10)-C(11)-C(12)	119.9(3)
C(1)-C(2)-C(3)	119.2(2)	C(7)-C(12)-C(11)	120.9(3)
C(1)-C(2)-C(7)	121.4(2)	C(6)-C(13)-C(14)	118.7(2)
C(3)-C(2)-C(7)	119.4(2)	C(6)-C(13)-C(18)	123.2(2)
C(2)-C(3)-C(4)	120.8(2)	C(14)-C(13)-C(18)	118.1(2)
C(3)-C(4)-C(5)	119.5(2)	C(13)-C(14)-C(15)	120.9(3)
C(4)-C(5)-C(6)	121.5(3)	C(14)-C(15)-C(16)	120.1(3)
C(1)-C(6)-C(5)	117.9(2)	C(15)-C(16)-C(17)	119.7(3)
C(1)-C(6)-C(13)	123.7(2)	C(16)-C(17)-C(18)	120.7(3)
C(5)-C(6)-C(13)	118.4(2)	C(13)-C(18)-C(17)	120.5(2)
C(2)-C(7)-C(8)	120.2(2)	C(3)-C(4)-O(2)	116.0(2)
C(2)-C(7)-C(12)	121.3(3)	C(5)-C(4)-O(2)	124.5(2)
C(8)-C(7)-C(12)	118.5(3)	C(4)-O(2)-C(19)	117.6(2)
		O(2)-C(19)-C(20)	107.0(2)

Bond lengths (in Å) and bond angles (in °) for molecule 3(B)

Bond	Length	Bond	Length
O(1)-H(1)	0.87(4)	C(10)-C(11)	1.381(6)
C(1)-O(1)	1.374(3)	C(11)-C(12)	1.397(5)
C(1)-C(2)	1.393(3)	C(12)-C(7)	1.390(4)
C(2)-C(3)	1.405(4)	C(6)-C(13)	1.491(4)
C(3)-C(4)	1.379(4)	C(13)-C(14)	1.389(4)
C(4)-C(5)	1.378(4)	C(14)-C(15)	1.387(5)
C(5)-C(6)	1.388(3)	C(15)-C(16)	1.383(4)
C(6)-C(1)	1.403(4)	C(16)-C(17)	1.369(5)
C(2)-C(7)	1.489(4)	C(17)-C(18)	1.375(5)
C(7)-C(8)	1.401(5)	C(18)-C(13)	1.384(4)
C(8)-C(9)	1.382(6)	C(4)-O(2)	1.379(3)
C(9)-C(10)	1.374(6)	O(2)-C(19)	1.414(4)
		C(19)-C(20)	1.489(5)

Bond	Angle	Bond	Angle
C(1)-O(1)-H(1)	110(2)	C(7)-C(8)-C(9)	120.3(3)
C(2)-C(1)-O(1)	123.0(3)	C(8)-C(9)-C(10)	120.6(4)
C(6)-C(1)-O(1)	115.8(3)	C(9)-C(10)-C(11)	120.0(4)
C(2)-C(1)-C(6)	121.2(2)	C(1)-C(11)-C(12)	120.1(3)
C(1)-C(2)-C(3)	118.2(3)	C(7)-C(12)-C(11)	120.2(3)
C(1)-C(2)-C(7)	122.2(2)	C(6)-C(13)-C(14)	119.4(2)
C(3)-C(2)-C(7)	119.6(3)	C(6)-C(13)-C(18)	122.2(2)
C(2)-C(3)-C(4)	121.0(3)	C(14)-C(13)-C(18)	118.4(3)
C(3)-C(4)-C(5)	119.8(2)	C(13)-C(14)-C(15)	121.0(3)
C(4)-C(5)-C(6)	121.3(3)	C(14)-C(15)-C(16)	119.4(3)
C(1)-C(6)-C(5)	118.5(3)	C(15)-C(16)-C(17)	119.8(3)
C(1)-C(6)-C(13)	121.9(2)	C(16)-C(17)-C(18)	120.9(3)
C(5)-C(6)-C(13)	119.6(3)	C(13)-C(18)-C(17)	120.5(3)
C(2)-C(7)-C(8)	119.6(3)	C(3)-C(4)-O(2)	124.8(3)
C(2)-C(7)-C(12)	121.6(3)	C(5)-C(4)-O(2)	115.4(3)
C(8)-C(7)-C(12)	118.8(3)	C(4)-O(2)-C(19)	118.2(2)
		O(2)-C(19)-C(20)	107.8(3)